Universidade de Aveiro Departamento de Química
Ano 2011

MARIA LUÍSA MOUTA FARIA LIMA DÓRIA

PERFIL FOSFOLIPÍDICO DE DIFERENTES LINHAS CELULARES DO CANCRO DA MAMA

PHOSPHOLIPID PROFILE OF DIFFERENT BREAST CANCER CELL LINES

Universidade de Aveiro Departamento de Química
Ano 2011

MARIA LUÍSA MOUTA FARIA LIMA DÓRIA

PERFIL FOSFOLIPÍDICO DE DIFERENTES LINHAS CELULARES DO CANCRO DA MAMA

PHOSPHOLIPID PROFILE OF DIFFERENT BREAST CANCER CELL LINES

Dissertação apresentada à Universidade de Aveiro para cumprimento dos requisitos necessários à obtenção do grau de Mestre em Bioquímica, com especialização em Métodos Biomoleculares, realizada sob a orientação científica da Doutora Maria do Rosário Gonçalves Reis Marques Domingues, Professora Auxiliar do Departamento de Química da Universidade de Aveiro, e da Doutora Luisa Alejandra Helguero Shepherd, Investigadora Auxiliar do Departamento de Química da Universidade de Aveiro

Dedico este trabalho à minha família e ao Adriano pelo incansável apoio.

o júri

Presidente

Prof. Doutor Francisco Manuel Lemos Amado
Professor Associado do Departamento de Química da Universidade de Aveiro

Doutora Bárbara M. Macedo
Investigadora responsável pela Unidade Metabolómica do IBMC

Doutora Luisa Alejandra Helguero Shepherd
Investigadora Auxiliar do Departamento de Química da Universidade de Aveiro

Prof. Doutora Maria do Rosário Gonçalves Reis Marques Domingues
Professora Auxiliar do Departamento de Química da Universidade de Aveiro

agradecimentos

Às minhas orientadoras, Professora Rosário Domingues e Professora Luisa Helguero agradeço pelos ensinamentos, orientação científica, incentivos, disponibilidade incondicional, confiança depositada e apoio ao longo da realização deste trabalho, bem como as críticas construtivas e as oportunas sugestões que me colocaram ao longo deste percurso e que em muito contribuíram para o meu enriquecimento científico.

Aos meus colegas de mestrado, pela amizade e companheirismo, compreensão e incentivo, entre a ajuda laboratorial e partilha de experiências com permanente disponibilidade, sem deixar de contar com todos os momentos de descontracção e diversão que passamos juntos.
Às meninas de doutoramento, por todos os desabafos, comentários, ajuda constante no laboratório, e pela disponibilidade, tornando os dias no laboratório mais agradáveis. Não posso deixar de lado todo o grupo de espectrometria de massa que me recebeu da melhor forma em especial à Cristina Barros por toda a ajuda, conselhos, ensinamentos e pela sua sempre boa disposição.

Também queria agradecer à Doutora Bárbara Macedo do IBMC por todo o tempo e paciência que despendeu, sempre com boa disposição e disponibilidade sendo uma ajuda preciosa e indispensável para a concretização deste trabalho.

E por último, mas não menos importante, agradeço à minha família e todos os meus amigos que “sobreviveram” a todas as crises e as intermináveis explicações sobre células e lípidos, esses seres que por muitas vezes me deixaram fora de mim.

palavras-chave Fosfolípidos, células epiteliais mamárias, cancro da mama, espectroscopia de massa, lipidómica

Resumo

O cancro da mama é a principal causa de morte por cancro nas mulheres. Alterações nas funções celulares de células cancerígenas levam a um crescimento celular descontrolado e mudanças morfológicas nestas. Membranas celulares estão intimamente envolvidas na regulação da sinalização celular; no entanto ainda muito está por compreender. Fosfolípidos são os principais constituintes das membranas biológicas e possuem um papel importante a nível funcional, estrutural e metabólico. O objectivo deste trabalho foi compreender se os perfis fosfolípidos de células epiteliais e de cancro da mama de ratinho e humanas diferem em relação a morfologia e grau de agressividade das células. Para este objectivo os fosfolípidos de linhas celulares foram analisados usando uma abordagem lipidómica.

Brevemente, os fosfolípidos foram extraídos de seis linhas celulares diferentes (três de ratinho e três humanas) usando o método de Bligh and Dyer, seguida de uma separação das classes de fosfolípidos por cromatografia em camada fina. As diferentes classes de fosfolípidos foram quantificadas pela quantificação de fósforo e analisadas por espectrometria de massa.

Diferenças e semelhanças importantes foram encontradas n entre células de ratinho e humanas, entre células não tumorais e células cancerígenas e entre células do cancro da mama com diferentes graus de malignidade. A espectrometria de massa e a análise por quantificação mostraram alterações no perfil das classes esfingomielina, cardiolipina e fosfatidilinositol. Alterações nas células mais agressivas foram observadas nas classes lisofosfatidilcolina, fosfatidiletanolamina e ácido fosfatídico.

Concluindo, os resultados indicam que as diferenças no perfil fosfolipídico tanto em células de ratinho como células humanas, podem ser associadas a morfologia, comportamento e expressão genética da célula, directamente relacionado com actividades enzimáticas e metabólicas que são conhecidas de estarem alteradas no cancro. Assim, a identificação das classes de fosfolípidos e sua estrutura abrem novas possibilidades para a exploração destas características no cancro e providenciam potenciais biomarcadores divulgando vias metabólicas com potencial para a terapia.

Keywords Phospholipids, mammary epithelial cells, breast cancer, mass spectrometry, lipidomics

abstract

Breast cancer is the leading cause of cancer-related death in women. Altered cellular functions of cancer cells lead to uncontrolled cellular growth and morphological changes. Cellular biomembranes are intimately involved in the regulation of cell signaling; however, they remain largely understudied. Phospholipids are the main constituents of biological membranes and play important functional, structural and metabolic role. The aim of this work was to establish if phospholipids profiles of mouse and human mammary epithelial cells and breast cancer cells differ in relation to morphology and degree of differentiation. For this purpose, phospholipids of cell lines were analyzed using a lipidomic approach.

Briefly phospholipids were extracted from six different cell lines (three from mouse and three from human) using Bligh and Dyer method, followed by a separation of phospholipid classes by thin layer chromatography. Phospholipid classes were quantified by phosphorus assay and analyzed by mass spectrometry.

Important differences and similarities were found in the relative phospholipid content between mouse and human cells, between non-tumorigenic and cancer cells and between breast cancer cells with different levels of aggressiveness. Mass spectrometry and quantification analysis showed substantial alterations in the profile of sphingomyelin, cardiolipin and phosphatidylinositol classes comparing non-tumorigenic with cancer cells. Alterations in the most aggressive cell lines were observed in lysophosphatidylcholine, phosphatidylethanolamine and phosphatidic acid classes.

Taken together, the results indicate that changes in phospholipid profile, either from mouse and human cell lines, can be associated to the difference in cell morphology, behavior and genetic expression, directly related to enzymatic and metabolic activities known to be altered in cancer. Thus, identification of phospholipid classes and their structure open new possibilities for exploration of such characteristics in cancer and provide novel biomarkers and disclose metabolic pathways with potential for therapy.

Index

Figures index

Tables index

Abbreviations:

AJ – adherent junctions

ATP – adenosine triphosphate

ATX – autotaxin

BSA – bovine serum albumin

C1P – ceramide 1 phosphate

CAM – cell adhesion molecules

CERT – ceramide transfer protein

CI – chemical ionization

CL – cardiolipin

Cyt c – cytochrome c

DAG – diacylglycerol

DAGK – diacyl glycerol kinase

DMEM/F12 – phenol red Dulbecco's modified Eagle medium

ECM – extracellular matrix

EI – electron impact

EGF – epithelial growth factor

ER – estrogen receptor

ESI – electrospray ionization

FA – focal adhesion

FAB – fast atom bombardment

FBS – fetal bovine serum

GC – gas chromatography

HER2 – human epidermal growth factor receptor 2

HPLC – high performance liquid chromatography

HS – horse serum

IgSF – immunoglobulin superfamily

LC – liquid chromatography

LPA – lysophosphatidic acid

LPAAT – lysophosphatidic acid acyltransferase

LPC – lysophosphatidylcholine

LPCAT1 – lysophosphatidylcholine acyltrasferase 1

LPP – phosphate phosphohydrolase

LSM – lysosphingomyelin

MALDI – matrix-assisted laser desorption/ionization

MS – mass spectrometry

NMR – nuclear magnetic resonance

PA – phosphatidic acid

PBS – phosphate buffer saline

PC – phosphatidylcholine

PE – phosphatidylethanolamine

PG – phosphatidylglycerol

PI – phosphatidylinositol

PI3K – phosphatidylinositol 3 kinase

PIP – phosphatidylinositol phosphate

PL – phospholipid

PLA2 – phospholipase A2

PLC – phospholipase C

PLD – phospholipase D

PR – progesterone receptor

PS – phosphatidylserine

PTN – Phosphatase and tensin homologue

Q – quadrupole

S1P – sphingosine – 1 – phosphate

S1PR – sphingosine – 1 – phosphate receptor

SM – sphingomyelin

TLC – thin layer chromatography

TOF – time of flight

I. Introduction

I. Introduction

1. Cancer

The human body is constituted by trillions of cells which reproduce by cell division. Under normal conditions this is an orderly and controlled process, responsible for the formation, growth and regeneration of healthy tissues in the body. Sometimes, however, the cells lose the ability to limit and control their own growth, thereby dividing and multiplying themselves very quickly and randomly [1]. As a consequence of this cellular dysfunction, an imbalance occurs in the formation of body tissues, originating what is known as a tumor. If the cells of the tumor have the ability to disseminate and invade, the malignant tumor is known as cancer. Cancer cells, receive signals which are transmitted inside the cell and nucleus to activate genes associated with the increase of angiogenesis, cell survival, proliferation and aggressiveness [2].

During metastasis, cancer cells invade the endothelium to reach the bloodstream and travel to other organs, being the metastasis process the fundamental step for cancer progression.

Is in this simplified scenario of the cancer cell physiology (i.e. proliferation, invasion and migration) that cells undergo major morphological and functional changes.

1.1. Breast cancer

Breast cancer is a disease with high incidence and, although it is not the cancer with higher mortality rate, is the leading cause of cancer-related death in women worldwide. Therefore, the study of this disease is very important [3]. Despite significant advances in diagnosis and treatment of breast cancer, several major unresolved clinical and scientific problems remain. These problems are related to prevention, diagnosis, tumor progression and recurrence, treatment and therapeutic resistance [1]. Resolving all these problems is complicated because breast cancer is not a single disease but is a highly

heterogeneous collection of different diseases with different risk factors, clinical presentations, pathological features, response to therapy and outcomes, which affect the same anatomical organ and is originated in the same anatomical structure, the terminal duct-lobular unit [4].

Cancer may be caused by several factors, including genetic and environmental factors. The various risk factors that modulate the development of breast cancer can be: age, country, socioeconomic status, reproductive events, exogenous hormones (hormone reposition therapy and contraceptives), life style risk factors (alcohol, diets, obesity and physical activity), familial history of breast cancer and mammographic density [5].

Breast cancer can be classified taking into consideration different aspects. The four characteristics most widely used are [4, 6]: stage of the tumor (based on tumor size: the greater the number of the stage, the worse prognosis), grade of the tumor (based on the loss of differentiation capacity: the higher grade, the worse prognosis), histopathology (ductal carcinoma when it is in the ducts or lobular carcinoma when it is in the lobules) and protein and gene expression. Each aspect influences the prognosis and the type of treatment selected.

Four main molecular classes of breast cancer have been distinguished by protein and gene-expression profiling [7] (Figure 1): basal like breast cancers, which mostly represent estrogen receptor (ER)-negative, progesterone-receptor (PR)–negative, and human epidermal growth factor receptor 2 (HER2)-negative tumors (also known as “triple-negative” tumors); luminal-A cancers, which are mostly ER-positive and histologically low-grade; luminal-B cancers, which are also mostly ER-positive but may express low levels of hormone receptors and are often high-grade; and HER2-positive cancers, which show amplification and high expression of the erbb2 gene and several other genes connected with this tyrosine kinase receptor [7].

There is a fifth type, recently cataloged as claudin-low, which is mostly triple negative but distinguished by having less cell – cell adhesion proteins and frequent infiltration of lymphocytes [4].

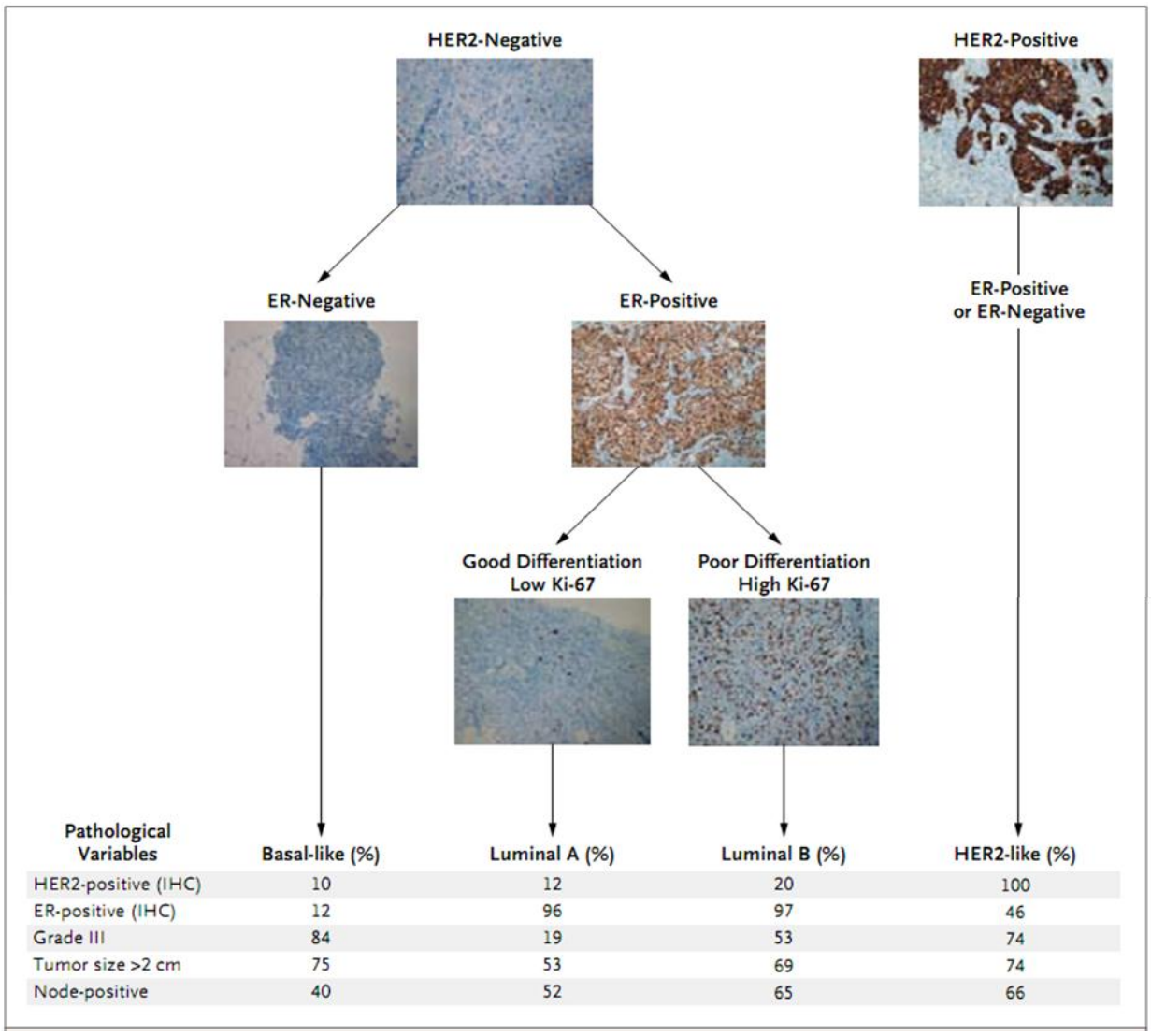

Pathological Variables	Basal-like (%)	Luminal A (%)	Luminal B (%)	HER2-like (%)
HER2-positive (IHC)	10	12	20	100
ER-positive (IHC)	12	96	97	46
Grade III	84	19	53	74
Tumor size >2 cm	75	53	69	74
Node-positive	40	52	65	66

Figure 1: Relation between molecular classes and clinical-pathologic characteristics of breast cancer [7]

More than 70 % of primary breast cancers in women are ER – positive, showing estrogen-dependent growth, and undergo regression when deprived of hormones (i.e. estrogens) that support the tumor [8] or when treated with ER antagonists [9]. Patients with this type of tumor have a better prognosis.

1.2. Metastasis

Metastasis is a fundamental step in cancer progression and, in 90% of the cases, is the death cause in women with breast cancer [10].

Much of metastasis research has focused on properties of the tumor cells with an increasing recognition of the importance of cell – cell and cell – extracellular matrix (ECM) interactions in the control of progression and differentiation of tumor cells [10]. Cell – cell and cell – ECM interactions are mediated by proteins known as cell adhesion molecules (CAMs; Figure 2). These proteins are important in cancer because abnormal subcellular localization and / or activity has been found in many types of cancer including breast cancer, and is associated to malignant progression and metastasis [11].

CAMs are transmembrane glycoproteins located on the cell surface and they are involved in binding to other cells or to the ECM in a process called cell adhesion. These receptor proteins are composed by three domains: an intracellular domain which interacts with the cytoskeleton, a transmembrane domain and an extracellular domain that interact with other CAMs or the ECM. The majority of CAMs belong to five families: immunoglobulin superfamily (IgSF CAMs), integrins, cadherins, selectins and lymphocyte T receptors [12]. In the literature the CAMs with more importance in cancer cell proliferation and invasion are cadherins and integrins [13, 14] and invasive cells undergo dramatic changes in the CAM´s level and affinity for substrates / ligands of the ECM.

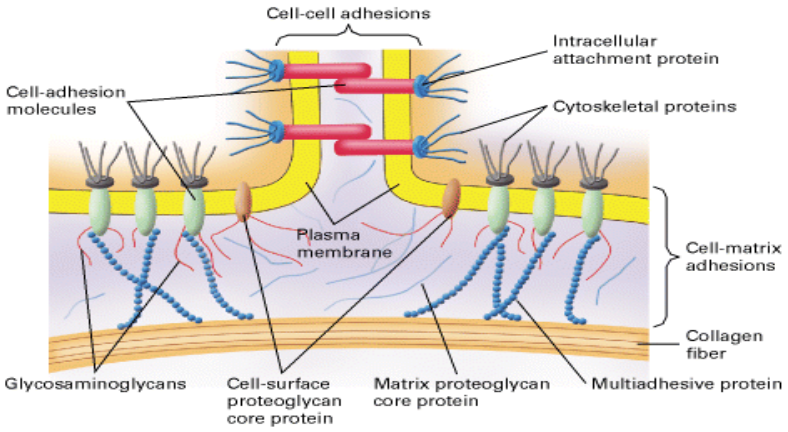

Figure 2: Schematic overview of the types of molecules that bind cells to each other and to the extracellular matrix - Cell-adhesion molecules http://tainano.com/chin/Molecular%20Biology%20Glossary.htm

In order to become activated, cadherins and integrins need to form clusters [15]. The cluster formation begins with the grouping of many CAM molecules in the plasmatic membrane, thus being able to bind their ligands with higher strength.

Clusters of integrins bound to the ECM and cytosqueleton are called focal adhesion (FAs). In the case of clusters of cadherins, these points of contacts are known as adherens junctions (AJs). Formation of clusters and CAM activation will activate intracellular signaling pathways that communicate to the cell the characteristics of extracellular space (outside – in signaling) [13]. Both FAs and AJs are dinamic molecular complexes regulated not only by binding to a substrate or partner but by the CAM availability at the membrane wich depends on the rate of protein uptake and recycling [16].

Therefore, FA and AJ formation and thus cell adhesion and intracellular signaling may be directly affected by the fluidity of cell membrane.

The cell membrane constitutes a meeting point between proteins and lipids and both molecular species have important roles in cellular processes. Lipids constitute at least 50% of the total mass of the membrane [17]. In this way, the cell responds to external stimuli, not only by regulating the expression of proteins but also by modulating the levels of lipids and phospholipids in the membrane. Thus changes in lipid environment of the cell can regulate function and availability of intrinsic membrane proteins, thus affecting inside out and outside in cell signaling (i.e. membrane transport). Therefore, adhesion and migration, two processes leading to metastasis converge at the cell membrane.

2. Lipids in the cell membrane

Living cells contain thousands rather than dozens of different lipids with different functions. The various functions of lipids make them essential to the survival of the cell

[18]. First, ligand – receptor interactions, endocytosis and vesicle recycling are controlled, at least in part, by membrane fluidity and by membrane specialized microdomains. This membrane fluidity and microdomains formation depend on lipid–lipid and lipid–protein interactions. In addition the cells have to synthesize huge amounts of lipids during replication to build more membranes. Second, lipids play an important role in various cellular functions by acting as signaling molecules (ceramide and phosphoinositides) or as precursors for second messengers (araquidonic acid, diacylglycerol-DAG). Thirdly, lipids can act as energy source, since fatty acids are the most reduced form of chemical energy [2].

Most of these cell functions occur in or around membranes. Membranes not only define the cell's boundary but they also create cellular compartments into which certain activities can be segregated to make them more efficient [17].

Singer and Nicolson were the first to propose that membranes were formed by a fluid bilayer in which proteins and lipids could move freely – the fluid mosaic model – contributing greatly to our concept of a cell membrane [18, 19]. Most biological membranes are asymmetrical, both laterally and in cross-section and their lipids participate in dynamic interactions that facilitate changes in their relative position in membranes, membrane thickness, surface packing, lateral and rotational mobility and other properties that complicate the study of membrane structure. Recent studies show that lipid modifications and the surrounding amino acids are not only involved in the interaction with membranes but that they also regulate membrane lipid structure, the formation of lipid domains in membranes and clustering of some proteins.

The basic structural constituent of biological membranes such as plasma membranes and cell membranes of intracellular organelles, are the phospholipids (PL; Figure 3), where phosphatidylethanolamine (PE), phosphatidylserine (PS) and phosphatidylinositol (PI) are found predominantly in the cytoplasmic leaflet of the membrane, and phosphatidylcholine (PC) is found predominantly on external leaflet of the membrane [17]. The PCs constitute more than 50% of phospholipids in eukaryotic membranes [20].

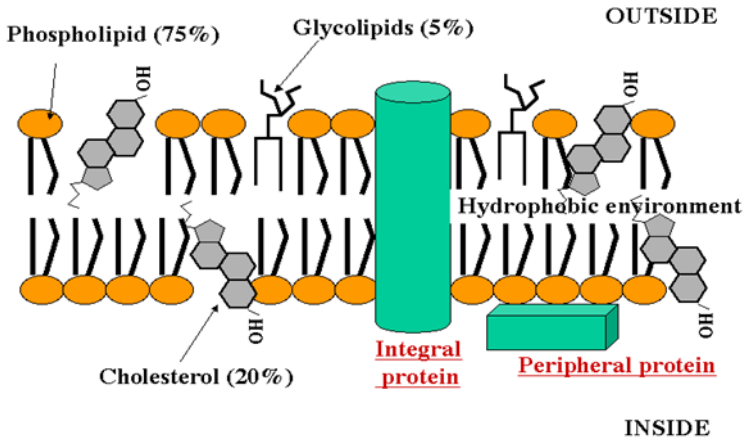

Figure 3: Schematic representation of plasmatic membrane and the percentage of its different compounds

The PL are amphipathic molecules, i.e., have a head constituted by a phosphate group linked to other specific group, depending on the class of lipid, which is polar or hydrophilic and a tail consisting of the fatty acid chains that are nonpolar or hydrophobic, both linked by a glycerol molecule. These characteristics make phospholipids singular molecules, which establish the organized structure of cell membranes [21].

Sphingomyelin (SM) and other related molecules, like ceramide and sphingosine, are another important class of membrane lipids, the sphingolipids. Cholesterol, another important component in the cell membrane, fills the spaces along the molecules of SM. These results in membrane regions with large concentrations of SM and cholesterol called lipid rafts [20]. These regions are very important because some protein components of signaling transduction (including MAP kinases and ER) have a great affinity for these lipid rafts [22]. The presence of SM and therefore lipid rafts suggests that sphingomyelin plays an important structural role in the cell membrane and participates in signal transduction pathways.

PLs can also be found in other parts of the cell besides plasmatic membrane, such as in the membrane of organelles and where they are synthesized. PE and cardiolipin (CL) are mainly synthesized in mitochondria, and PC, PI, PS and some PE are synthesized in the endoplasmatic reticulum while SM and some PC are synthesized in Golgi complex [23].

Many lipids in the plasma membrane are involved in signaling cascades, being vital for signal transduction pathways in the cell. Lipid signaling is an essential part of cellular

functions and refers to any event involving a signaling lipid messenger that binds to a target protein, such as receptors, kinases or phosphatases, which translate the message from the lipids into a specific cellular response [24]. Different lipid categories have been identified as signaling molecules and cellular messengers. These lipids include: sphingosine-1-phosphate (S1P), a sphingolipid derivative of ceramide which is a potent messenger involved in regulating calcium mobilization, cell growth and apoptosis; prostaglandins, which are derived from arachidonic acid involved in inflammation and immune process; DAG and phosphatidylinositol phosphate (PIP), the latter two being involved in calcium-mediated activation of protein kinase C and PI3K-AKT survival pathway, among others [24-27].

All of the lipid functions (membrane dynamics, energy homeostasis, and molecular machinery regulation) are critical aspects of cell proliferation, inflammation, immunity, apoptosis and invasion. An unbalance in cellular lipid composition and quantity seems to lead to variations in these cellular functions, and can be involved in uncontrolled cell growth which contribute to the onset of cancer and its progression [2, 22]

3. Lipids and cancer

There is some knowledge regarding specific lipids that may be involved in cancer (in [2, 28]), however, research in this area is far from being complete. In the following text we will present a brief review of the most important lipids that are thought to be involved in this complex disease, cancer.

High levels of PC, the most abundant PL in membrane, and PE were detected in breast cancer cells. Some mechanisms behind the increase in PC levels observed in cancer cells include an increase of choline kinases expression and activity and a higher rate of choline transport. Choline kinase is an enzyme responsible for PC formation from choline, and its overexpression was also detected in several human cell lines of breast cancer [29].

PIs, their metabolites such as phosphatidic acid (PA) and DAG and PI derivatives like PIP are very important contributors to cellular signaling cascades that activate

proliferation, maintain survival and promote migration [27]. Imbalances in their relative levels lead to changes in cellular functions that may contribute to the onset of cancer. Products of PI´s phosphorylation, as PIPs, are precursors of second messengers and regulate various cellular responses such as cell growth, proliferation, and motility via specific interactions of proteins that bind to their phosphorylated polar heads. For example, phosphatidylinositol 3 kinase (PI3K) phosphorylates phosphatidylinositol 4,5 bisphosphate (PIP2) resulting in phosphatidylinositol 3,4,5 trisphosphate (PIP3), which acts as second messenger and controls cell growth, survival, proliferation, motility and morphology [30]. Dual specificity of the protein phosphatase (PTEN - Phosphatase and tensin homologue), has PIP3 as main targets, the opposite function of PI3K [31]. Overexpression of PI3Ks and inactivation by genetic and epigenetic mutations of Pten gene results in accumulation of PIP3 and play a crucial role in the development of different tumors. High PIP3 levels lead to a cytoskeleton rearrangement that is subsequently stimulated, increasing migration and metastasis. This hyperactivation of PI3K with mutations in Pten are associated with the development of resistance to hormonal therapy with ER antagonists [32].

Lysophosphatidic acid (LPA), structurally similar to sphingosine – 1 – phosphate (S1P), appears to be important in the metastases process and high levels of LPA were observed in plasma samples of patients with ovarian cancer [33]. LPA activates PI3K leading to increase of PIP3 and induction of cell proliferation and cell survival. Therefore the LPA signaling pathway regulates cell proliferation, invasion and angiogenesis in cancer cells [34].

Sphingolipids and their metabolites are molecules involved in the regulation of various aspects of cancer pathology and its therapy, including apoptosis, cell proliferation, cell migration, inflammation or senescence [35]. As an example, ceramides and sphingosines are lipids with pro-apoptotic and anti-proliferative activities. When these lipids are converted in ceramide – 1 – phosphate (C1P) and S1P respectively, they promote cell growth and proliferation and revert the apoptotic stimuli [35, 36]. Recently it was reported that changes in the sphingolipid metabolism by ceramide transfer protein, CERT, could confer survival advantages to cancer cells and be therefore implicated in

cancer biology. High levels of S1P promote proliferation and survival in cancer cells and S1P receptors (S1PR) were recently discovered and are consider as a requirement for tumor angiogenesis [37].

There is a subset of lipid rafts domains that is enriched in ceramides and sphingomyelin and generally promotes apoptosis. These domains rich in ceramides allow to amplify a weak primary signal, for example death receptors that transmit a strong signal to the cell and thus trigger apoptosis. When ceramide in these domains is replaced by cholesterol, these domains become involved in normal cell signaling. The deregulation of these domains rich in colesterol promotes cell transformation and tumor progression [22, 38].

4. Lipids and metastases

There is an important relationship between lipid domains in the membrane, such as lipid rafts, and the proteins involved in metastases process, the CAM´s. Sphingolipids, represented by SM, are one of the main phospholipid classes in membrane [39], mostly due to their high content in raft domains. Studies have emphasized that sphingolipids are associated with integrins and can modulate their activity and functions. Binding of cells to proteins of the ECM is deficient when cells are totally deprived of sphingolipids [40].

Integrin clustering is regulated by their recruitment to membrane lipid rafts, the microdomains rich in sphingolipids and cholesterol. These two compounds have specific roles in regulation of integrin activation and function [40]. Reduction of cholesterol concentration in plasmatic membrane can lead to the loss of lipid raft signaling function, being important for signal transduction and cellular adhesion.

The association of cadherins with lipid rafts promotes cell – cell adhesion [41] as N-cadherin (highly expressed in migratory cells) can be trapped and immobilized in lipid rafts. The effect of lipid rafts disruption in the cadherin mobility can be explained by the structural organization of lipid rafts that can act as a brake on the plasma membrane proteins movement that must pass through or around this structure [42]. This indicates

that lipid rafts have an important role in organizing signal transduction pathways in a specific area of the membrane [22].

5. Lipidomic approach using Mass spectrometry

The study of lipids and their classes in their natural environment is called lipidomic. This is a new field of study that focuses on a large-scale study of lipids functions and metabolic pathways in biological systems [43]. Lipidomic approaches extensively examine the various lipid classes, both qualitatively and quantitatively, their interactions with other lipids, proteins and other molecules in vivo, lipid function and the changes that occur during pathophysiological disorders [44]. Lipidomic was an area of intense research in the 60´s; however, due to limitations in the analytical techniques, the evolution of this research area was much slower relative to the progress made in the areas of molecular biology, genomics and proteomics [45]. Thus, although lipidomic was a field already known in several studies, this name has only recently become in use [46].

There is a huge structural diversity of lipids in the biological systems, approximately 200 000. There are several approaches to classify lipids, one based on the definition of Christie [47], considering two classes: simple lipids, also known as neutral or non-polar lipids and polar or complex lipids. Another classification used and described in a review by Fahy et al [48] divides the lipids into eight groups: fatty acyls, glycerolipids, glycerophospholipids or PLs, sphingolipids, sterol lipids, prenol lipids, saccharolipids and polyketides.

In most mammalian cells, PLs represent approximately 60% of total lipids and sphingolipids comprise roughly 10% of total lipids. Due to the importance of these two groups, our study focused on them.

Phospholipids (Figure 4) are almost everywhere in nature and are key components in the lipid bilayer of cells, being involved in metabolism and cell signaling. These compounds can be divided into different classes, based on the nature of the polar head

group: PA, PC, PE, PI, PS, phosphatidylglycerol (PG) and CL. Each class comprise different molecular species depending on the fatty acid composition of each phospholipid.

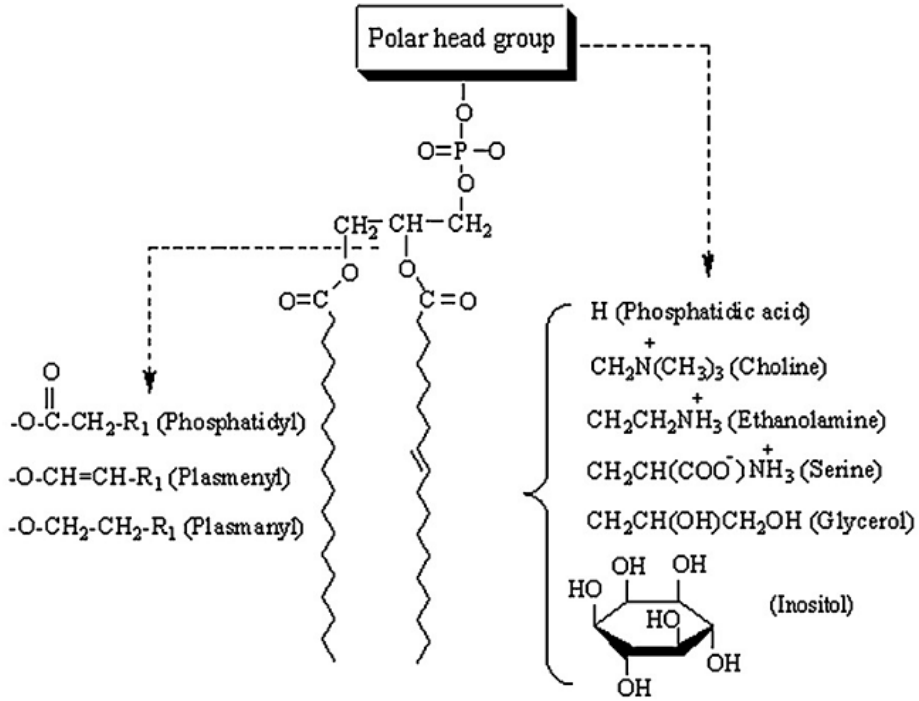

Figure 4: Molecular structure of the main types of phospholipids [49]

The second major group of polar lipids corresponds to the sphingolipids, a complex group of molecules that share a common structural feature, a sphingoid base backbone, which in mammals is known as sphingosine. Based on the covalent bond nature between the different possible polar molecules (Figure 5) and sphingosine, the sphingolipids can be classified as: the sphingoid bases and their simple derivatives (such as the S1P), the sphingoid bases with an amide-linked fatty acid (e.g., ceramides), and more complex sphingolipids with head groups that are attached via phosphodiester linkages (the phosphosphingolipids as SM), via glycosidic bonds (the simple and complex glycosphingolipids such as cerebrosides and gangliosides), and other groups (such as phosphono- and arseno-sphingolipids). Within the same class the species can still be distinguished through the different fatty acyl composition [50].

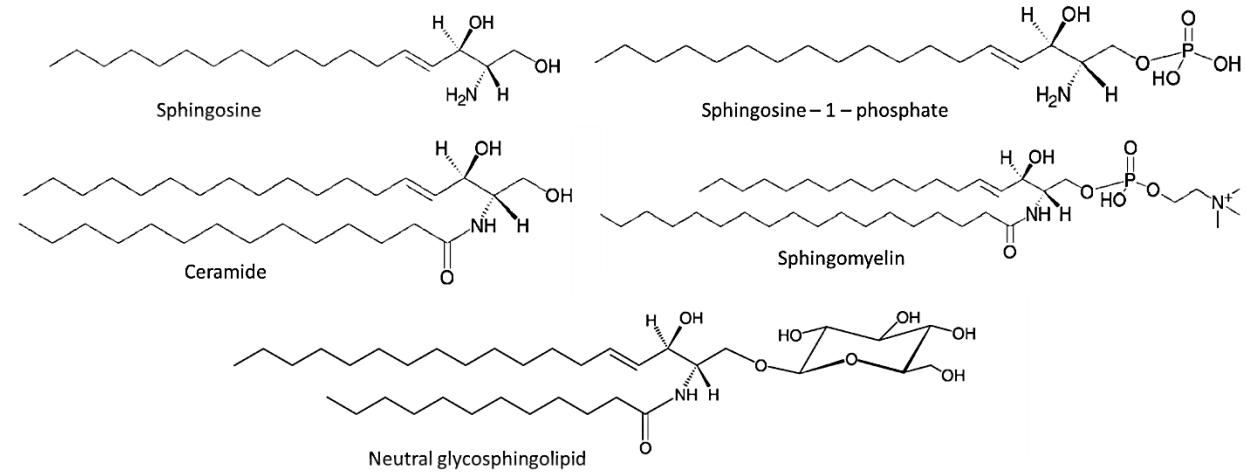

Figure 5: Molecular structure of the main types of sphingolipids [48]

The strategy underlying the lipidomic methodology (Figure 6) involves, firstly, the preparation of the biological sample, which in our case was non-tumor and breast cancer cells in culture. Secondly, the extraction of lipids in a fraction free of proteins and other components. Once extracted, the lipids are then fractionated, which usually requires a step of chromatography for identification and quantification of each molecular class. Finally these various classes of lipid extracts are then analyzed by mass spectrometry, thereby creating a lipid profile [51].

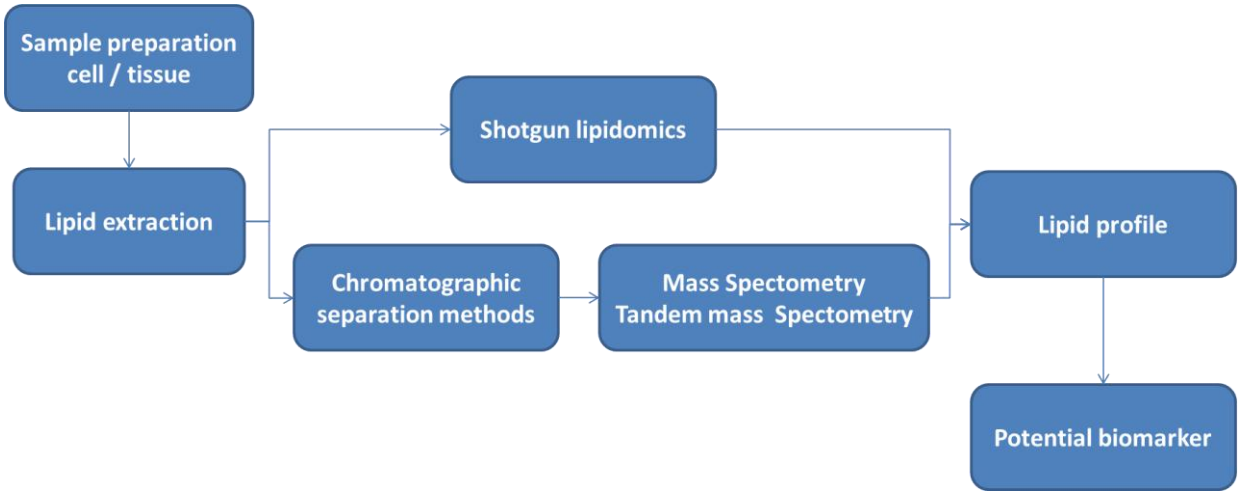

Figure 6: Schematic representation of a lipidomic approach

5.1. Extraction

Lipids can be extracted from biological samples by a vast number of organic solvents, and these extractions can be adapted for a specific class of lipids (for example phospholipids, sphingolipids, etc) [50]. Since this analysis is centered in phospholipids, extraction is focused in this lipid class. The chemistry of PL molecules require the presence of a more polar solvent, like alcohol, followed by a non-polar solvent, like chloroform, for a complete extraction.

The mixture of chloroform, methanol and water in different proportions is efficient for phospholipid extractions. This approach was developed in the 50´s by Folch [52] that used chloroform / methanol 2:1 and a high amount of water to wash the non-lipid components. Although this extraction procedure is efficient, the formation of emulsions is a big disadvantage, despite Folch´s attempts to tackle this issue by the addiction of salts.

The Bligh and Dyer method [53] is a variation of Folch´s extraction and is advantageous for tissues with a high percentage of water content because it calculates the amount of water in the sample so that the final composition of chloroform / methanol / water will be 1:2:0,8, creating a single phase of extraction. The extraction is very efficient and quick. After the addition of water and chloroform, the lipids are recovered from the bottom phase, rich in chloroform, followed by a wash with water and methanol. The non lipidic contaminants can be eliminated in this wash. To augment the recovery of phospholipids, the methanol proportion can be increased.

To minimize the risk of fatty acid oxidation or the lipids hydrolysis during the isolation process it is recommended that all extractions be made at low temperature (4ºC), as fast as possible after the lipids removal from the tissue or cell culture.

5.2. Chromatographic separation method: thin layer chromatography

The chromatographic techniques are very useful in the analysis of lipids extracted from biological samples since it allow to separate the different classes of phospholipids. Chromatography takes advantage of different affinity of analyte with the mobile phase and stationary phases to achieve separation of complex mixtures, i. e., it involves passing the mixture dissolved in a "mobile phase" through a stationary phase, which separates the analyte to be measured from other molecules in the mixture based on differential partitioning between the mobile and stationary phases.

The most popular techniques of chromatography are: thin-layer chromatography (TLC), gas chromatography (GC), liquid chromatography (LC) and high-performance liquid chromatography (HPLC) [54]. These techniques can also function as a pre-separation when coupled with mass spectrometry (MS), facilitating further analysis and identification of lipids, already divided by their families. The techniques more used for PLs analysis are TLC and HPLC, but in this study only TLC was used.

TLC was the first form of chromatography used for analysis of phospholipids. It is the simplest method for lipids separation and is widely used today. It is a technique in which the stationary phase is a solid phase and the mobile phase is a liquid phase. TLC is then a solid – liquid adsorption technique in which the solvent molecules compete with the molecules of the sample for binding sites on the stationary phase.

For phospholipids separation glass plates coated with alumina or silica are used as the stationary phase, the latter being most common. In the surface of the silica gel particles, there are hydroxyl groups which render the surface of silica gel highly polar. Thus, the polar functions of the organic analyte interact strongly with the surface of the gel particle and the nonpolar functions interact only weakly. For silica gel chromatography, the mobile phase is normally an organic solvent or mixture of them, chosen based on the type and class of lipids to separate. As the liquid phase travels along the surface of the solid phase it transports the analyte particles along the silica gel surface. However, the analyte molecules are only free to move with the solvent if they are not bound to that surface. Thus, the fraction of time that the analyte is bound to the

surface of the silica gel relative to the time it spends in solution determines the retention factor of the analyte.

Despite being less sensitive than other chromatography methods, TLC is commonly used to separate PL classes from total lipid extracts with the advantage of being a relatively easy and fast technique. It can separate, the nonpolar lipids (triglycerides, free fatty acids, cholesterol and DAGs) from more complex lipids like phospholipids, and also achieve separation even within the phospholipids, when using an adequate mixture of solvents [55]. After separation in classes, lipids and phospholipids are nowadays usually analyzed by mass spectrometry.

5.3. Mass spectrometry

Mass spectrometry (MS) is a powerful analytical technique that can be used to identify unknown compounds. This technique allows the separation and detection of gas phase ions according to their mass / charge (*m/z*) value. Using this technique it is possible to detect compounds at very low concentrations in chemically complex mixtures, since the identification can be made from very small quantities.

All mass spectrometers consist essentially in three basic units (Figure 7) [56]: the ionization source, where ions are produced from the sample under study, the mass analyzer, which gives the actual separation of ions according to their *m/z* value and the detector, where the separated ions are collected and characterized by producing a signal whose intensity is related to the number of detected ions. These detectors are connected to a computer that provides mass spectra recording the *m/z* corresponding to each ion and the correspondent relative abundance. An important feature of these instruments is the high vacuum present that allows free movement of ions through the spectrometer without simultaneous reactions or changes of the ions.

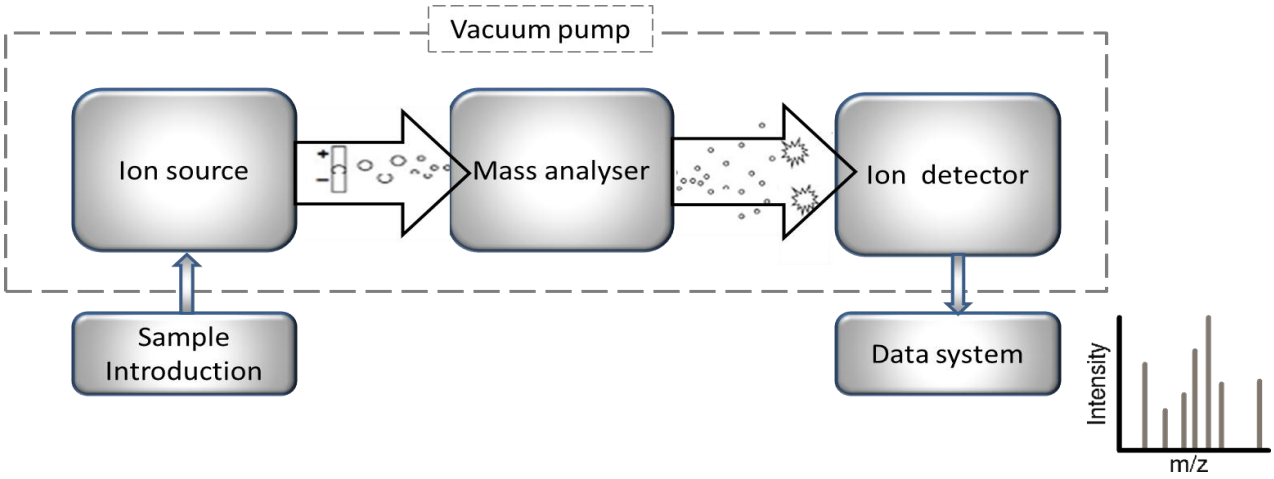

Figure 7: Components of a mass spectrometer

Ionization methods

Over time, there have been different ionization methods. The first ionization method to emerge was the electron impact (EI) and later the chemical ionization (CI), which are only applicable to volatile and thermally stable compounds. To overcome this limitation the use of ionization by bombardment with fast ions or atoms (FAB) allowed analysis of non-volatile and thermally unstable samples by MS. More recently the electrospray ionization (ESI) and laser desorption ionization by matrix-assisted (MALDI) were developed and are the ionization methods most commonly used today in the analysis of biomolecules.

The development of ionization by FAB allowed the analysis of natural PLs and the ability to analyze directly intact PL structures and preserve the information inherent to their chemical structure. However there were some associated problems, the complications of the spectrum with ions of the matrix and the decomposition of molecular ions during ionization [57]. With the advent of electrospray ionization (ESI), a softer ionization method than FAB, these problems were solved and the level of sensitivity for the detection of phospholipids was increased. The ionization sources commonly used in lipidomics are ESI and MALDI [57, 58]. Since PLs have a relatively low

molecular weight (600 to 1000 Da), ESI is the most used in PL analysis. Under ESI conditions, PLs ionize as single charged ions which facilitates their analysis by ESI-MS.

ESI was developed in 1989 by John Fenn and his colleagues [59] and involves dissolving the sample in a solvent and the formation of spray. The sample is injected in a metal needle using a syringe pump and a high voltage is applied in the needle. This high voltage will charge the solvent and the sample molecules, creating a spray of electrically charged droplets. After release of the droplets, they undergo further division and with the assistance of nitrogen gas the solvent will gradually evaporate, until each droplet corresponds to a single charged ion after the solvent being completely evaporated (Figure 8).

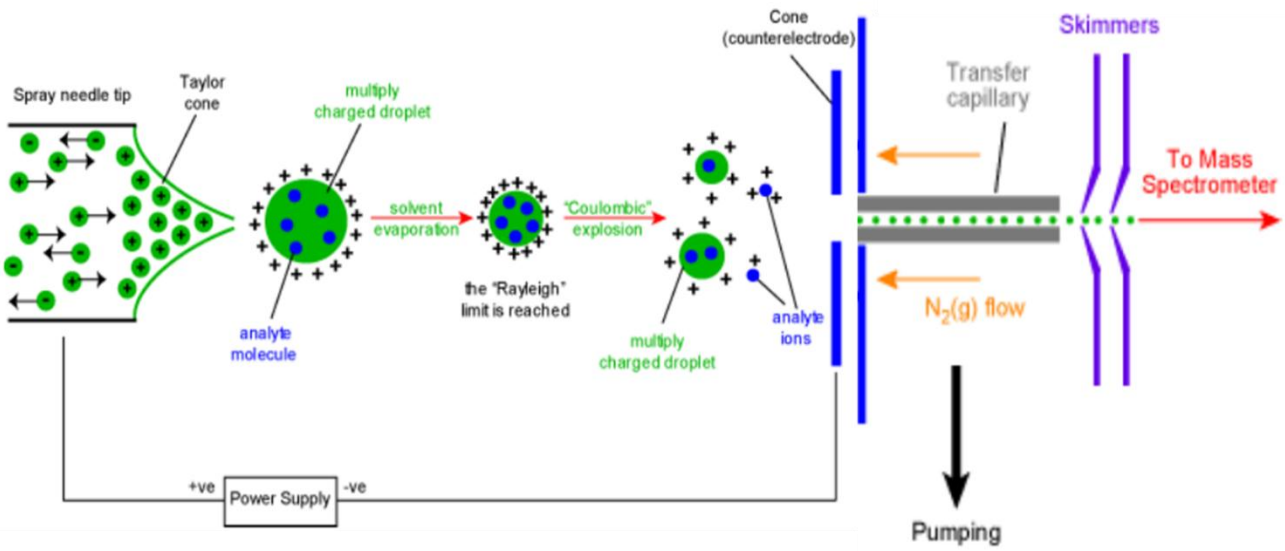

Figure 8: A schematic representation of an ESI source and the mechanism of ion formation (http://www.chm.bris.ac.uk/ms/theory/esi-ionisation.html)

Depending on the chemical properties of the molecules (i. e. the polarity) both negative ions (molecules that have lost protons) and positive ions (molecules that have gained protons) can be formed. This ionization has the advantage that the molecules are not broken apart, instead they remain intact; this is why this ionization is called soft ionization.

Analyzers

After sample ionization, ions are separated based on their *m/z* ratio by the analyzer. There are three main types of analyzers that are commonly used for phospholipids analysis by mass spectrometry: quadrupole (Q), ion trap and time of flight (TOF).

The Qs have many advantages such as being relatively low-cost, easy to use and capable of providing accurate results. However their resolution is limited and the transmission decrease linearly, being the upper limit of *m/z* around 3000. A quadrupole consists of four parallel rolls, which applies a current that affects the trajectory of ions traveling through the central route between the 4 rolls. For certain voltages, only ions of a specific *m/z* ratio can pass through the quadrupole filter, while others are carried away as uncharged molecules. By varying the electrical signals from one quadrupole, it is possible to vary the range of the *m/z* transmitted.

Linear ion trap is an analyzer which consists of a multi-pole, producing a three-dimensional field where the ions are confined (trapped). For this analyzer there is a stability diagram, where the ions whose coordinates are within the diagram, and whose kinetic energy do not exceed the potential of the trap, are enclosed in the field until they are removed by collision. To make them leave, a radio - frequency of small amplitude voltage is applied. This amplitude is then scanned in an ascending way and increasing mass ions are sequentially ejected from the trap and detected by a detector to produce a mass spectrum.

A time of flight analyzer (TOF) uses the differences on time that accelerated ions leads to reach the detector based on their mass differences. The ions are accelerated by pulsed electric field and the accelerated particles pass through a flight tube of varying length. The essential principle of flight time analyzer is based on all ions accelerated to the same energy, i.e. with equal energy and will travel at speeds inversely proportional to the square roots of their masses. So the lighter ions with high-speed reach the detector earlier than heavier ions with low speed [60, 61].

Detectors

The signal obtained by the analyzer has to be detected by a detector. The detectors can be of two categories: direct measurement detectors that detect the charge when it reaches the detector, and multiplier detectors, which use an electron multiplier to increase the intensity of the signal generated. The direct detectors include the plate detector and the Faraday box detectors. The multiplier detectors include the electron multiplier detectors, electronic channel multipliers and the scintillators. From these the most widely used are electron multipliers, since they have a lifetime exceeding a limit of detectable masses. The operating principle of these detectors is as follows: when an ion reaches the first electrode it produces emissions of secondary electrons, which are in turn accelerated in direction to the second electrode and so on.

The detector is connected to a computer that integrates the information received and converts it into a mass spectrum, which shows the ion mass / charge ratio on the abscissa (values of *m/z*), and the relative abundance of these same ions after a normalization in relation to the ion abundance on the ordinate [60, 61].

Tandem mass spectrometry (MS/MS)

The main characteristics of mass spectra obtained with soft ionization method are the absence of fragmentation, which allows the accurate determination of molecular masses of mixtures of components. However, in these conditions little information is obtained about the ion´s molecular structure. To achieve this goal, several analyzers are coupled in series to proceed the fragmentation of the desired ion by inducing dissociation of the ions formed at the source by collision. However some instruments (linear ion trap) with just one analyzer are able to perform multiple MS (MSn), becoming efficient instruments in the structural identification of several molecules including the phospholipids. Using this technology we can draw several conclusions about the structure

of the analyzed molecules and the spectra obtained gives us not only the most frequent molecular fragmentation but also as the most favorable [50].

The type of MS / MS most commonly used in mass spectrometry is called product ion scan. In this way the first analyzer selects a specific *m/z* value (precursor ion) of the mixture, ionizes and transmits to the second analyzer, a collision cell, were the ion will be fragmented. At last, the fragmented ions are separated based on their *m/z* value by the last analyzer. Analyzing the ion fragments and knowing the mass of the precursor ion, the structural information of lipid can be deduced, as the assembly of a puzzle. So, each peak corresponding to the phospholipid of interest is subjected to collision-induced dissociation and molecular structure of this phospholipid is determined by its spectrum of product ion spectra or MS / MS [62].

Another type of MS / MS is precursor ion scan, which makes use of a characteristic fragment produced by certain compounds in the sample. In this type all ionic species are separated in the first analyzer and will be sequentially transmitted to the cell collisions. However, the third analyzer is set to transmit a single *m/z* value of a fragment formed in the second analyzer, the cell collision. The computer analysis will show the precursors of the specific ion formed in the third analyzer.

Fragmentation in the second analyzer not only gives a single precursor ion, but can give a rise of fragments with a characteristic mass loss of a particular class of compounds. This type of MS / MS is called a common neutral loss, where the first and third analyzer are scored together, separated by an equal amount of a neutral loss mass that occurs in the second analyzer. All ions are sequentially separated in the first analyzer and transmitted to the second analyzer. The third analyzer separates the ions coming out of the second analyzer by the *m/z* value equal to the neutral loss mass [63].

5.4. Phospholipids and mass spectrometry

MS has played a key role in the study of phospholipids, because it allows the detection and determination of the structures of these molecules. The combination of

sensitivity, specificity, selectivity and speed makes MS an ideal technique for the analysis of this type of lipids.

Information on the molecular weight of each lipid species can be determined from a first analysis on the MS spectrum. In a second approach, a certain ion with a specific *m/z* value, corresponding to a single phospholipid, can be further analyzed by MS / MS. The fragmentation pattern observed in MS / MS normally contains information about the polar head group and fatty acyl composition, which determines not only the class of phospholipid but also in particular the phospholipid structure. Other modes of MS / MS, precursor ion scan and neutral loss scan, are also useful for detecting characteristic phospholipids of each class.

Almost all PLs are ionizable in ESI, some more in the positive mode, others more in the negative mode. The positive mode by ESI-MS can ionize the following classes: PC, PS, CL, PE, and SM, which is a sphingolipid analogous to PC containing the same polar head attached to a ceramide [50]. The lyso forms of these phospholipids, ie without one of the fatty acid chains, can also be detected in this mode. All these classes form [M + H] + ions. In this mode, the formation of these ionic species and lipids fragmentation are greatly affected by the concentration of ions in solution. Ions that are commonly used to bind to phospholipids are: Li^+, Na^+ and K^+.

The classes PI, PS, PG, PA, PE, CL and ceramides, and their lyso forms, can be detected in negative mode, all forming ions $[M-H]^-$ [64]. The fragmentation patterns of these species in negative mode, compared to the positive mode, results in richer structural information of the phospholipids. In each case the fragmentation of the polar head and the fatty acids is shown, helping in the lipid identification process [57].

PA is the simplest polar head group, and serves as a precursor and metabolite of biosynthetic pathways and catabolism of phospholipids. Although it is possible to observe $[M + H]^+$ and $[M-H]^-$ ions, the most abundant are negative ions [65].

PC was the first to be analyzed by mass spectrometry due to its high abundance in the cell. The PC an SM fragmentation is similar because they share the same polar choline head group. The fragmentation of their protonated ions ($[MH]^+$) form a ion with a *m/z* value of 184, characteristic of the choline polar head, as the ion $[MH-59]^+$, corresponding

to the neutral loss of $(CH_3)_3N$. Precursor ions scan of 184 will allow the identification of all PCs in the lipid extract.

PE constitutes one of the major classes of lipids found in cell membranes. The fragmentation of PE protonated in the positive mode produce an abundant ion of [M + H-141] $^+$, resulting from the neutral loss of ethanolamine polar head. The fragmentation pathways of these classes in negative mode ([M-H] $^-$) results in an ion with a *m/z* value of 196 related to head of the group with dihydrate glycerol, as well as informative carboxylate ions of the fatty acids.

PG is the less abundant phospholipid class in eukaryotic cells, since they are more characteristic of prokaryotic cells. In tandem mass spectrometry, this class produces a characteristic ion from the neutral loss of its polar head, the ion [M + H-171] $^+$.

PI, a very important lipid in the cell signaling, is a phospholipid class containing a sugar, inositol, consisting of six carbons as polar head. In the MS / MS spectra PI, when deprotonated ([M-H] $^-$), shows a characteristic ion with *m/z* value of 241 from the dihydrate head group, in addition to the carboxylate ions of the fatty acids.

PS is an important phospholipid with a unique feature: it is predominantly found on the inside of the membrane and the appearance of this phospholipid on the outer membrane initiates many biological events, such as cell adhesion, and apoptosis. The fragmentation of PS in the positive mode produced an ion resulting from neutral loss of polar head of serine ([M + H-185] $^+$) in the MS / MS spectrum. In the negative mode this class can be identified with a neutral loss of 87 ([M-H-87] $^-$), corresponding to neutral loss of the serine head.

CL is the most complex phospholipid present in eukaryotic cells being involved in mitochondrial stability and function. Despite being ionizable in both modes (negative and positive) its analysis is easier in the negative mode. Once cardiolipine structure is two phosphatidic acids with a glycerol bond, electrospray ionization can generates abundant negative ions, including the double charged $[M-2H]^{2-}$ ions. The fragmentation of CL in the negative mode ($[M-H]^-$ and $[M-2H]^{2-}$) led to a rich set of information that was consistent with the elimination of each fatty acid by a neutral loss [57].

The characteristic fragmentation of the most important PL classes is presented in Table 1.

Table 1: Characteristic fragmentation pathways of the most important PL classes

Class	Head group	Analysis Charge / method
PC Phosphatidylcholine	Choline	+ / precursor *m/z* 184
SM Sphingomyelin	Choline	+ / precursor *m/z* 184
PE Phosphatidylethanolamine	Ethanolamine	+/ neutral loss 141 Da - / precursor *m/z* 196
PS Phosphatidylserine	Serine	- / neutral loss 87 Da + / neutral loss 185 Da
PA Phosphatidic acid	Acid	- / precursor *m/z* 79
PG Phosphatidylglycerol	Glycerol	- / neutral loss 74 Da + / neutral loss 172 Da
PI Phosphatidylinositol	Inositol	- / precursor *m/z* 241

Information about PL profiles and the molecular species that belong to each PL class in breast cancer is scarce. There has been some evaluation of lipid profiles using magnetic nuclear resonance (MNR) which allowed correlation of PL classes with histopathology features of human breast surgical tissue specimens. As such, SM and PC amounts were inversely correlated to cellular infiltration and linfatic invasion, respectively; and PC levels were higher in ER negative tumors [66, 67]. MS has been used to analyse PLs in canine cell carcinoma of the urinary bladder [68] and is frequently used to study PIs in cancer (in [69]). Recently, identification of PL profiles in urine of patients with breast cancer was carried out using LC/MS/MS and showed an increase in PC and PE in patients with breast cancer, which after surgery, reverted to the initial pre-surgical levels [70, 71]. So far this is the closest methodological approach to our work; no studies have focused on the identification of PL profiles in breast cancer cells using MS. This is probably because analysis of lipids by MS is time consuming due to lack of bioinformatic

tools for spectra interpretation and requires the individual interpretation of each detected PL molecular specie [57].

6. Aim

Lipid research in cancer is relatively scarce. Therefore our work focused on the analysis of phospholipid profiles using MS. Since lipid roles and classes may influence CAMs activation and function, in this work, it is proposed that changes in lipid classes and profiles are associated to cancer progression. Thus, the general aim of this work is to compare the phospholipid profile between normal mammary cells and breast tumor cells with different degrees of malignancy with the help of a lipidomic approach involving TLC separation and MS. This work will be separated into three specific aims:

1) Use of mouse cell lines to analyze differences and similarities in PL profiles of a non-tumorigenic cell line and two cancer cell lines with different metastatic potential.

2) Use of human cell lines to analyze differences and similarities in PL profiles of a non-tumorigenic cell line and two cancer cell lines with different metastatic potential.

3) Cross comparison of results obtained between mouse and human species.

II. Material and Methods

II. Material and Methods

1. Cell culture and extraction

In this work, we used both human and mouse tumor and non-tumor cell lines. The use of different species is valuable as most relevant changes should be conserved across species. The mouse cell lines used were: EpH4, MC4-L5 and MC4-L2; and the human cell lines used were: MCF10A, T-47D, MDA-MB-231. The characteristics of each cell line are summarized in Table 2.

EpH4 cells are mammary epithelial, non-tumorigenic and derived from normal mouse mammary glands [72]. This cell line was used as a control to compare changes in PL profile, in MC4-L2 and MC4-L5 mouse cancer cells. All mouse cell lines are derived from Balb/c mice and express high levels of ER and PR. MC4-L2 is very migratory and metastatic, while the MC4-L5 cell line is more rounded epithelial, poorly migratory and rarely metastatic [73]. MCF10A cell line is derived from a mammary gland of a patient with cystic fibrosis and has the morphology of normal mammary epithelial cells. Thus, although these cells are not malignant, they form cysts. However, this cell line is commonly used as a non-malignant control in studies of breast cancer in the human model. T-47D is a cancer cell line of the luminal A group, with low metastatic potential. This cell line was isolated from the pleural effusion of a woman with breast ductal carcinoma. MCF10A and T-47D cells have receptors for a variety of steroids. The MDA-MB 231 cell line was derived from the mammary gland tissue of patients with metastatic breast adenocarcinoma. MDA-MB 231 belong to the triple-negative group which are very migratory and highly metastatic.

Table 2: Main features of mouse cell lines used.

	MC4-L2	MC4-L5	EpH4	MDA-MB-231	T-47D	MCF10A
Tissue of origin	Mammary adeno carcinoma (HD)	Mammary adeno carcinoma (HD)	Mid pregnant mammary gland	Mammary adeno carcinoma	Mammary adeno carcinoma	Cystic fibrosis
In vitro morphology	Spindle shape	Polygonal	Polygonal	Spindle shape	Polygonal	Epithelial or Spindle shape*
ER	+	+	+	-	+	-
PR	+	+	+	-	+	-
c-erbB2	+	ND	ND	-	+	-
E-cadherin	+	+	+	-	+	+
Tumour morphology	Biphasic carcinoma	Ductal carcinoma	Non-tumorigenic	Ductal carcinoma	Ductal carcinoma	Non-tumorigenic
Local invasion	High	Low	None	High	Low	None
Metastasis	Axiliary limph node and lungs	Axiliary limph node and lungs	None	Axiliary limph node and lungs	None	None

* When MCF10A cells are confluent, their morphology is polygonal. ND: not detected. HD: hormone dependent.

T-47D, MDA-MB-231 and all mouse cell lines were grown in phenol red Dulbecco's modified Eagle medium (DMEM/F12, Invitrogen) with 10% fetal bovine serum (FBS; Gold, PAA) and 5 mg/L gentamicin (Invitrogen). MCF10A were grown in DMEM/F12 with 5% horse serum (HS; Invitrogen), epithelial growth factor (EGF, Sigma-Aldrich) 20ng/ml, Hydrocortisone (Sigma-Aldrich) 0,5mg/ml, Cholera toxin (Sigma-Aldrich) 100ng/ml, insulin (Sigma-Aldrich) 10µg/ml and with Penicillin Streptomycin (Sigma-Aldrich).

The cells were grown at 37ºC, 5% CO_2 changing the medium of the flasks whenever necessary. When two 150 cm^2 dishes (≈4x10^7cells) of cells reached 60% density they were washed with 10 ml of phosphate buffer saline (PBS) and medium of T-47D, MDA-MB-231 and all mouse cell lines was changed to DMEM without phenol red and high

glucose (PAA), without FBS and with 5µg/ml insulin (Sigma-Aldrich) for 24h. MCF10A were changed to their growth medium but without FBS. Cells were grown in medium without serum to be sure that no compounds from serum interfere in the lipid analysis. Three different cultures for each cell type were analyzed in order to verify the reproducibility of the results.

After 24h, the process of cell extraction started by the removal of the medium and washing of the dishes with 10 ml of PBS, twice. To detach the cells, 5 – 6ml of trypsin (Invitrogen) were added and left for ± 3 min at 37ºC. After verifying that all the cells were detached, cells were removed and placed in a 50 ml falcon tube to which the same volume of PBS (10-12 ml) was added. The dishes were washed with 10 ml of PBS to recover some cells that were still in the dishes.

After mixing, the cell suspension very well, 100 µl were separated to an eppendorf, to count the amount of cells, and 1 ml to another eppendorf to make a whole cell extract and quantify the amount of proteins. The rest of the suspension was centrifuged 10 min at 2000 rpm (Mixtasel centrifuge, Selecta). The supernatant was discarded and the pellet ressuspended in 1 ml of PBS, passing to an eppendorf, followed by centrifugation at 2000 rpm, 4min (Minispin plus, Eppendorf). This step was repeated three times. The final pellet was ressuspended in 1 ml of mili-Q H_2O (Millipore).

In order to confirm that lipid content per cell was similar in the different types of cells, tripsinized cells were counted in a Neubauer chamber before the lipid extraction.

2. Lipid extraction

Total lipids from all cell lines were extracted with the Bligh and Dyer method [53]. We used HPLC solvents (chloroform and methanol) and milli-Q purified water. For 1 ml of sample, 3,75 ml chloroform /methanol 1:2 (v/v) was added, vortexed well, and incubated on ice for 30 min. Then, and additional volume of 1,25 ml chloroform was added and finally 1,25 ml mili-Q H_2O. Following vigorous vortex, samples were centrifuged at 1000

rpm for 5 min at room temperature to obtain a two-phase system: aqueous top phase and organic bottom phase with chloroform from which lipids were obtained. The organic phase was separated into a new tube, dried in a nitrogen flow and ressuspended in 300 µl of chloroform making our extracts ready for the following analysis.

3. Thin layer chromatography

PL classes from the total lipid extract were separated by thin layer chromatography (TLC) using silica gel plates with concentrating zone 2,5x20cm (Merck). Prior to separation, plates were washed in a methanol : chloroform mixture (1:1, v/v) and left in the safety hood for 15 min. Plates were then sprinkle with boric acid (2,3% m/v) (DHB chemicals) and dried in an oven at 100ºC during 15min. It was applied in the plates 20 µl of phospholipid solution in chloroform (with a concentration of 150 µg of phospholipid per 100 µl). The plates were dried in a nitrogen flow and developed in solvent mixture with chloroform, ethanol (Panreac), water and triethylamine (Merck). The proportion between chloroform/ethanol/water/triethylamine was 30:35:7:35 (v/v/v/v). When the elution was completed, the plates were left in the safety hood until the eluent was completely dried. Lipid spots on TLC plates were observed after spraying a primuline (Sigma-Aldrich) solution of 50µg/100 ml dissolved in a mixture of acetone (Sigma-Aldrich) and mili-Q H_2O, (acetone : water 80:20, v/v), and visualized with a UV lamp (λ=254 nm).

Identification of the different classes of PLs was carried out with the use of patterns (LPC, SM, PC, PI, PS, PE, PA, CL) from Avanti Polar Lipids, Inc, run side by side in the TLC plate. Then, 5 spots from each classes were scraped off the plates to glass tubes: one spot were scraped to quantify amount of phosphorus with a phosphorus assay to calculate the percentage of each PL class in the total amount of PL in the sample, and the remaining four spots from each class were scraped to extract PL classes for subsequent identification by MS.

The extraction of lipid classes from silica to further MS analysis was carried out with a mixture of chloroform / methanol. First the samples were solubilized in 450 µl of chloroform, vortexed well and left to stand for 5 min, in order to be able to extract the phospholipids from the silica. Second, the samples were filtered by vacuum and 450 µl of chloroform/methanol (2:1, v/v) were added to the tubes, vortexed well and also filtered. Finally, the total extracted was passed in a syringe (GASTIGHT 1ml, Sigma-Aldrich) with a filter (Syring Driver Filter Unit 0,22 µm, Millipore-Millex), in order to obtain a complete free – silica extract. The filtered samples were dried under nitrogen stream and were re-suspended in 100 µl of chloroform to store at -4°C for further analysis.

For MS analysis in both positive and negative modes, samples were diluted with methanol.

4. Phospholipid quantification

In order to quantify the total amount of PL as well as amounts of each PL class separated by TLC, a phosphorus assay was performed according to Bartlett and Lewis [74]. To quantify the total PL extract, 15 µl of sample was used, and dried with a nitrogen flow, and to quantify the different classes separated by TLC, the spots were scraped off from the plates directly to the quantification tubes. Next, 6,5 ml of perchloric acid (70%) (Panreac) was added to samples which were then incubated in a heating block (Stuart) 45min at 180°C. After cooling, 3,3 ml of mili-Q H_2O, 0,5 ml of 2,5% ammonium molybdate (Riedel – de Haën) and 0,5 ml of 10% ascorbic acid (VWR BDH Prolabo) were added to all samples, vortexing always after each solution, followed by incubation for 5 min at 100°C in a water bath. Standards from 0,1 to 2 µg of phosphorous (P), made from a phosphate standard solution of dihydrogenphosphate dihydrated (NaH_2PO_4 . $2H_2O$) (Riedel – de Haën) with 100 µg/ml of P, underwent the same treatment as the samples. The absorbance of the samples, after cooling, was measured at 800 nm (Multiskan 90, Thermoscientific). In the case of TLC separated lipid classes, prior to spectrophotometric determination, samples were centrifuged 5 min at 4000 rpm to separate PLs from silica.

The amount of phosphorus present in each sample was calculated by linear regression through the graph relating the amount of phosphorus present in the patterns (X-axis) with absorbance obtained from duplicates of various concentrations (Y-axis). The amount of phospholipid was calculated by multiplying the amount of result phosphorus by 25. The percentage of each PL class was calculated by relating the amount of PL in each TLC spot to the total amount of PL in the sample, thus giving the relative PL content (%) of each PL class.

5. Protein quantification by DC assay

The amount of protein in the sample was determined by the DC *protein assay* (BioRad). Protein concentration was used to normalize the data and compare the amount of lipids and proteins per cell. The 1ml of sample separated in the cell extraction was centrifuged 2 min at 10 000 rpm. The supernatant was discarded and the pellet ressuspended in 50 µl of PBS-TDS (PBS with SDS 0,1%, Triton X-100 1% and Na Deoxy cholate 0,5%). The sample was again centrifuged 2 min at 10 000 rpm and the supernatant was recovered to a new eppendorf. Twenty µl of S reagent from the BioRad kit was added to 1 ml of A reagent to make A´ reagent. Then, 10 µl of sample was separated to a new eppendorf 50 µl of A´reagent and 400 µl of B reagent was added. Standard solutions of bovine serum albumin (BSA) between 0,3 to 5 mg/ml were treated in the same way as the samples. At last, the absorbance of all the samples was measured at 750 nm.

6. Electrospray mass spectrometry conditions

Analysis of PLs, classes and total extract, was carried out by mass spectrometry using ESI ionization and three distinct mass spectrometers: linear ion trap

(ThermoFinnigan, San Jose, CA, USA), triple quadrupole (QqQ, Walters, Manchester, UK) and Q-ToF 2 (Micromass, Manchester, UK).

ESI conditions in electrospray linear ion trap mass spectrometer were as follows: electrospray voltage was 4.7 kV in negative mode and 5 kV in positive mode; capillary temperature was 275ºC and the sheath gas flow was 25 U. An isolation width of 0.5 Da was used with a 30 ms activation time for MS/MS experiments. Full scan MS spectra and MS/MS spectra were acquired with a 50 ms and 200 ms maximum ionization time, respectively. Normalized collision energy TM (CE) was varied between 17 and 20 (arbitrary units) for MS/MS. Data acquisition of this mass spectrometer was carried out with an Xcalibur data system (V2.0).

ESI conditions in electrospray triple quadrupole mass spectrometry were as follows: electrospray voltage was 3.5 kV in positive mode; capillary temperature was 300ºC and the sheath gas flow was 32 U. Full scan MS, neutral loss and parent scan spectra were acquired between a 50 ms and 200 ms maximum ionization time. Normalized collision energy TM (CE) was varied between 20 and 30V for MS/MS. Data acquisition was carried out with a Mass Lynx data system (V4.0).

ESI conditions in electrospray Q-Tof mass spectrometer were as follows: electrospray voltage was 3 kV in the positive mode with a cone voltage of 30V. The temperature of the source was 80ºC and the solvation was 150ºC. MS/MS spectra were performed using argon as collision gas, with energy between 20 - 35 V. Data acquisition was carried out with a Mass Lynx data system (V4.0).

III. Results and Discussion

III. Results and Discussion

In this work three different types of cells from two different animal species (three from mouse and three from human) were used. First we used mouse mammary epithelial cells, using non tumorigenic cells (EpH4) as control, and two cells from a mouse mammary adenocarcinoma with different degrees of malignancy (less metastatic MC4-L5 cells and more metastatic MC4-L2 cells). In a second stage, we used human mammary epithelial cells, MCF10A as control non tumorigenic cells, and two types of breast cancer cells, T-47D (no metastatic) and MDA-MB-231 (very metastatic).

Using these different cells with distinct metastatic potentials we were able to evaluate possible modifications in the lipidome that appear in the cell during cancer progress. In addiction the comparison between human and mouse cells is useful in one hand to identify how far it is possible to use another animal model to obtain the same results. On the other hand, if the same pattern were found in the group of cells from the two species, then we can infer that the differences between metastatic and non-metastatic cells or between cancer and control cells are likely to be conserved among species. This will make these results more important and more likely to represent, at least in part, the human pathology.

In this chapter, the lipid profile of control and breast cancer cell lines will be characterized using mass spectrometry (MS) with electrospray ionization, and a lipidomic approach. Inside this methodology, two complementary strategies were used: a) after separation of PL by TLC, each class content was analyzed by quantification of PL content with phosphorus assay and b) after TLC separation analysis of each class by MS was carried out. Results and discussion are presented in the following three chapters:

1. Phospholipid profiling of mouse mammary epithelial and breast cancer cell lines
2. Phospholipid profiling of human mammary epithelial and breast cancer cell lines
3. Cross comparison between results of mouse and human species

1. Phospholipid profiling of mouse mammary epithelial cell lines

In order to evaluate the possible alterations in PL profile as cell progress in breast cancer, PL content and profile of lipid extracts was obtained from non-tumorigenic EpH4 mammary epithelial cells, MC4-L5 epithelial low-metastatic and MC4-L2 spindle-shaped, metastatic mammary cancer cell lines. For this purpose, PL classes were separated by TLC and analyzed by MS and MS/MS using ESI ionization and quantified by phosphorus assay.

To know the approximate amount of PLs and proteins per cell we counted the number of cells and quantified the lipid and protein content in each extract (Table 3).

Table 3: Amount of PLs and proteins per cell in µg in all three types of cells

	PLs per cell (µg)	**Proteins per cell (µg)**
EpH4	2,79E-05 ± 3,63E-06	7,39E-04 ± 2,27E-04
MC4-L5	5,99E-06 ± 3,68E-06	2,67E-04 ± 2,93E-05
MC4-L2	2,62E-05 ± 1,43E-05	3,32E-04 ± 6,95E-05

Phospholipid class separation by TLC and quantification

Separation of PL classes was accomplished by TLC which allowed the fractionation of the PL content into the major classes namely LPC, SM, PC, PI, PS and PE (Figure 9).

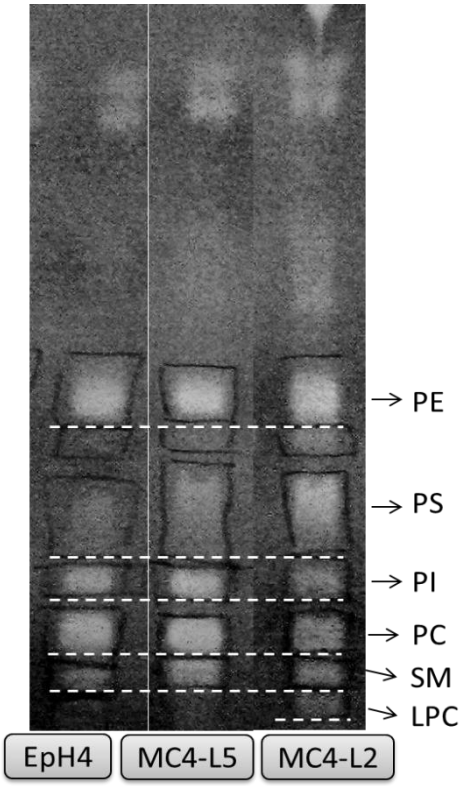

Figure 9: Separation of PL major classes (LPC, SM, PC, PI, PS and PE) by thin layer chromatography in the three mouse epithelial cell lines

Synthesis of PL classes occurs from PA and DAG through different pathways (Figure 10).

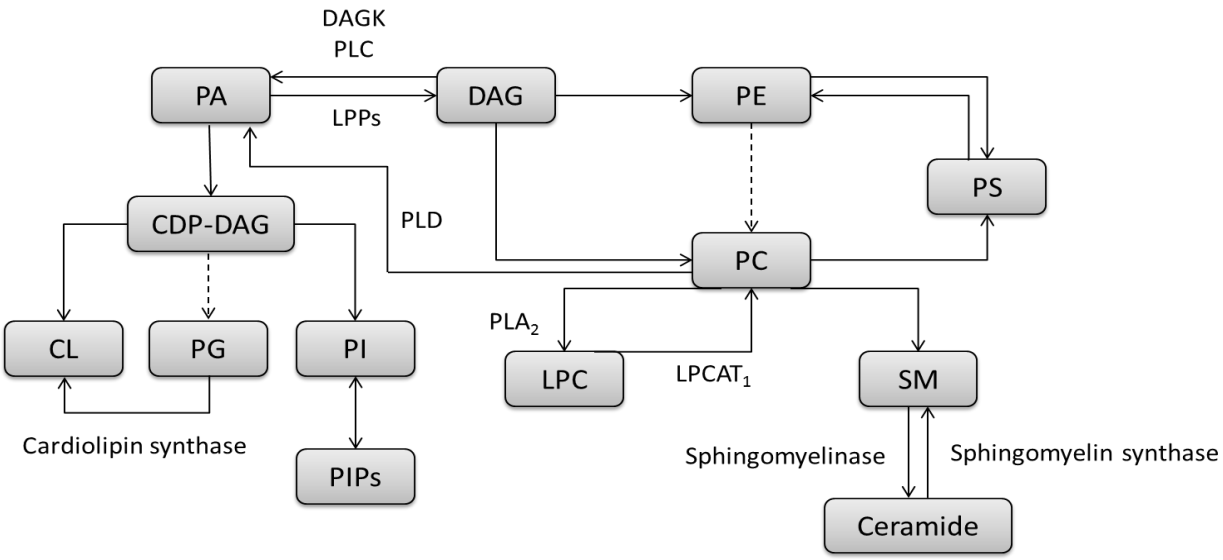

Figure 10: Main cellular phospholipid synthesis routes. Note: broken arrows indicate more than one step. DAGK: diacylglycerol kinase, PLC: phospholipase C, LPPs: phosphate phosphohydrolases, PLD: phospholipase D, PLA_2: phospholipase A2, $LPCAT_1$: lysophosphatidylcholine acyltrasferase 1

Relative PL content (%) of each PL class in the total lipid extract was evaluated by quantifying the amount of PL in each spot using the phosphorus assay, as shown in Figure 11.

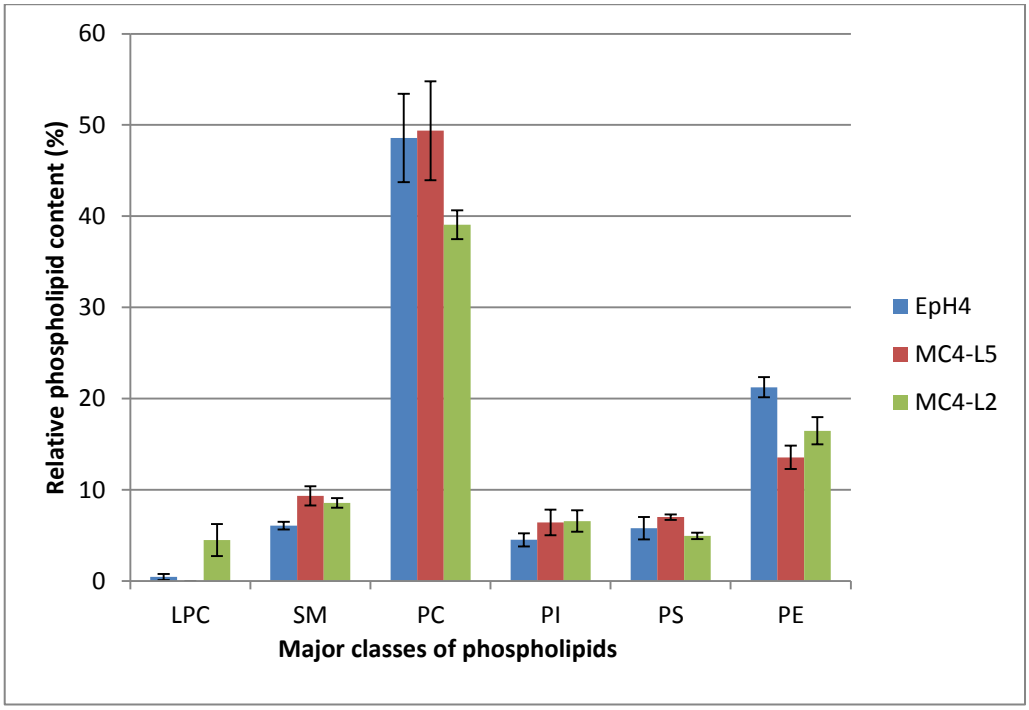

Figure 11: Relative phospholipid (PL) content (%) in PL classes separated by thin layer chromatography in mouse non – tumorigenic and cancer cell lines. PL content in each spot was related to total phosphate content in the sample. Mean +/- SD from three independent experiments is shown

The most abundant PL class in all cell lines was PC, followed by PE. Major differences were found in the LPC content which was nearly undetectable in EpH4 cells, absent in MC4-L5 cells, but dramatically increased in the metastatic MC4-L2 cells. On the other hand, decrease in PCs was detected in MC4-L2 cells as compared to the two polygonal EpH4 and MC4-L5 cells. Increased PCs levels have been reported in malignant cells with low level of progression [75], while PCs decrease was reported in metastatic breast cancer cells. These observations are in agreement with our results. MC4-L5 and MC4-L2 cancer cells showed slightly higher levels of SM and lower levels of PE as compared to EpH4 mammary epithelial cells. Interestingly, PI known to be actively

involved in growth and cell migration [27] only increased slightly in cancer vs non tumorigenic cells, while PS did not substantially change.

To evaluate if in addition to differences in percentages of each PL class considering the total extract, it was possible to see differences in molecular composition among each PLs classes, lipid extract from each PL class spot was analyzed by MS and MS/MS and class members were identified. PI and PS classes were analyzed in the negative mode, presented in Table 4 with the indication of the *m/z* values of the ions $[M-H]^-$.

Table 4: Identification of $[M-H]^-$ ions observed in the MS spectra of PI and PS.

	Diacyl			
	$[M-H]^-$	**C:N**	**Fatty acids**	
PI	835	34:01	16:00	18:01
	835	34:01	16:01	18:00
	837	34:00	16:00	18:00
	861	36:02	18:02	18:00
	861	36:02	18:01	18:01
	863	36:01	18:00	18:01
	865	36:00	18:00	18:00
	885	38:04	20:04	18:00
	887	38:03	20:03	18:00
	889	38:02	20:02	18:00
PS	760	34:01	16:00	18:01
	760	34:01	16:01	18:00
	788	36:01	18:00	18:01
	790	36:00	18:00	18:00
	812	38:03	20:00	18:03
	812	38:03	20:03	18:00
	814	38:02	20:02	18:00
	836	40:05	18:00	22:05
	872	42:01	22:00	20:01

The attribution of the fatty acyl composition of each PL molecular species was done accordingly to the interpretation of the correspondent MS/MS spectra. C:N: number of carbons in the fatty acid chain : number of double bonds; fatty acids (#:#): the first value indicates # of carbons in the fatty acid chain and the second value, the # of double bonds in that chain; PI: phosphatidylinositol; PS: phosphatidylserine

PC, SM, LPC and PE classes were analyzed in the positive mode and molecular species identified are presented in Table 5 with the indication of the *m/z* values of the ions $[M+H]^+$.

Table 5: Identification of $[M+H]^+$ ions observed in the MS spectra of LPC, PC, SM and PE.

	Diacyl			Akylacyl			
	$[M+H]^+$	**C:N**	**Fatty acids**	**$[M+H]^+$**	**C:N**	**Fatty acids**	
LPC	496	16:00	16:00	482	16:00	O-16:00	
	522	18:01	18:01	508	18:01	O-18:01	
	524	18:00	18:00	510	18:00	O-18:00	
PC	706	30:00	14:00	16:00	692	30:00	O-14:00	16:00
	732	32:01	14:00	18:01	718	32:01	O-14:00	18:01
	732	32:01	16:00	16:01	744	34:02	O-16:00	18:02
	758	34:02	16:01	18:01	746	34:01	O-16:00	18:01
	760	34:01	16:00	18:01	772	36:02	O-16:00	20:02
	762	34:00	16:00	18:00	774	36:01	O-16:00	20:01
	786	36:02	18:01	18:01				
	788	36:01	18:00	18:01				
	790	36:00	18:00	18:00				
	812	38:03	20:01	18:02				
	814	38:02	20:01	18:01				
	842	40:02	22:01	18:01				
SM	703	34:01	18:01	16:00				
	705	34:00	18:00	16:00				
	787	40:01	18:01	22:00				
	813	42:02	18:01	24:01				
	815	42:01	18:01	24:00				

PE	690	32:01	14:00	18:01	702	34:02	O-16:01	18:01
	690	32:01	16:00	16:01	704	34:01	O-16:00	18:01
	716	34:02	16:01	18:01	728	36:03	O-18:02	18:01
	718	34:01	16:01	18:00	730	36:02	O-18:01	18:01
	718	34:01	16:00	18:01	732	36:01	O-18:00	18:01
	742	36:03	18:01	18:02	750	38:06	O-18:02	20:04
	744	36:02	18:01	18:01	750	38:06	O-16:01	22:05
	744	36:02	18:00	18:02	752	38:05	O-16:01	22:04
	746	36:01	18:00	18:01	752	38:05	O-18:01	20:04
	748	36:00	18:00	18:00	776	40:07	O-18:02	22:05
	768	38:04	20:04	18:00	778	40:06	O-18:01	22:05
	768	38:04	20:03	18:01				
	772	38:02	20:01	18:01				
	792	40:06	22:06	18:00				

The attribution of the fatty acyl composition of each PL molecular species was done accordingly with the interpretation of the correspondent MS/MS spectra. C:N: number of carbons in the fatty acid chain : number of double bonds; fatty acids (#:#): the first value indicates # of carbons in the fatty acid chain and the second value, the # of double bonds in that chain; PC: phosphatidylcholine; LPC: lysophosphatydilcholine; SM: sphingomyelin; PE: phosphatidylethanolamine.

In general, for the three different types of cells, we see the same molecular species in each PL class. However, in some cases the relative abundances were different and resulted in different PL profiles. Due to its very low abundance in EpH4 and MC4-L5 cells, the LPC class was only analyzed in the MC4-L2 cells. The PL profile observed for each class in each cell type is described in the following section.

Phosphatidilcholine and Lysophosphatidylcholine profile

The most abundant PLs in the cell are PCs, which are also the most important structural PL in the plasmatic membrane. PCs obtained from the three different types of cells were analysed by ESI-MS in positive mode, with formation of both $[MH]^+$ and $[MNa]^+$. In order to identify exclusively the $[MH]^+$ ions, precursor ion scanning of the ion at *m/z* 184 was obtained in a triple quadrupole, as typical approach for the detection of choline lipids [76, 77]. Precursor ion scan is possible because fragmentation of protonated

ions ($[MH]^+$) gives rise to a typical product ion at *m/z* 184, characteristic of its choline head. This approach allowed to obtain the spectra shown in Figure 12, which revealed the $[MH]^+$ ions of PCs isolated in the extract from the TLC spot.

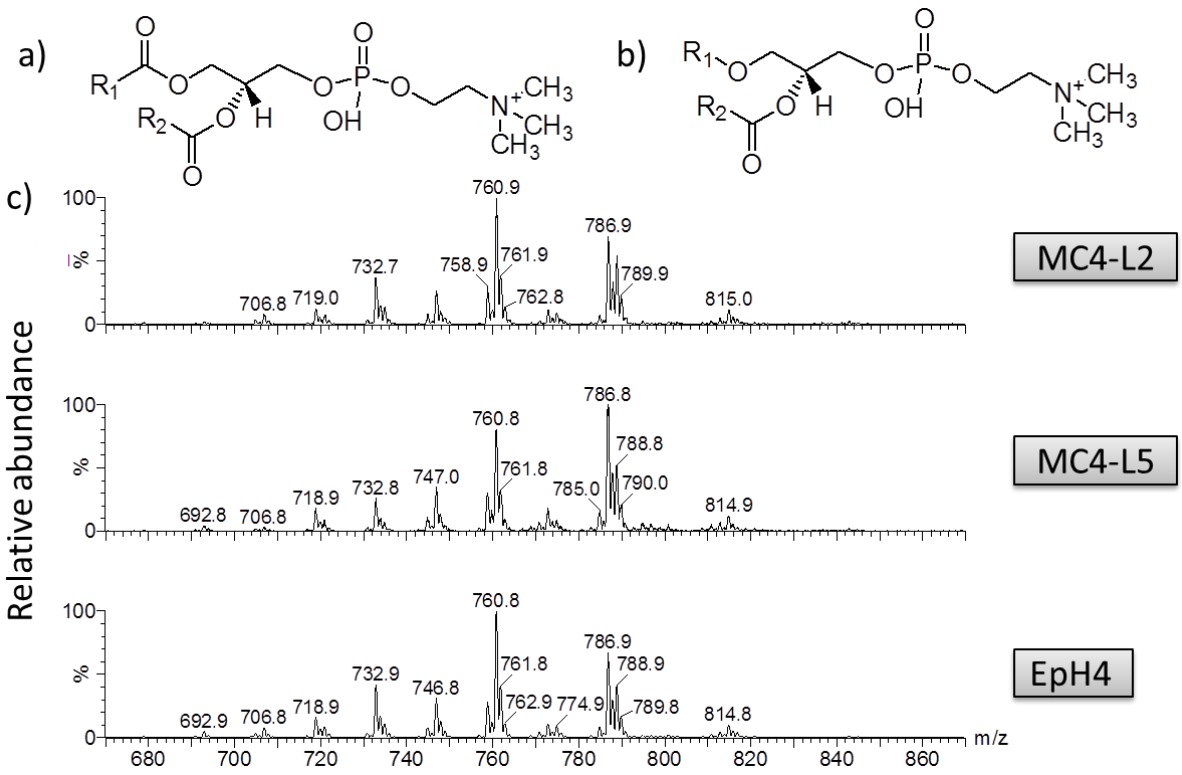

Figure 12: Phosphatidylcholine (PC) spectra. A. Diacyl PC structure; B: Alkylacyl PC structure; C. MS spectra obtained by electrospray ionization mass spectrometry analysis of PC extracted from the correspondent spots separated by thin layer chromatography. PCs were selectively detected by diagnostic precursor ion scan of the product ion at *m/z* 184 in the positive mode of obtained using an electrospray triple quadrupole. Y-axis: Relative abundance considering the highest abundant ion as 100 %; x-axis: *m/z* for each ion.

Analysis and interpretation of PCs spectra allowed identification of diacyl and acylalkyl PCs. This identification of both daicyl and acylalkyl PLs as well as their fatty acyl chain composition and location along the glycerol backbone was achieved by direct analysis and interpretation of MS/MS spectra of each ion identified in the MS spectra (Table 5). Fragmentation observed in MS/MS spectra of the $[MNa]^+$ give more product ions and thus gives more structural information, namely ion of $[MNa\text{-}59]^+$, which corresponds to the neutral loss of choline ($(CH_3)_3N$), the loss of sodiated choline polar

head group ([MNa-205]$^+$) and the ions corresponding to the loss of fatty acyls chains ([MNa-R_1COOH]$^+$ > [MNa-R_2COOH]$^+$), in diacyl PCs (Figure 13), and the loss of R_2COOH in acylalkyl PCs [77].

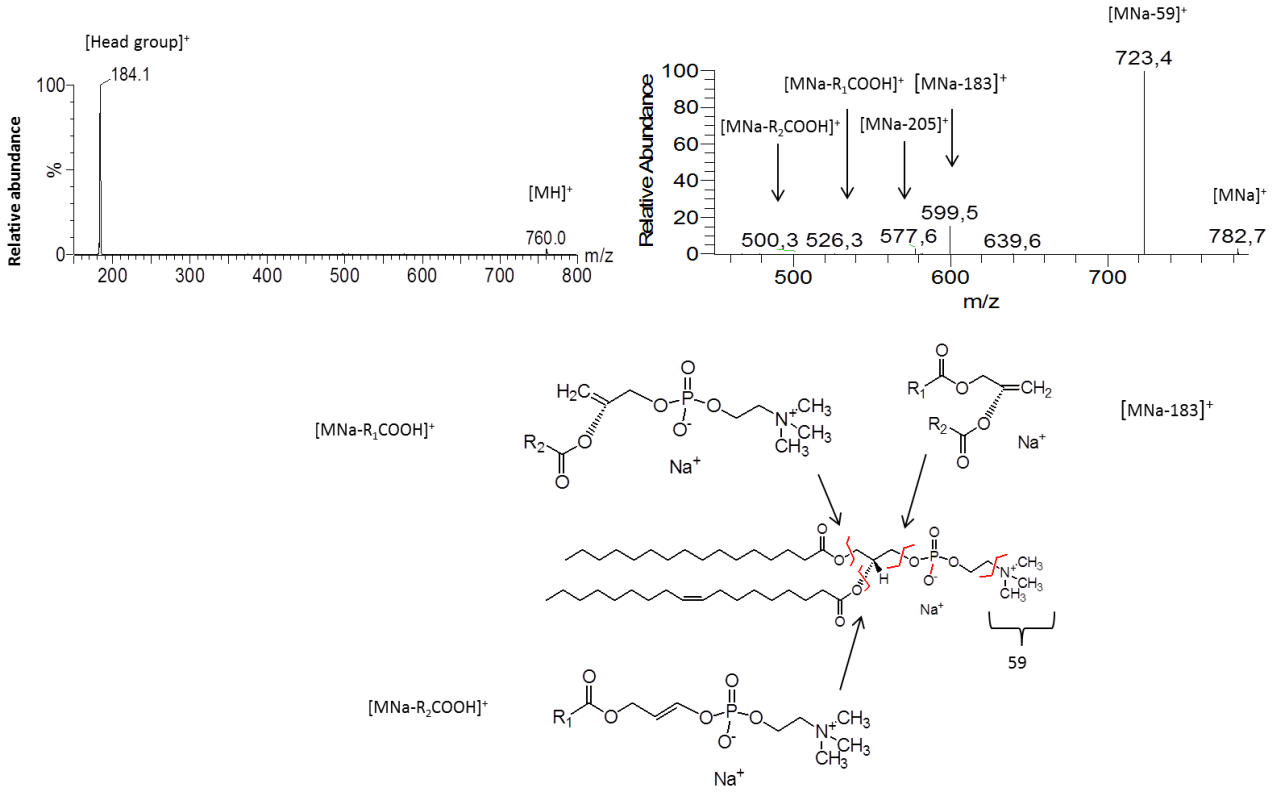

Figure 13: ESI – MS/MS spectrum of the [MH]+ at *m/z* 760 (left) and [MNa]+ at *m/z* 782 (right), corresponding to PC (16:00/18:01). Molecular structure of phosphatidylcholine (PC) is shown in presenting main cleavages correspondent to the fragmentation observed in the MS/MS spectrum of [MNa]+ ion. Fragmentation of [MH]+ ions originated the characteristic ion of *m/z* 184 corresponding to the phosphatidylcholine head group of PCs (left spectrum obtained in ESI-Q TOF), and additional ions from [MNa]+ providing more structural information (right spectrum obtained in ESI-ion trap)

The three cell types showed high relative abundance of PC (16:00/18:01) and PC (18:01/18:01) corresponding to [MH]$^+$ at *m/z* 760 and 786, respectively; followed by PC (14:00/18:01 and 16:00/16:01) and PC (O-16:00/18:01) corresponding to [MH]$^+$ at *m/z* 732 and 746 respectively (Figure 12 and Table 5). Additionally, PC (18:01/18:01) and PC (O-16:00/18:01) (*m/z* 786 and 760 respectively), although not substantially, were present in higher relative abundance in MC4-L5 cells, which did not happen in the other types of

cells (EpH4 and MC4-L2). However, there were no substantial differences between the three spectra which indicate no variations in the type of PCs found, even though there was a decrease in the percentage of PCs in MC4-L2 cells (Figure 11).

A study about the distribution of PLs in human MCF7 and T-47D breast cancer cells, compared with other primary cells (HMECs), revealed similarities in composition of diacyl PLs, including diacyl PC [78], comparable with our results. The lipid transfer protein StARD10 – a PC and PE binding protein involved in their shuttling across membranes and net transfer of these PLs between subcellular compartments – cooperates with c-erb signalling, is over-expressed in mammary tumors from Neu/ErbB2 transgenic mice [79], and its loss is significantly associated with decreased patient survival [80]. Therefore, specific PC molecular species and the total PC content in the cell may not vary [81] but the PC content in the different cellular compartments can be altered. Interestingly, this is in agreement with our results in the three spectra and the percentage of PCs in EpH4 and MC4-L5 cells. The percentage of PCs in MC4-L2 cells was lower than in the more differentiated EpH4 and MC4-L5 cells, which could be related to the increase of LPC, once the percentage of LPC in this more metastatic cells is substantially higher and PC can be a precursor of LPC by PC enzymatic hydrolysis due to the enzyme phospholipase A2 (PLA2; Figure 10).

Due to its very low abundance in EpH4 and MC4-L5 cells, the LPC class was only analyzed in the more aggressive, metastatic MC4-L2 cells. LPC class was analyzed by ESI-MS in positive mode, with formation of both $[MH]^+$ and $[MNa]^+$. Both acyl and alkyl PLs were identified (Table 5). This identification of acyl and alkyl lyso PLs as well as their fatty acyl chain composition along the glycerol backbone was achieved by direct analysis and interpretation of MS/MS spectra of each ion identified in the MS spectra. As explained in the class of PCs, this is possible because fragmentation of protonated ions ($[MH]^+$) form a typical ion of *m/z* 184, characteristic of its choline head. Fragmentation of $[MNa]^+$ give more product ions thus providing more structural information, namely ion of $[MNa\text{-}59]^+$, which correspond to the neutral loss of choline polar head ($(CH_3)_3N$), the loss of sodiated

polar head group ($[MNa-205]^+$) and the ions corresponding to the loss of fatty acyl chain ($[MNa-RCOOH]^+$) in acyl LPCs as in the class of PCs.

The most abundant LPC found is LPC (18:01) with $[MH]^+$ at *m/z* 522 and LPC (18:00) at $[MH]^+$ *m/z* 524, followed by LPC (16:00) at $[MH]^+$ *m/z* 496. The less abundant were alkyl LPC.

It was observed an increase in LPC content in MC4-L2 cells, which may be the result of higher PC enzymatic hydrolysis due to PLA2 influence, which correlated to the decrease in PC content observed in this type of cells. This alteration could be related to the metastatic phenotype as it was shown that the levels of PC were increased in malignant cells with low level of progression, and decreased in breast cancer cells with high level of progression [75]. Activation of cytosolic PLA2 is responsible for the hydrolysis of the sn-2 ester bond of PC to yield free LPC and fatty acid, predominantly arachidonic acid [82]. The activity and expression of several PLA2 isoforms are increased in several human cancers [83]. In addition, many of LPC functions are thought to be due to the actions of autotaxin (ATX) and LPA production. ATX promotes metastasis as well as cell growth, survival, and migration of cancer cells. These actions could depend on the catalytic activity of ATX, which converts LPC into LPA in the extracellular fluid surrounding the tumor [84]. In breast cancer cells, ATX is associated with invasiveness [85] and higher plasma LPA levels are present in patients with ovarian cancer and other gynecologic malignancies, like breast cancer, compared with healthy controls [86]. Elevated levels of LPC in the plasma of patients with ovarian cancer were also described [87].

Sphingomyelin profile

SM is synthesized from ceramide by SM synthases [88] (Figure 10) and are also precursors of ceramide; SM can serve as a substitute for phosphatidylcholine as a building block of membranes and, when in specific domains like membranes “rafts”, can coordinate various signaling pathways. SMs extracted from TLC spots were analyzed by ESI-MS in positive mode, with formation of both $[MH]^+$ and $[MNa]^+$. In order to identify

exclusively the $[MH]^+$ ions, precursor ion scan of the ion at *m/z* 184 was obtained in the triple quadrupole, as explained for PC class [65, 76]. This approach allowed to obtain the spectra, which revealed the $[MH]^+$ ions of SMs present in the TLC spot (Figure 14).

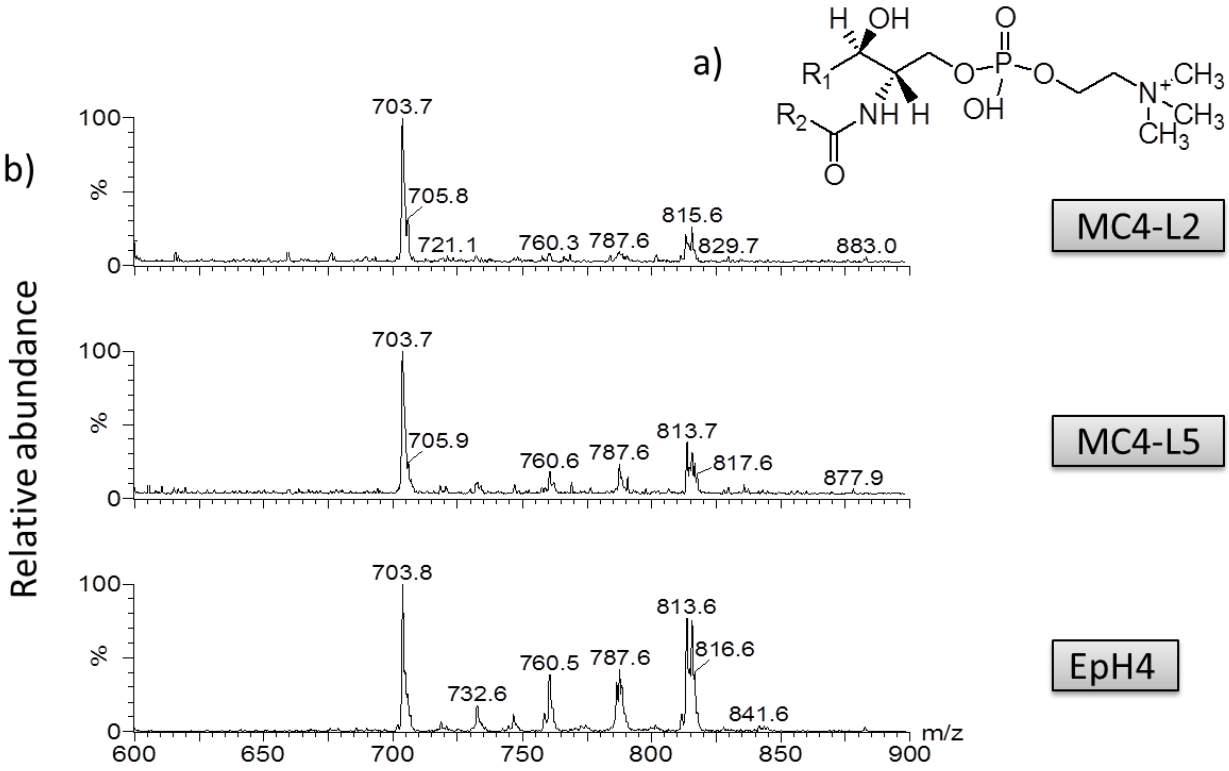

Figure 14: Sphingomyelin (SM) spectra. A. Diacyl SM structure; B: MS spectra obtained by electrospray ionization mass spectrometry analysis of SM extracted from the correspondent spots separated by thin layer chromatography. SMs were selectively detected by diagnostic precursor ion scan of the product ion at *m/z* 184 in the positive mode obtained using an electrospray triple quadrupole. Y-axis: Relative abundance considering the highest abundant ion as 100 %; x-axis: *m/z* for each ion.

Analysis of SMs species allowed to identify diacyl PLs as summarized in Table 5. This identification of diacyl PLs, as well as their fatty acyl chain composition, was achieved by direct analysis and interpretation of MS/MS spectra of each ion identified in the MS spectra. As in PCs, fragmentation of $[MNa]^+$ ions gave more product ions thus providing additional structural information, inclusive the ions corresponding to the loss of fatty acyl chain with water ($[MNa\text{-}R_2CO\text{-}H_2O]^+$) (Figure 15).

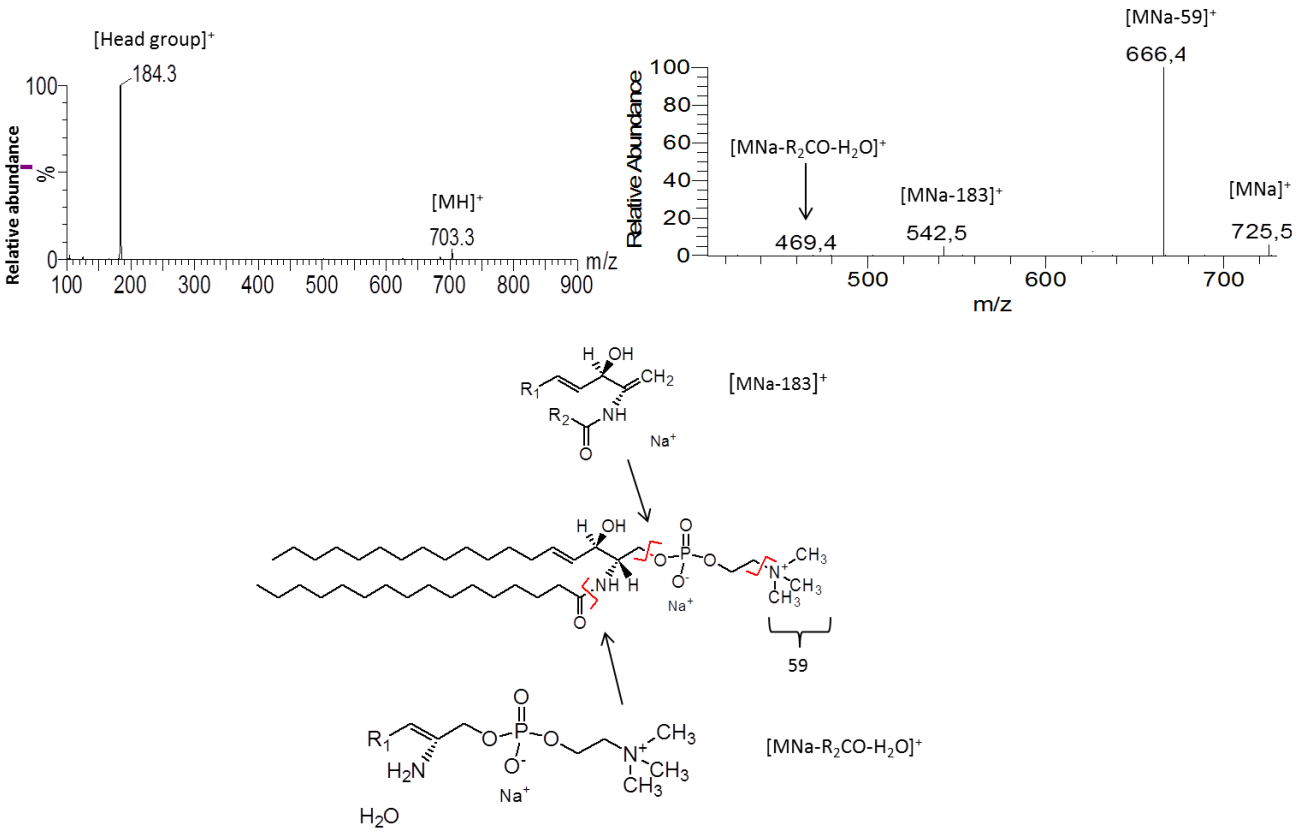

Figure 15: ESI – MS/MS spectrum of the $[MH]^+$ at *m/z* 703 (left) and $[MNa]^+$ at *m/z* 725 (right), corresponding to SM (18:01/16:00). Molecular structure of Sphingomyelin (SM) is shown below and present main cleavages correspondent to the fragmentation pathways observed in the MS/MS spectrum of $[MNa]^+$ ion. Fragmentation of $[MH]^+$ ions originated the characteristic ion at *m/z* 184 corresponding to the choline head of SMs (left spectrum obtained in ESI-Q TOF). Fragmentation of $[MNa]^+$ ions gave more product ions thus providing additional structural information (right spectrum obtained in ESI-ion trap), inclusive the ions corresponding to the loss of fatty acyl chain with water ($[MNa\text{-}R_2CO\text{-}H_2O]^+$)

As it is observed in the Figure 14, the major SM found was SM (18:01/16:00) corresponding to $[MH]^+$ at *m/z* ion of 703, followed by SM (18:01/24:01) $[MH]^+$at *m/z* 813 and SM (18:01/24:00) of $[MH]^+$ at *m/z* 815. SM (18:00/16:00) and SM (18:01/22:00) corresponding to the $[MH]^+$ at *m/z* 705 and 787, respectively, appeared with less relative abundance.

Some differences in the sphingomyelin profile appear evident, comparing tumor cells with control cells. The relative amount of SM (18:01/24:01), SM (18:01/24:00) and SM (18:01/22:00) (*m/z* 813, 815 and 787, respectively) compared to SM (18:01/16:00) (*m/z* 703) was inversely correlated to cells aggressiveness (i.e. higher in EpH4>MC4-L5>MC4-L2). Curiously, the total percentage of SM increased in both tumor cells,

comparing to our control cells, which can suggest an increase of SM (18:01/16:00) and SM (18:00/16:00).

SM is synthesized from ceramide, an important lipid with roles in apoptosis and cell growth through the action of SM synthases [88]. Interestingly, recent data showed that the levels of C16-ceramide are significantly high in different types of tumors, compared to other healthy tissue [89]. These results are in agreement with high levels of SM (18:01/16:00) and SM (18:00/16:00) (*m/z* 703 and 705, respectively) observed in MC4-L5 and MC4-L2 cancer cells.

In the context of tumor growth, higher SM content maybe important for cell survival as SM containing vesicles have been shown to have angiogenic activity [90]. SM is important for maintenance of membrane bilayer structure, macrodomain formation and signaling, which are altered in breast cancer [91]. An example of specialized domains rich in SM are lipid rafts, which, when enriched with ceramide generally promotes apoptosis, but when enriched in cholesterol, they are involved in normal cell signaling. This lipid raft with cholesterol, when deregulated promotes cell transformation and tumor progression, and it is known to be higher in cancer cells [91]. Due to this alteration in cancer cells, the lipid rafts enriched in ceramide would be lower and the ceramide could generate SM, increasing the levels of SM in the cell.

Phosphatidilethanolamine profile

Ethanolamine phospholipids are the key membrane fluidizing phospholipids. Due to its cone-shaped form, PE is a typical non-bilayer preferring lipid, which may regulate the fluidity of membranes and modify the Ca^{+2} transport process [75]. PE was analyzed by ESI-MS in positive mode, with formation of $[M+H]^+$, and confirmation by neutral loss scan (neutral loss of polar head, -141 Da) was obtained in the triple quadrupole, as typical approach for PEs [76, 77]. This is possible because fragmentation of protonated ions ($[M+H]^+$) originates a typical ion formed due to the loss of 141 Da, characteristic from its

ethanolamine head. This approach permitted to obtain the spectra, which revealed the $[M+H]^+$ ions of PEs present in the extracts obtained from the PE TLC spot (Figure 16).

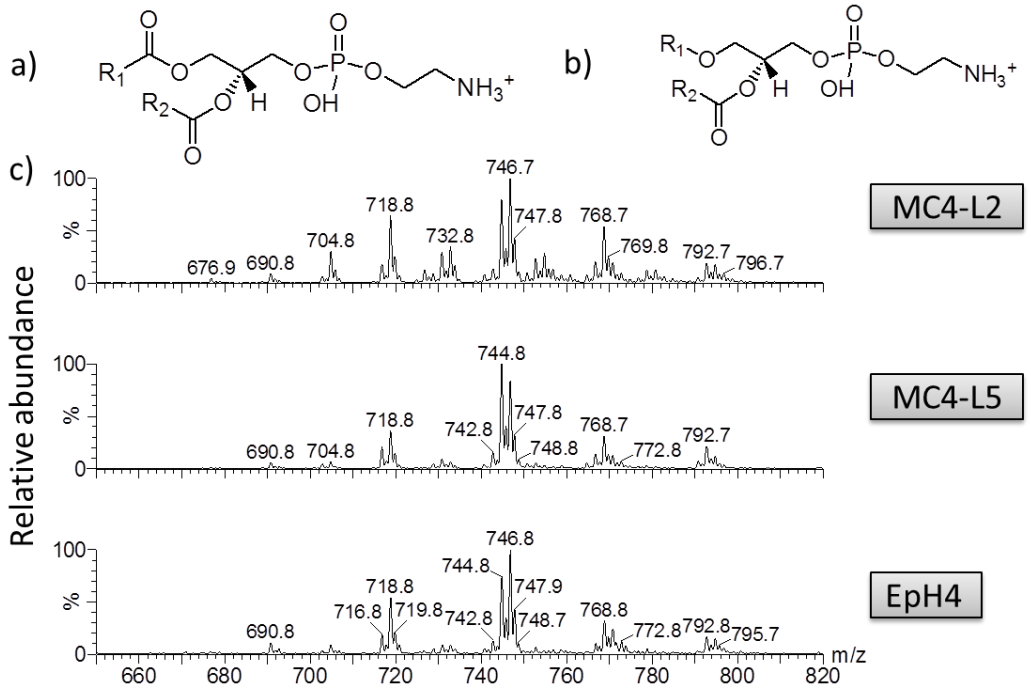

Figure 16: Phosphatidylethanolamine (PE) spectra. A. Diacyl PE structure; B: Alkylacyl PE structure; C. MS spectra obtained by electrospray ionization mass spectrometry analysis of PE extracted from the correspondent spots separated by thin layer chromatography. PEs were selectively detected by diagnostic neutral loss scan correspondent to the neutral loss of PE polar head (neutral loss of 141 Da) in the positive mode obtained using an electrospray triple quadrupole. Y-axis: Relative abundance considering the highest abundant ion as 100 %; x-axis: *m/z* for each ion.

Analysis of PEs species allowed to identify both diacyl and acylalkyl PLs as resumed in Table 5. This analysis of both diacyl and acylalkyl PLs was achieved by direct analysis and interpretation of MS/MS spectra of each ion identified in the MS spectra, as explained before. Fragmentation observed in MS/MS spectra of the $[MNa]^+$ give more product ions and thus more structural information. Since the analysis of a MS/MS spectrum cannot discriminate between an alkenylacyl from an alkylacyl, it was considered always to be alkylacyl PEs. Fragmentation of $[M+Na]^+$ showed loss of fatty acyl chains ($[M+Na\text{-}R_1COOH]^+ > [M+Na\text{-}R_2COOH]^+$), in diacyl PEs, and the lost of $[M+Na\text{-}R_2COOH]^+$ in acylalkyl PEs. Also, the relative abundance of the ion $[M+Na\text{-}R_2COOH]^+$ was higher than [M+Na-

$R_1COOH]^+$ in this class and allowed the identification of both the fatty acyl composition and its location along the glycerol backbone (Figure 17).

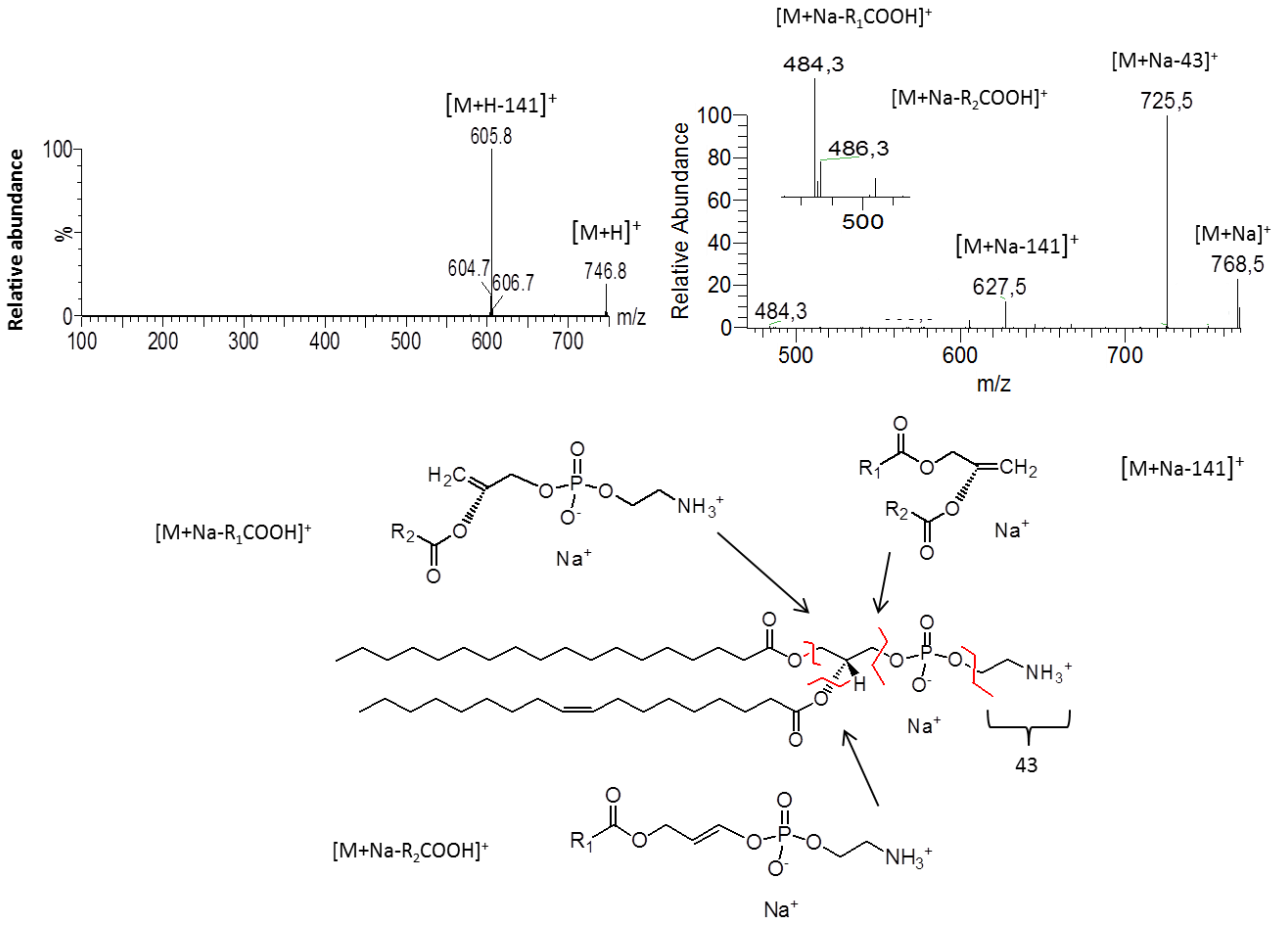

Figure 17: ESI – MS/MS spectrum of the $[M+H]^+$ at *m/z* 746 (left) and $[M+Na]^+$ at *m/z* 768 (right), corresponding to PE (18:00/18:01). Molecular structure of phosphatidylethanolamine (PE) is shown below presenting main cleavages correspondent to the fragmentation observed in the MS/MS spectrum of $[M+Na]^+$ ion. Fragmentation of $[M+H]^+$ form a typical ion due to neutral loss of 141 Da, characteristic from its phosphatidylethanolamine head group (left spectrum obtained in ESI-QTOF). Fragmentation of $[M+Na]^+$ ions gave more product ions thus providing additional structural information (right spectrum obtained in ESI-ion trap)

In all cell types, the most abundant PEs molecular species observed were PE (18:01/18:01 and 18:00/18:02) and PE (18:00/18:01), corresponding to *m/z* values of 744 and 746 (Figure 16).

However, differences were particularly evident in the spectrum of MC4-L2 compared to the other two types of cells (MC4-L5 and EpH4), indicating that this class of PLs are modified in the more aggressive cells. The most evident alteration occurred in PE (O-18:00/18:01) corresponding to *m/z* value 732 and PE (20:04/18:00 and 20:03/18:01), corresponding to *m/z* value 768, as both ions showed higher relative abundance in the MS spectra of MC4-L2 cells, compared to the other two types of cells.

PE content is significantly elevated in malignant tumors compared to benign tumors and to non involved breast tissue [67], and altered in different meningiomas [92]. Further, malignant breast tumors appear to be particularly rich in PEs [66]. At first impression, these results are in clear contrast with our findings where in EpH4 mammary epithelial cells, relative PEs amount was higher than in both cancer cells. However, differences may be explained by the source of material used (tissue vs cell culture) and the absolute values obtained by ^{32}P-NMR while in our case PE content was calculated relative to all PL levels. Alternatively, certain molecular species of PEs (O-18:00/18:01, 20:03/18:01 and 20:04/18:00) were observed with higher relative abundance in the highly metastatic MC4-L2 cells.

Higher PE levels have also been reported in hormone resistant, highly metastatic cell lines such as MDA-MB 231 [75]. In our spectra, it can also be confirmed that the PE profile is more altered in metastatic MC4-L2 cells compared to the control and not metastatic cells, EpH4 and MC4-L5, respectively.

Low levels of alkylacyl PE in ER+ breast cancer lines with low metastatic potential versus normal breast epithelium have been reported [75]. This study is in agreement with our results where higher levels of PE (O-18:00/18:01), PE (O-16:00/18:01) and PE (O-16:00/22:05) were found in the more aggressive MC4-L2 cells, compared to mammary epithelial or cancer cells with low metastatic potential were observed.

Phosphatidylserine profile

PS is a negatively charged phospholipid that constitutes approximately 2–10% of total cellular lipid [93]. PS is normally localized in membrane leaflets that face the cytosol. However, certain conditions can cause translocation of PS to the outer leaflet of the plasma membrane where it may initiate and participate in cellular processes such as blood coagulation [94] and apoptosis [66, 95].

PSs were analyzed by ESI-MS in negative mode, with formation of $[M-H]^-$. This approach permitted to obtain the spectra, which revealed all $[M-H]^-$ ions of the PSs present in the extract obtained from TLC spot (Figure 18). The MS spectra of the PS for the three cell lines were similar.

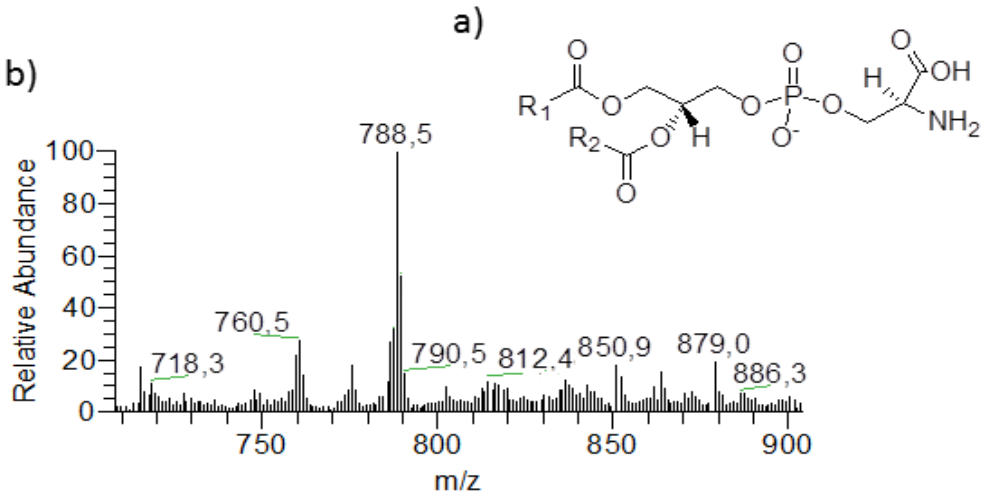

Figure 18: A. Diacyl PS structure; B. MS spectrum obtained by electrospray ionization mass spectrometry analysis of PS extracted from the correspondent spots separated by thin layer chromatography of EpH4 mammary epithelial cells. The MS spectra of the other cell lines were identical. The PS spot was extracted and acquired in the negative mode obtained using an electrospray ion trap. Y-axis: Relative abundance considering the highest abundant ion as 100 %; x-axis: *m/z* for each ion.

Interpretation of MS/MS spectra of each ion identified in the MS spectra allowed identification of diacyl PSs as well as their fatty acyl chain composition and location along

the glycerol backbone (Table 4). This is possible because fragmentation of deprotonated ions ($[M-H]^-$) lead to the formation of a typical ion from the loss of 87 Da ($[M-H-87]^-$), characteristic from its serine polar head, and the ions corresponding to the fatty acyls as carboxylate anions chains ($[R_2COO]^-$ > $[R_1COO]^-$) [77] as shown in Figure 19.

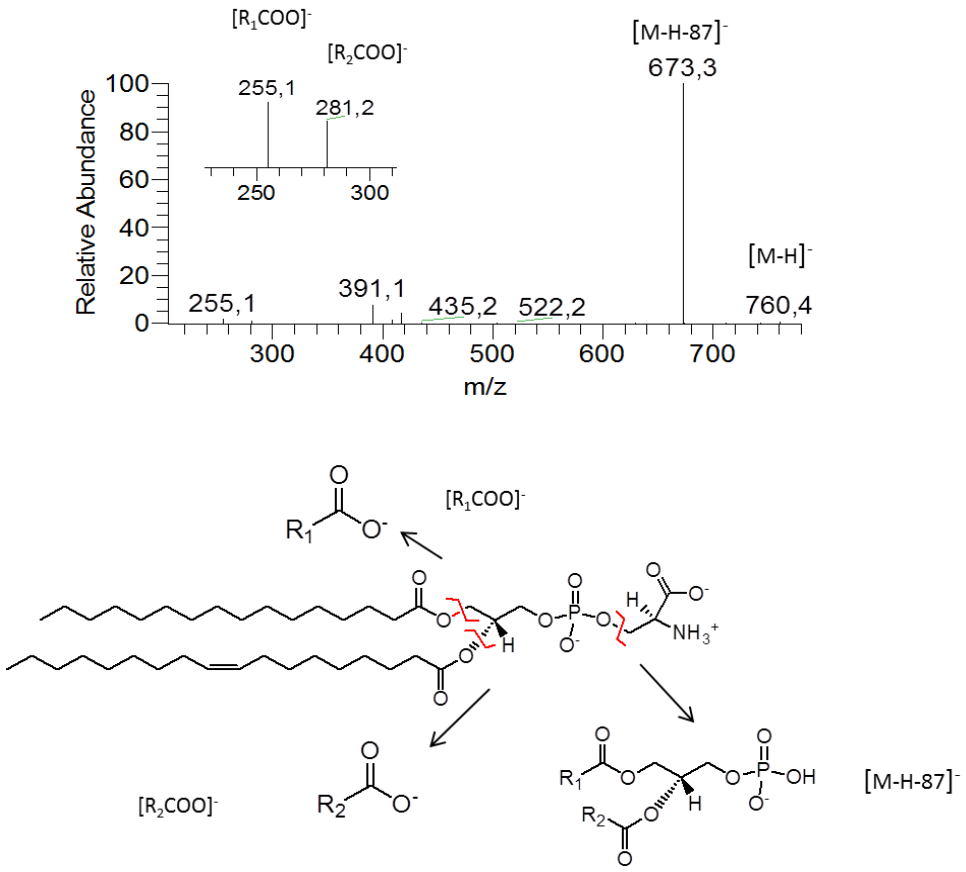

Figure 19: ESI – MS/MS spectrum of the $[M-H]^-$ at *m/z* 760, corresponding to PS (16:00/18:01). Molecular structure of phosphatidylserine (PS; below) presenting main cleavages correspondent to the fragmentation observed in the MS/MS spectrum of $[M-H]^-$ ion obtained in ESI-ion trap. Fragmentation of $[M-H]^-$ gave the typical neutral loss of 87 ($[M-H-87]^-$), characteristic of its serine polar head, and ions corresponding to the fatty acyls chains carboxylate anions ($[R_2COO]^-$ and $[R_1COO]^-$).

The three cell types showed similar ESI-MS spectra in terms of molecular species and their relative abundance (Figure 18, only spectrum from EpH4 cells). The most abundant PS, observed and identified, was the PS (18:00/18:01), corresponding to the ion

$[M-H]^-$ at *m/z* of 788. The rest of PSs found have almost the same relative abundance and also showed similar relative abundance in all cell lines.

In addition to a structural function, PS is involved in signaling pathways such as protein kinase C pathways [96] and in localization of intracellular proteins to the cytosolic membrane leaflets [97]. These PS functions make this PL important in the cell and its distribution in cancer is altered [98], but the total amount seems to remain identical in cell lines [75] and tumor tissue [67]; which confirm our results where no differences in PS relative amounts or molecular species were observed.

Phosphatidylinositol profile

PIs mediate communication between cell surface receptors and intracellular organelles. This is possible by PIs single or combinatorial phosphorylation of the 3, 4 and 5 positions on the inositol ring of PI which can generate at least seven unique PIPs, with diverse roles in receptor-mediated signal transduction, cytoskeletal remodeling, nuclear events and membrane trafficking [27].

PIs were analyzed by ESI-MS in negative mode, with formation of $[M-H]^-$. This approach permitted to obtain the spectra shown in Figure 20, which revealed the PI $[M-H]^-$ ions present in the lipid extract obtained from the TLC spot.

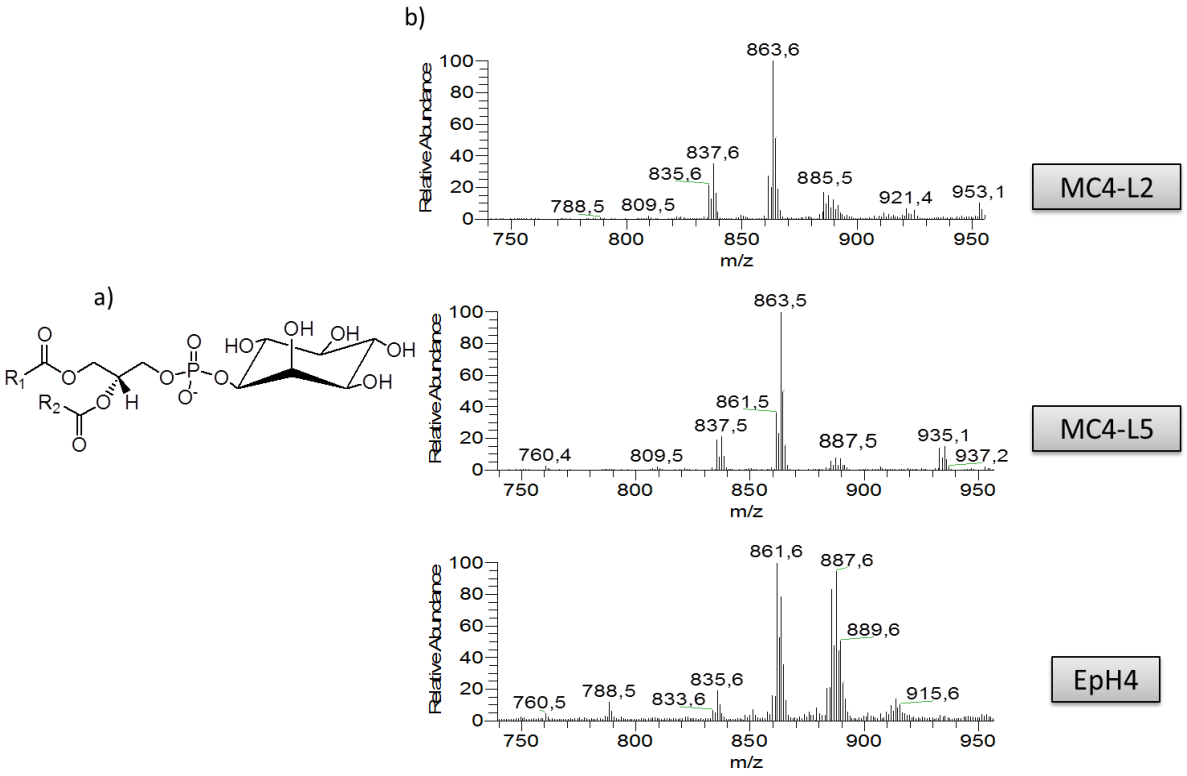

Figure 20: A. Diacyl PI structure; B. MS spectra obtained by electrospray ionization mass spectrometry analysis of PI extracted from the correspondent spots separated by thin layer chromatography. The PE spot was extracted and MS spectra were acquired in the negative mode obtained using an electrospray ion trap. Y-axis: Relative abundance considering the highest abundant ion as 100 %; x-axis: *m/z* for each ion.

Analysis of PIs species allowed to identify diacyl PIs as shown in Table 4. Similar to PS, this analysis was achieved by direct interpretation of MS/MS spectra of each ion identified in the MS spectra. This is possible because fragmentation of deprotonated ions ($[M-H]^-$) form typical ions as the loss of fatty acyls with the inositol ($[M-H-R_1COOH-162]^-$ and $[M-H-R_2COOH-162]^-$), the loss of fatty acyls chains ($[M-H-R_1COOH]^-$ and $[M-H-R_2COOH]^-$), and, like PSs, the ions corresponding to the fatty acyls chains ($[R_2COO]^-$ > $[R_1COO]^-$) [77] (Figure 21).

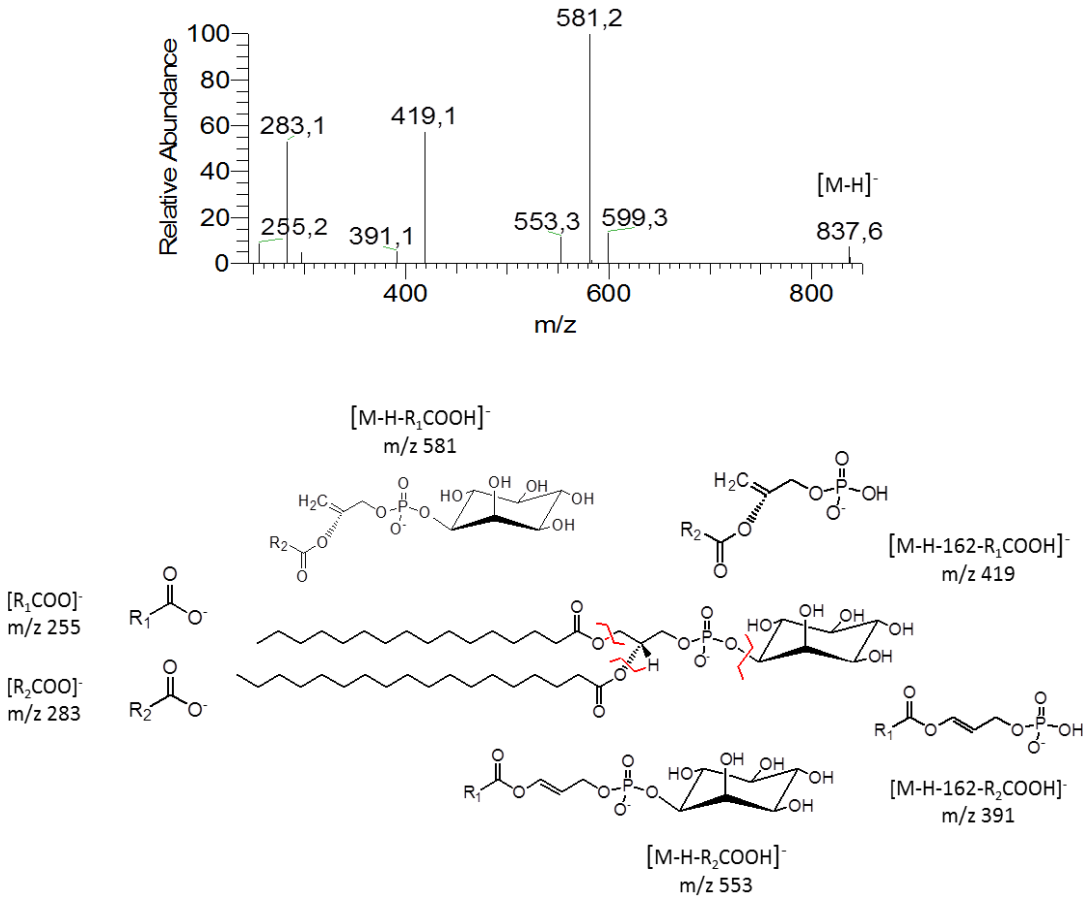

Figure 21: ESI – MS/MS spectrum of the $[M-H]^-$ at *m/z* 837, corresponding to PI (16:00/18:00). Molecular structure of phosphatidylinositol (PI; below) presenting main cleavages correspondent to the fragmentation observed in the MS/MS spectrum of $[M-H]^-$ ion obtained in ESI-ion trap. Fragmentation of $[M-H]^-$ gave the typical ions as the loss of fatty acyls with the inositol ($[M-H-R_1COOH-162]^-$ and $[M-H-R_2COOH-162]^-$), loss of fatty acyls chains ($[M-H-R_1COOH]^-$ and $[M-H-R_2COOH]^-$), and ions corresponding to the fatty acyls chains carboxylate anions ($[R_2COO]^-$ > $[R_1COO]^-$)

Differences in PIs profile, between cancer cells and control cells were observed (Figure 20). Curiously, the PI profile of both cancer cells was similar although different compared to EpH4 mammary epithelial cells, suggesting that PI molecular species may be target of, or reflect malignant transformation.

The most abundant PIs in EpH4 non malignant cells were PI (18:00/18:02 and 18:01/18:01) at *m/z* of 861 and PI (20:03/18:00) at *m/z* 887, followed by PI (18:00/18:01) at *m/z* 863 and PI (20:04/18:00) at *m/z* 885. In cancer cells, the most abundant ion was PI (18:00/18:01) at *m/z* 863, followed by less abundant PI (18:00/18:02 and 18:01/18:01) at *m/z* 861. It is interesting that the unsaturated PIs found in EpH4 were replaced by

saturated PIs, not just considering ions at *m/z* 863 and 861 but also PI (16:00/18:01) and PI (16:01/18:00) at *m/z* 835, PI (16:00/18:00) at *m/z* 837. The most remarkable change was observed in PI (20:03/18:00) at *m/z* 887, and PI (20:04/18:00) at *m/z* 885, which were present in less relative abundance in cancer cells compared to EpH4 cells.

PIs are precursors of PIP3, a signaling lipid that modulates cell growth, proliferation and motility [32]. In malignant cells, this messenger process is altered by various mechanisms. The formation of PIP3 is promoted by PI3K of which the gene encoding the catalytic subunit was found to be amplified and overexpressed in several types of cancers including breast cancers [99]. PTEN is a tumor suppressor that removes the 3rd phosphate of PIP3 and attenuates signaling downstream of activated PI3K and is frequently mutated or lost in different breast cancers [99]. In this work, levels of PIP3 precursors (PIs) were slightly higher in both tumor cells which is consistent with results shown by others in breast cancer cells [75] and tissues [67]. However, it is evident from the small differences that enzymatic activity regulating PIPs levels is a major if not more important signaling regulatory point.

In some studies it is found that arachidonic acid caused significant increase of cell growth and a significant portion of this growth depended on PI3K activation [100]. This can justify our changes in the PI (20:03/18:00) and PI (20:04/18:00). It has been reported that high levels of DAG (C20:04/C18:00) and polyunsaturated PIs increase fluidity of liposomes, even at low temperatures [101]. Curiously, the MS/MS profile showed that in cancer cells, the unsaturated fatty acyl substitution was replaced by the saturated fatty acyl one, which suggests that low fluidity of cell membrane may be characteristic of malignant cells. Whether the level of saturation / membrane fluidity has an impact on cell signaling by PIPs, remains to be investigated.

2. Phospholipid profiling of human mammary epithelial cell lines

With a similar approach as that used in mouse cell lines, PL content and profile of lipid extracts was obtained from non-tumorigenic MCF10A mammary epithelial cells, T-47D epithelial, non-metastatic and MDA–MB-231 spindle-shaped, metastatic mammary cancer cell lines. For this purpose, the PL classes separated by TLC were analyzed by MS and MS/MS using ESI ionization and quantified by phosphorus assay.

To know the approximate amount of lipids and proteins per cell we counted the number of cells and quantified the PL and protein content in each extraction (Table 6).

Table 6: Amount of PL and proteins per cell in µg in all three types of cells

	PLs per cell (µg)	**Proteins per cell (µg)**
MCF10A	1,23E-05 ± 2,58E-06	3,35E-04 ± 1,30E-04
T-47D	4,15E-05 ± 1,02E-05	5,67E-04 ± 2,15E-04
MDA-MB-231	2,10E-05 ± 7,02E-06	3,61E-04 ± 1,70E-04

Phospholipid class separation and quantification

Separation of PL classes was accomplished by TLC permitting the fractionation and identification of LPC, SM, PC, PI, PS, PE, PA and CL classes in distinct spots (Figure 22).

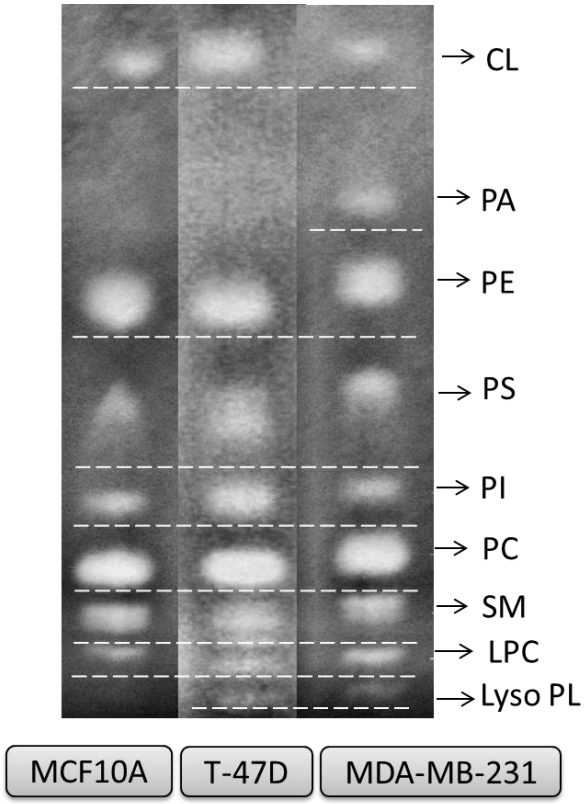

Figure 22: Separation of PL classes by thin layer chromatography. The class named as Lyso PL could not be identified with any standard used.

Relative PL content (%) of each PL class in total lipid extract was evaluated by quantifying the amount of PL in each spot by phosphorus assay and results obtained are shown in Figure 23.

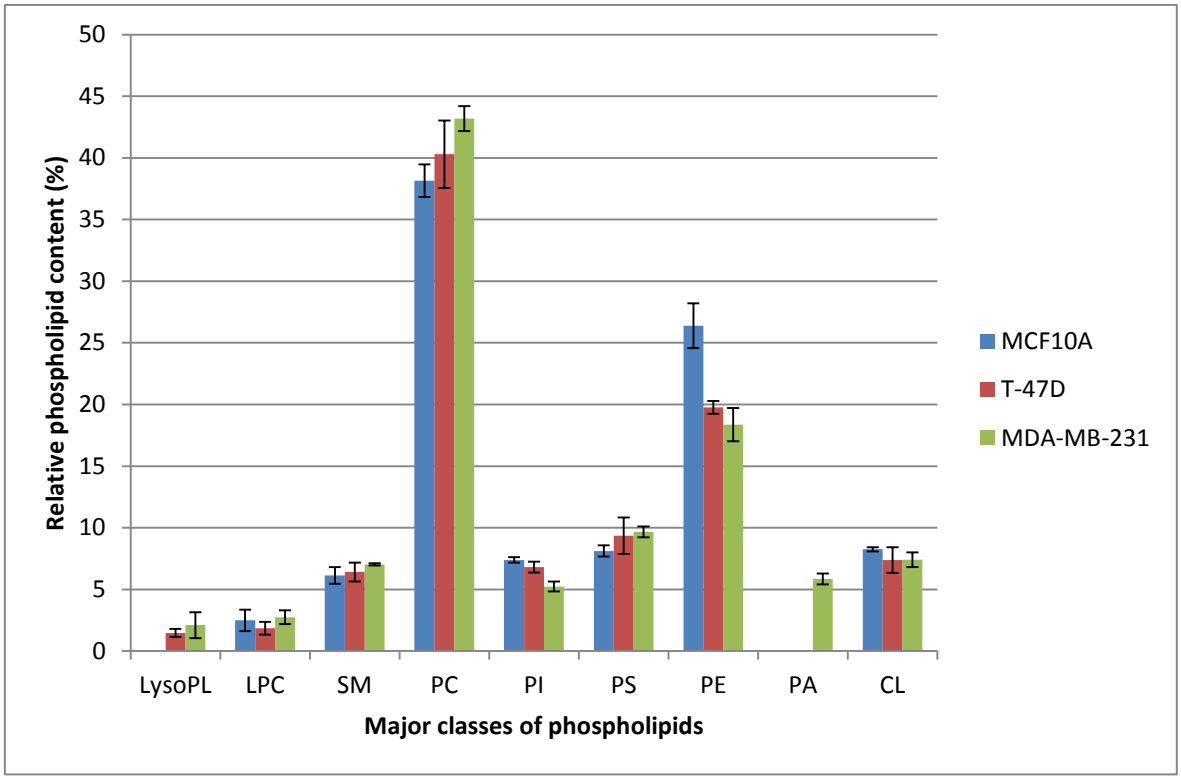

Figure 23: Relative phospholipid (PL) content (%) of PL classes in human non-tumorigenic and cancer cell lines. Phosphate content in each spot was related to total phosphate content in the sample. Mean +/- SD from three independent experiments is shown

The most abundant PL class in all cell lines was PC, followed by PE. The lyso PL was a class found in both cancer cells but with no correspondence to any standard used in the TLC and since its abundance was very low, it was impossible to analyze by MS. However, due to its position in the TLC plate, it appears to be a lyso SM. LPC was slightly lower in the less metastatic T-47D cell line compared to the other cell lines, MDA-MB-231 and MCF10A. Many studies refer that lyso PLs are more abundant in cancer cells [102], as appears to happen in our results. Increased PC levels have been reported in malignant cells compared to non-tumorigenic cell, but with no substantial differences between malignant cells with low and high level of progression [75]. These observations are in agreement with our results. Curiously, levels of PI, the precursors of PIPs known to be actively involved in growth and cell migration [27] have a slight decrease in cancer vs non tumorigenic cells, while PS, CL and SM did not substantially change. The percentage of PE class decreased with the increase of aggressiveness, being more evident the difference

between non-tumorigenic cells and both cancer cells. PAs were only detected in the most metastatic cells, MDA-MB-231, which could indicate that this PL class exist in very low abundance in the other two types of cells, MCF10A and T-47D.

Each PL class was analyzed by MS and MS/MS and the molecular species of each class were identified in order to evaluate if, in addition to differences in relative PL classes content, differences in molecular composition of each PL class could be observed. PI, PS, CL and PA classes were analyzed in the negative mode, and the results obtained are summarized in Table 7 with the indication of the *m/z* values of the ions $[M-H]^-$.

Table 7: Identification of $[M-H]^-$ ions observed in the MS spectra of PA, PI, PS and CL.

	Diacil			
	$[M-H]^-$	**C:N**	**Fatty acids**	
PA	647	32:00	16:00	16:00
	673	34:01	16:00	18:01
	675	34:00	16:00	18:00
	701	36:01	18:00	18:01
	703	36:00	18:00	18:00
PI	835	34:01	16:00	18:01
	835	34:01	16:01	18:00
	837	34:00	16:00	18:00
	861	36:02	18:02	18:00
	861	36:02	18:01	18:01
	863	36:01	18:00	18:01
	865	36:00	18:00	18:00
	885	38:04	20:04	18:00
	887	38:03	20:03	18:00
	889	38:02	20:02	18:00
	909	40:06	22:06	18:00
	911	40:05	22:05	18:00
	913	40:04	22:04	18:00

PS	734	32:00	16:00	16:00
	760	34:01	16:00	18:01
	760	34:01	16:01	18:00
	786	36:02	18:00	18:02
	786	36:02	18:01	18:01
	788	36:01	18:00	18:01
	812	38:03	20:00	18:03
	812	38:03	20:03	18:00
	814	38:02	20:02	18:00
	836	40:05	18:00	22:05
	844	40:01	18:00	22:01
	872	42:01	22:00	20:01

CL	1377	66:01	16:00	16:00	16:00	18:01
	1399	68:04	16:00	16:01	18:01	18:02
	1403	68:02	16:00	16:00	18:01	18:01
	1423	70:06	16:01	18:01	18:02	18:02
	1425	70:05	16:01	18:01	18:01	18:02
	1427	70:04	16:01	18:01	18:01	18:01
	1429	70:03	16:00	18:01	18:01	18:01
	1447	72:08	18:02	18:02	18:02	18:02
	1449	72:07	18:01	18:02	18:02	18:02
	1451	72:06	18:01	18:01	18:02	18:02
	1453	72:05	18:01	18:01	18:01	18:02
	1455	72:04	18:01	18:01	18:01	18:01
	1475	74:08	18:01	18:02	18:02	20:03
	1475	74:08	18:02	18:02	18:02	20:02
	1477	74:07	18:01	18:01	18:02	20:03
	1477	74:07	18:01	18:02	18:02	20:02

The attribution of the fatty acyl composition of each PL molecular species was done accordingly with the interpretation of the correspondent MS/MS spectra. C:N: number of carbons in the fatty acid chain : number of double bonds; fatty acids (#:#): the first value indicates # of carbons in the fatty acid chain and the second value, the # of double bonds in that chain; PI: phosphatidylinositol; PS: phosphatidylserine; PA: phosphatidic acid; CL: cardiolipin

PC, SM, LPC and PE classes were analyzed in the positive mode and molecular species identified are summarized in Table 8 with the indication of the *m/z* values of the ions $[M+H]^+$.

Table 8: Identification of $[M+H]^+$ ions observed in the MS spectra in LPC, PC, SM, PE and PS

	Diacil			Alquilacil		
	$[M+H]^+$	**C:N**	**Fatty acids**	**$[M+H]^+$**	**C:N**	**Fatty acids**
LPC	494	16:01	16:01	508	18:01	O-18:01
	522	18:01	18:01	510	18:00	O-18:00
	524	18:00	18:00			

PC	706	30:00	14:00	16:00	718	32:01	O-14:00	18:01
	732	32:01	14:00	18:01	720	32:00	O-14:00	18:00
	732	32:01	16:00	16:01	744	34:02	O-16:00	18:02
	734	32:00	16:00	16:00	746	34:01	O-16:00	18:01
	734	32:00	14:00	18:00	748	34:00	O-16:00	18:00
	758	34:02	16:01	18:01	772	36:02	O-16:00	20:02
	760	34:01	16:00	18:01	774	36:01	O-16:00	20:01
	762	34:00	16:00	18:00				
	784	36:03	18:01	18:02				
	786	36:02	18:01	18:01				
	788	36:01	18:00	18:01				
	808	38:05	20:04	18:01				
	808	38:05	20:03	18:02				
	810	38:04	20:01	18:03				
	812	38:03	20:01	18:02				
	814	38:02	20:01	18:01				
	834	40:06	20:03	20:03				

SM	703	34:01	18:01	16:00
	705	34:00	18:00	16:00
	785	40:02	18:01	22:01
	787	40:01	18:01	22:00
	813	42:02	18:01	24:01
	815	42:01	18:01	22:00
	841	44:02	18:01	26:01
	843	44:01	18:01	26:00

PE	690	32:01	14:00	18:01	702	34:02	O-16:01	18:01
	690	32:01	16:00	16:01	704	34:01	O-16:00	18:01
	716	34:02	16:01	18:01	732	36:01	O-18:00	18:01
	718	34:01	16:01	18:00				
	718	34:01	16:00	18:01				
	740	36:04	18:02	18:02				
	742	36:03	18:01	18:02				
	744	36:02	18:01	18:01				
	744	36:02	18:00	18:02				
	746	36:01	18:00	18:01				
	748	36:00	18:00	18:00				
	766	38:05	20:04	18:01				
	768	38:04	20:04	18:00				
	768	38:04	20:03	18:01				
	770	38:03	20:02	18:01				
	790	40:07	22:06	18:01				
	792	40:06	22:06	18:00				
	794	40:05	22:05	18:00				
	796	40:04	22:04	18:00				

PS	736	32:00	16:00	16:00
	762	34:01	16:00	18:01
	762	34:01	16:01	18:00
	788	36:02	18:00	18:02
	788	36:02	18:01	18:01
	790	36:01	18:00	18:01
	814	38:03	20:00	18:03
	814	38:03	20:03	18:00
	816	38:02	20:02	18:00
	838	40:05	18:00	22:05
	846	40:01	18:00	22:01
	874	42:01	22:00	20:01

The attribution of the fatty acyl composition of each PL molecular species was done accordingly with the interpretation of the correspondent MS/MS spectra. C:N: number of carbons in the fatty acid chain : number of double bonds; fatty acids (#:#): the first value indicates # of carbons in the fatty acid chain and the second value, the # of double bonds in that chain; PC: phosphatidylcholine; LPC: lysophosphatydilcholine; SM: sphingomyelin; PE: phosphatidylethanolamine; PS: phosphatidylserine

In general for the three different types of cells we see the same molecular species in each PL class. However, in some cases the relative abundances were different and

resulted in different PL profiles. The profile of PA class is just from MDA-MB-231 cell line, since it was only detected in this type of cells. A profile of either both lyso classes could not be traced due to their low abundance; however, some LPCs presented in the spot could be identified. The PL profile observed for each class in each cell type is described in the following section.

Phosphatidilcholine and Lysophosphatidylcholine profile

PCs obtained from the three different types of cells were analyzed by ESI-MS in positive mode, with formation of both $[MH]^+$ and $[MNa]^+$. In order to identify exclusively the $[MH]^+$ ions, precursor ion scan of the ion at *m/z* 184 were obtained in the triple quadrupole, as typical approach for choline lipids and described previously for mouse mammary epithelial cells. This approach permitted to obtain the spectra shown in Figure 24, which revealed the $[MH]^+$ ions of all PCs present in the extract from the spot obtained after TLC separation.

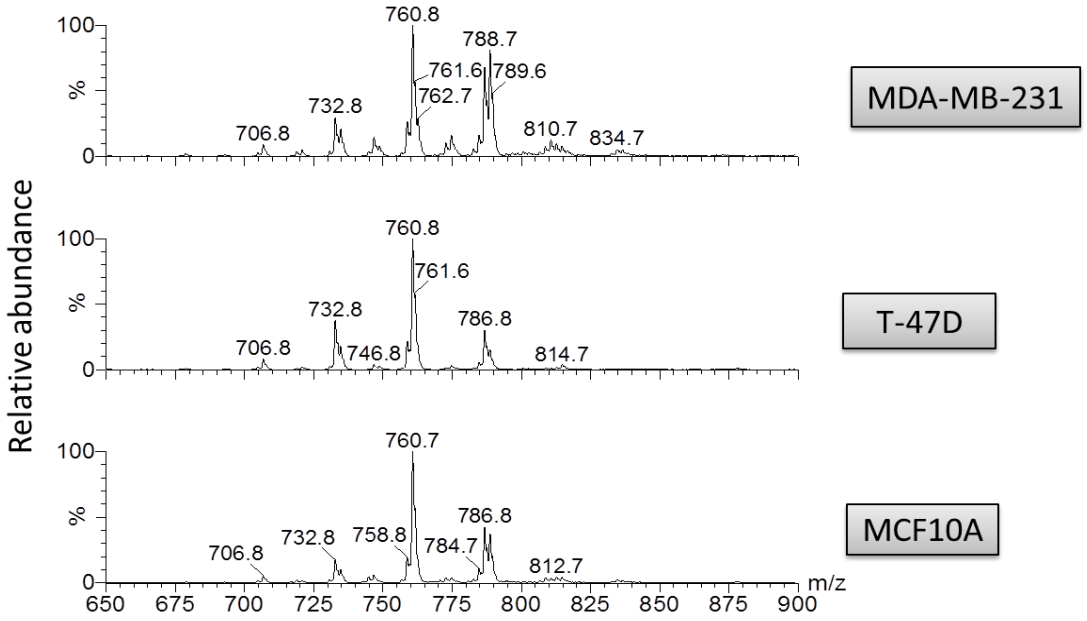

Figure 24: Phosphatidylcholine (PC) spectra obtained by electrospray ionization mass spectrometry analysis of PC extracted from the correspondent spots separated by thin layer chromatography. PCs were selectively detected by diagnostic precursor ion scan of the product

ion at *m/z* 184 in the positive mode obtained using an electrospray triple quadrupole. Y-axis: Relative abundance considering the highest abundant ion as 100 %; x-axis: *m/z* for each ion.

Identification of both diacyl and alkilacyl PCs as well as their fatty acyl chains composition along the glycerol backbone was achieved by direct analysis and interpretation of MS/MS spectra of each ion identified in the MS spectra, as resumed in Table 8.

The major PCs found were PC (16:00/18:01) corresponding to $[MH]^+$ at *m/z* 760, followed by PC (18:01/18:01), PC (18:00/18:01) and PC (14:00/18:01 and 16:00/16:01) corresponding to $[MH]^+$ at *m/z* 786, 788 and 732 respectively. The less abundant PCs appears to be the alkylacyl PCs, as PC (O-16:00/18:01) and PC (O-16:00/20:01) corresponding respectively to $[MH]^+$ at *m/z* 746 and 774.

Slightly relative PC levels were observed between the three cell lines, where there appeared to be an increase in the amount of PC with the increase of metastatic potential, i.e., MCF10A <T-47D<MDA-MB-231. Looking to the spectra, some differences were also found as PC (18:01/18:01) (*m/z* 786) and PC (18:00/18:01) (*m/z* 788), were higher in the metastatic cell line, MDA-MB-231. In addition, an increase of alkylacyl PCs was observed in MDA-MB-231 cells. There is another difference in both cancer cells comparing to non-tumorigenic cell line MCF10A, where PC (14:00/18:01 and 16:00/16:01) seemed to be increased.

Augmented synthesis of PC was reported in the T-47D cell line compared to normal breast tissue, but revealed similarities between the composition of diacyl PC, which is consistent with our results, both at the relative PL content levels (Figure 23) and the appearance of the spectrum [78]. The amount of PCs did not vary substantially between both tumor cell lines, in agreement with the literature [75], and as mentioned previously in our study in mouse cell lines.

It has been proposed that low levels of ether PCs are characteristic of breast cancer versus normal breast tissue [78]. Further, reduced levels of ether PCs were found to be characteristic of early stages of breast cancer progression, but not in all stages, being reported higher levels of ether PCs in malignant versus benign breast tumors [75].

Despite being detectable in all three cell types it was not possible to trace a LPC class profile due to its very low abundance. However, some LPC species could be identified in the LPC MS spectra with formation of both $[MH]^+$ and $[MNa]^+$. Both acyl and alkyl LPCs were identified in Table 8 . This identification of acyl and alkyl LPCs as well as their fatty acyl chain composition along the glycerol backbone was achieved by direct analysis and interpretation of MS/MS spectra of each ion identified in the MS spectra, as explained in mouse cell line analysis.

In the spectra it was identified five LPC, including diacyl LPC (16:01), LPC (18:01) and LPC (18:00) corresponding to $[MH]^+$ at *m/z* 494, 522 and 524 respectively, and akyl LPC (O-18:01) and LPC (O-18:00) corresponding respectively to $[MH]^+$ at *m/z* 508 and 510.

Interestingly, the relative PL content of LPC class decreased slightly in the low metastatic T-47D cells but increased in the MDA-MB-231 cells. One of the main sources of LPC comes from the hydrolysis of the sn-2 ester bond of PC by PLA2, to yield free LPC and fatty acid, predominantly arachidonic acid, as described previously [82]. The activity and expression of several PLA2 isoforms are increased in several human cancers. Therefore, we propose that the increase of LPC in our sample is probably due to higher PLA2 levels or enzymatic activity [83].

Sphingomyelin profile

SMs were analyzed by ESI-MS in positive mode obtained for the three different types of cells, with formation of both $[MH]^+$ and $[MNa]^+$. In order to obtain exclusively the $[MH]^+$ ions, precursor ion scan of the ion at *m/z* 184 was obtained in the triple quadrupole, as typical approach for choline lipids and described previously for mouse mammary epithelial cells. This approach permitted to obtain the $[MH]^+$ ions of all PCs present in the spot obtained after TLC separation, as the spectra shown in Figure 25.

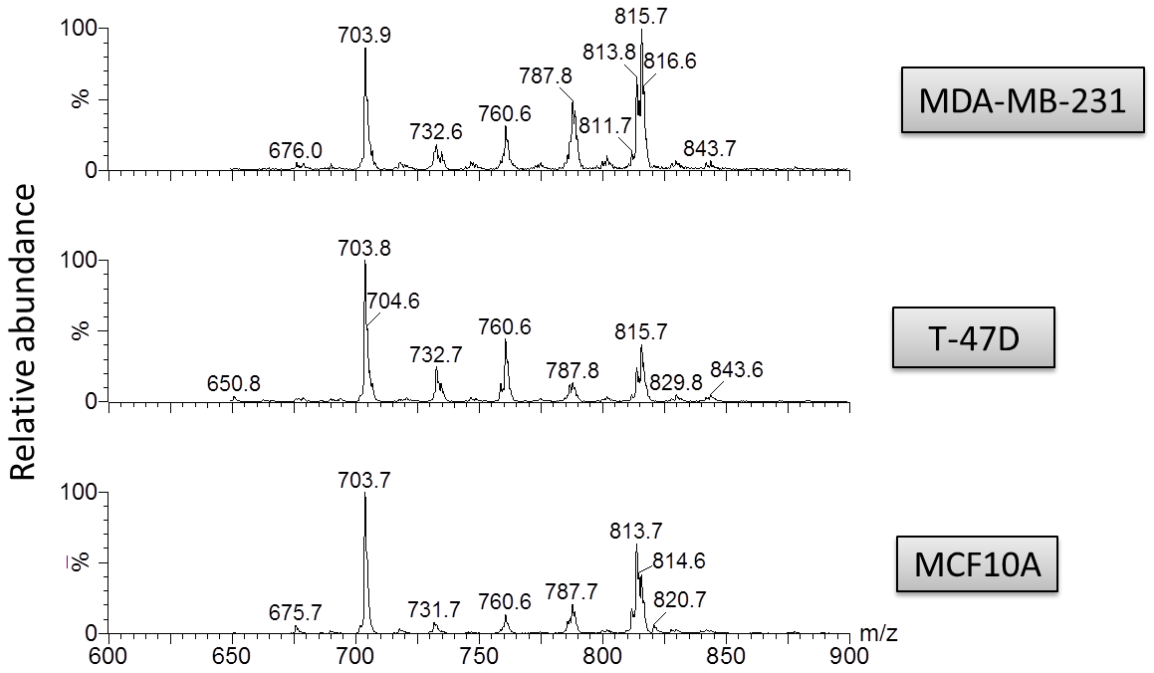

Figure 25: Sphingomyelin (SM) spectra obtained by electrospray ionization mass spectrometry analysis of SM extracted from the correspondent spots separated by thin layer chromatography. SMs were selectively detected by diagnostic precursor ion scan of the product ion at *m/z* 184 in the positive mode obtained using an electrospray triple quadrupole. Y-axis: Relative abundance considering the highest abundant ion as 100 %; x-axis: *m/z* for each ion

Interpretation of MS/MS spectra of each ion identified in the MS spectra allowed the identification of diacyl SMs as well as their fatty acyl chains composition along the glycerol backbone, as resumed in Table 8.

Observing the three spectra, SMs ions with higher relative abundance are SM (18:01/16:00), SM (18:01/24:01) and SM (18:01/24:00), corresponding to $[MH]^+$ at *m/z* 703, 813 and 815 respectively followed by SM (18:01/22:00) corresponding to $[MH]^+$ at *m/z* 787. Due to their high abundance and because they elute close to each other, we can see some PCs species in this spot, ions 760 and 732. However, PCs and SMs are easily to differentiate since PC species form ions with *m/z* even and SM species form ions with *m/z* odd.

Differences among the three spectra could be observed. First, a slight decrease in the relative abundance of SM (18:01/24:01), SM (18:01/24:00) and also SM (18:01/22:00) in T-47D comparing with non-tumorigenic MCF10A cells, which was more pronounced

when compared to MDA-MB-231 cells. Evident differences in the MDA-MB-231 profile compared with the other two types of cells, MCF10A and T-47D were observed and include: the relative abundance of SM (18:01/22:00), SM (18:01/24:01) and SM (18:01/24:00) increased substantially in the most metastatic cell line. Interestingly, looking to the relative SM abundance we see an increase of SMs, despite not substantially, in the MDA-MB-231 cells in addition to the differences in the SM profile which could be correlated.

As explained in the previous section (mouse cell lines), sphingolipids, such as SM, have important roles in basic cellular processes, such as proliferation, apoptosis, transformation, differentiation, motility and angiogenesis and also in maintain the bilayer structure, macrodomain formation and signaling, all of which are altered in breast cancer [91]. High levels of C16-ceramide, a precursor of SM biossynthesis, have been found in different types of tumors, compared to other healthy tissue [89]. These results are in agreement comparing our observations in non-tumorigenic cell line MCF10A and the low metastatic cell line T-47D, where the relative abundance of all SM is lower compared to SM (18:01/16:00) and (18:00/16:00). Highly metastatic cell line MDA-MB-231 profile have some similarities with MCF10A profile probably because these type of cells share some features, i. e. not express the three hormone receptors, ER, PR and HER2 and cluster within the same group of expressed genes. However, they obviously present important differences since MDA-MB-231 are cancer cells and MCF10A are not.

Phosphatidilethanolamine profile

PE was analyzed by ESI-MS in positive mode, with formation of $[M+H]^+$, and confirmation of neutral loss scan (neutral loss of polar head, -141 Da) was obtained in the triple quadrupole, as typical approach for PEs [76, 77] and as described previously for mouse mammary epithelial cells. This approach permitted to obtain the spectra in the Figure 26, which revealed the $[M+H]^+$ ions of PEs present in the TLC spot.

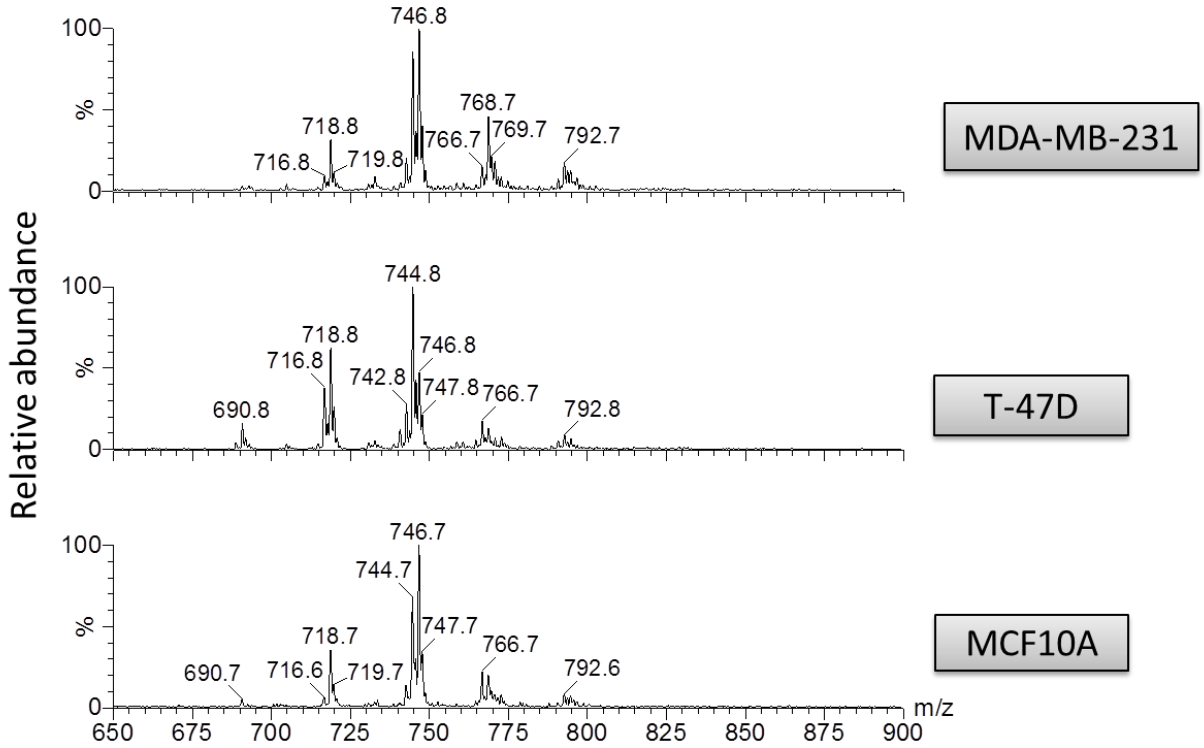

Figure 26: Phosphatidylethanolamine (PE) spectra obtained by electrospray ionization mass spectrometry analysis of PE extracted from the correspondent spots separated by thin layer chromatography. PEs were selectively detected by diagnostic neutral loss scan correspondent to the neutral loss of PE polar head (neutral loss of 141 Da) in the positive mode obtained using an electrospray triple quadrupole. Y-axis: Relative abundance considering the highest abundant ion as 100 %; x-axis: *m/z* for each ion

Analysis of both diacyl and alkylacyl PEs was achieved by direct interpretation of MS/MS spectra of each ion identified in the MS spectra, permitting the identification of both their fatty acyl chains composition along the glycerol backbone, as described previously and resumed in Table 8.

The most abundant PEs in all cell types were PE (18:01/18:01 and 18:00/18:02) and PE (18:00/18:01) corresponding respectively to the ion $[M+H]^+$ at *m/z* of 744 and 746 by followed PE (16:01/18:00 and 16:00/18:01), PE (20:04/18:01) and PE (20:04/18:00 and 20:03/18:01) with *m/z* of 718, 766 and 768 respectively.

There was a difference in the highly metastatic MDA-MB-231 cell line profile; the PE (20:04/18:00 and 20:03/18:01) (*m/z* 768) and PE (22:06/18:00) (*m/z* 792) had a higher relative abundance compared to the other two types of cells, MCF10A and T-47D cells,

which could be related to the metastatic phenotype. In addition, when we compare the mass range of the PE spectra between m/z of 700 and 740, a higher relative abundance of PE (O-18:00/18:01) and PE (O-16:00/18:01) which correspond to the ion $[M+H]^+$ at *m/z* of 732 and 704 respectively was observed in the high metastatic MDA-MB-231 cells. T-47D cell line present also some differences, as a higher relative abundance of PE (16:01/18:00 and 16:00/18:01) and, more notorious in the PE (18:01/18:01 and 18:00/18:02) which had a higher relative abundance than PE (18:00/18:01), in contrast to MCF10A and MDA-MB-231 cell lines.

As explained in the mouse cell lines section, malignant tumors appear to be particularly rich in PEs [66] which were found to be significantly altered in malignant tumors compared to benign tumors and to non-involved breast tissue [67]. Curiously once again, these results are in clear contrast with ours, since in the non-tumorigenic MCF10A cells, the relative PE amount was higher than in both cancer cells.

PEs have also been demonstrated to be significantly increased in MDA-MB-231 [75]. These is in agreement with our results, using the same cells, where certain molecular species of PEs (per example PE (20:04/18:00 and 20:03/18:01) and PE (O-18:00/18:01)) were found with the highest relative abundance.

Phosphatidylserine profile

PSs were analyzed by ESI-MS in negative mode, with formation of $[M-H]^-$. This approach permitted to obtain the spectra in Figure 27, which revealed $[M-H]^-$ ions present in the TLC spot.

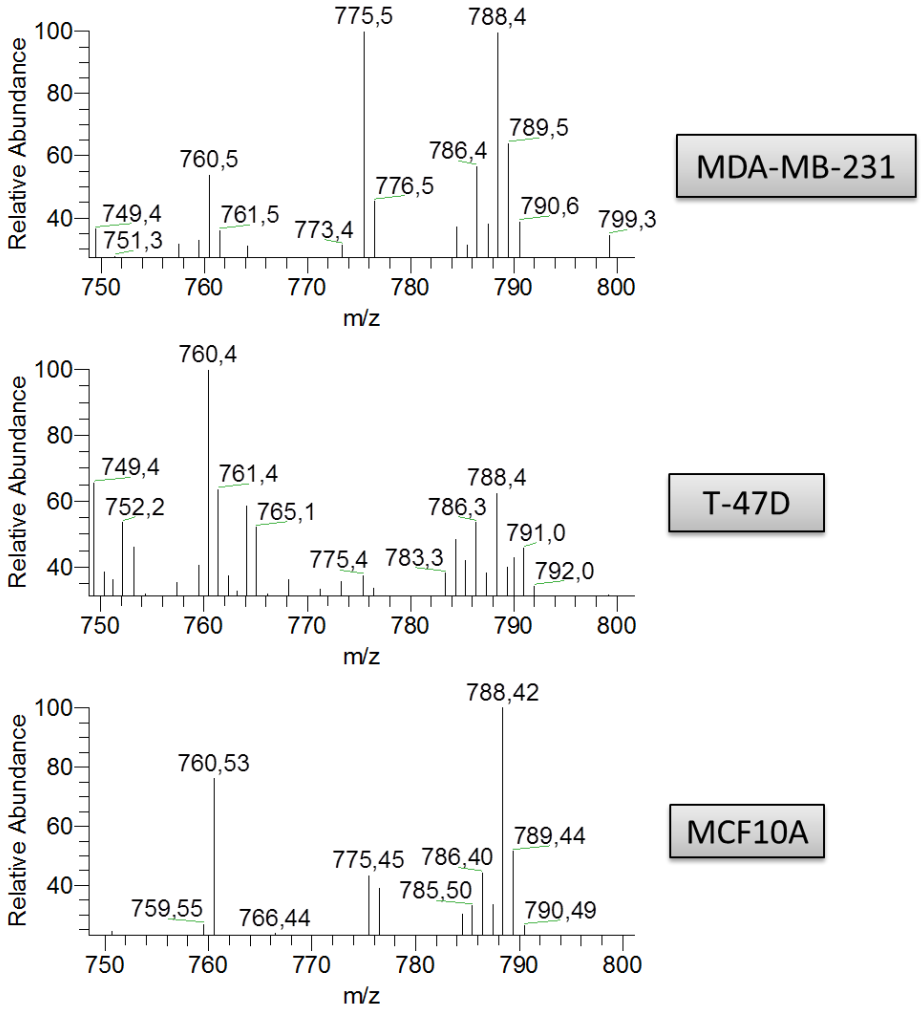

Figure 27: MS spectrum obtained by electrospray ionization mass spectrometry analysis of PS extracted from the correspondent spots separated by thin layer chromatography. The PS spot was extracted and acquired in the negative mode obtained using an electrospray ion trap. Y-axis: Relative abundance considering the highest abundant ion as 100 %; x-axis: *m/z* for each ion.

PS profile was also confirmed with a neutral loss scan in the positive mode (neutral loss of polar head, -185 Da) in the triple quadrupole in order to identify all PSs content in the TLC spot. This approach permitted to obtain the spectra in Figure 28, which revealed all $[M+H]^+$ PS ions present in the TLC spot.

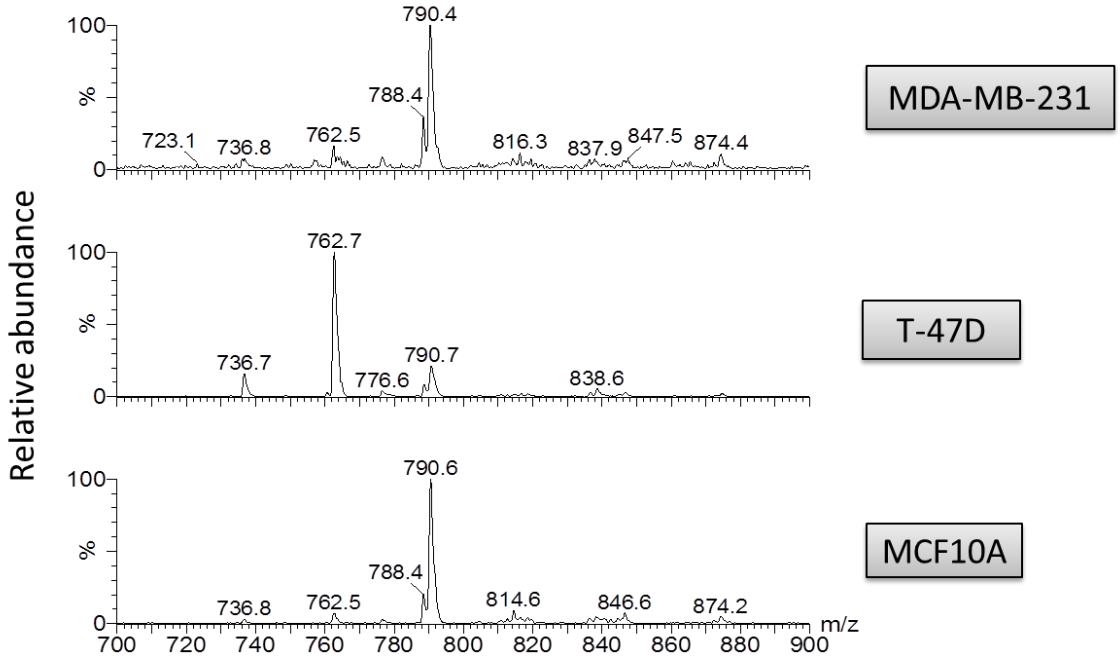

Figure 28: Phosphatidylserine (PS) spectra obtained by electrospray ionization mass spectrometry analysis of PS from spots separated by thin layer chromatography. PSs were selectively detected by diagnostic neutral loss scan correspondent to the neutral loss of PE polar head (neutral loss of 184 Da) in the positive mode obtained using an electrospray triple quadrupole. Y-axis: Relative abundance considering the highest abundant ion as 100 %; x-axis: *m/z* for each ion.

Interpretation of MS/MS spectra of each ion identified in the MS spectra allowed identification of diacyl PSs as well as their fatty acyl chain composition as described in mouse cell lines, as present in Table 7 and Table 8.

The most abundant PS in the MCF10A and MDA-MB-231 cells was PS (18:00/18:01) corresponding to the ion $[M-H]^-$ at *m/z* of 788 and to the ion $[M+H]^+$ at *m/z* of 790, followed by PS (16:00/18:01 and 16:01/18:00) corresponding to the ion $[M-H]^-$ at *m/z* of 760 and to the ion $[M+H]^+$ at *m/z* of 762. In the T-47D cells, we observed exactly the opposite, the most abundant ion was PS (16:00/18:01 and 16:01/18:00) followed by PS (18:00/18:01). Curiously there was a significant alteration in PS (16:00/18:01 and 16:01/18:00) (*m/z* 760 in the negative mode and *m/z* 762 in the positive mode) that were found with a high relative abundance in T-47D cells but with a very low relative abundance in the MCF10A and MDA-MB-231 cells. On the other hand, PS (18:00/18:01) (*m/z* 788 in the negative mode and *m/z* 790 in the positive mode) had a high relative

abundance in the MCF10A and MDA-MB-231 cells but a very low abundance in the T-47D cells.

As previously described, PS, a PL found predominantly on the inner membrane leaflets, plays very important roles in cellular homeostasis, and is therefore very important in the cell. PS is involved in signaling pathways and in localization of intracellular proteins to the cytosolic membrane leaflets, in addition to a structural function [96, 97]. The appearance PS on the outer leaflet of a lipid bilayer initiates many biological events, including platelet aggregation, cell adhesion, and is an indication of cellular apoptosis.

It has been described that PS distribution in cancer cells is altered [98]. Our results showed differences between low metastatic T-47D cells and highly metastatic MDA-MB-231 cells, but the highly metastatic cells have a very similar profile to non-tumorigenic MCF10A cells, which puts in doubt whether or not these differences are related to cancer development and aggressiveness or cellular morphology. In addition, gene expression profiles of MCF10A and MDA-MB-231 are very similar, and both cells are classified as basal-like.

Phosphatidic Acid profile

This class of PLs has the simplest polar head group, and serves as a precursor and metabolite in the PL biosynthetic and catabolism pathways.

PAs were analyzed by ESI-MS in negative mode, with formation of $[M-H]^-$. This approach permitted to obtain the spectra shown in Figure 29, which revealed the PA $[M-H]^-$ ions present in the TLC spot.

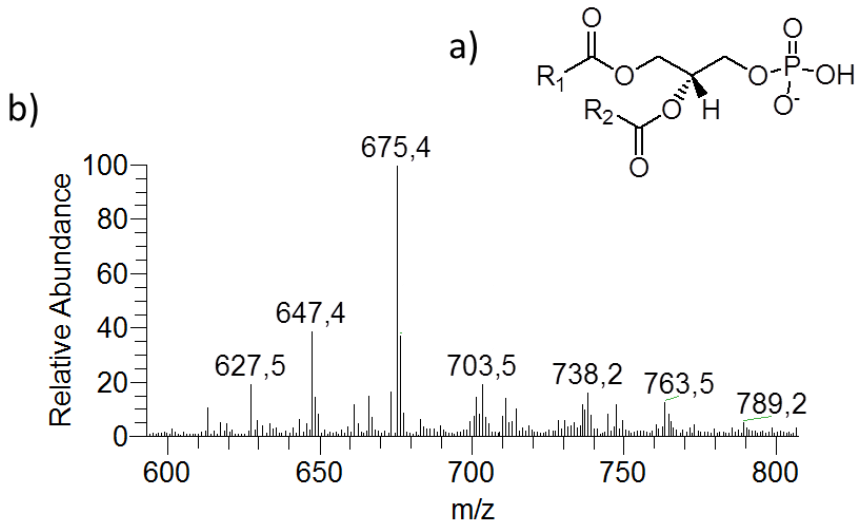

Figure 29: A. Diacyl PA structure; B. MS spectrum obtained by electrospray ionization mass spectrometry analysis of PA extracted from the correspondent spot separated by thin layer chromatography of MDA-MB-231 mammary cancer cells. The PA spot was extracted and acquired in the negative mode obtained using an electrospray ion trap. Y-axis: Relative abundance considering the highest abundant ion as 100 %; x-axis: *m/z* for each ion.

Analysis of PAs species allowed to identify diacyl PAs as resumed in Table 7. This identification as well as their fatty acyl chain composition and location along the glycerol backbone was achieved by direct analysis and interpretation of MS/MS spectra of each ion identified in the MS spectra. This is possible because fragmentation of deprotonated ions ($[M-H]^-$) is characteristic only for the ions from the loss of the fatty acyls chains ($[M-H-R_1COOH]^-$ and $[M-H-R_2COOH]^-$) and the ions corresponding to the fatty acyls chains themselves ($[R_2COO]^- > [R_1COO]^-$) [77] (Figure 30).

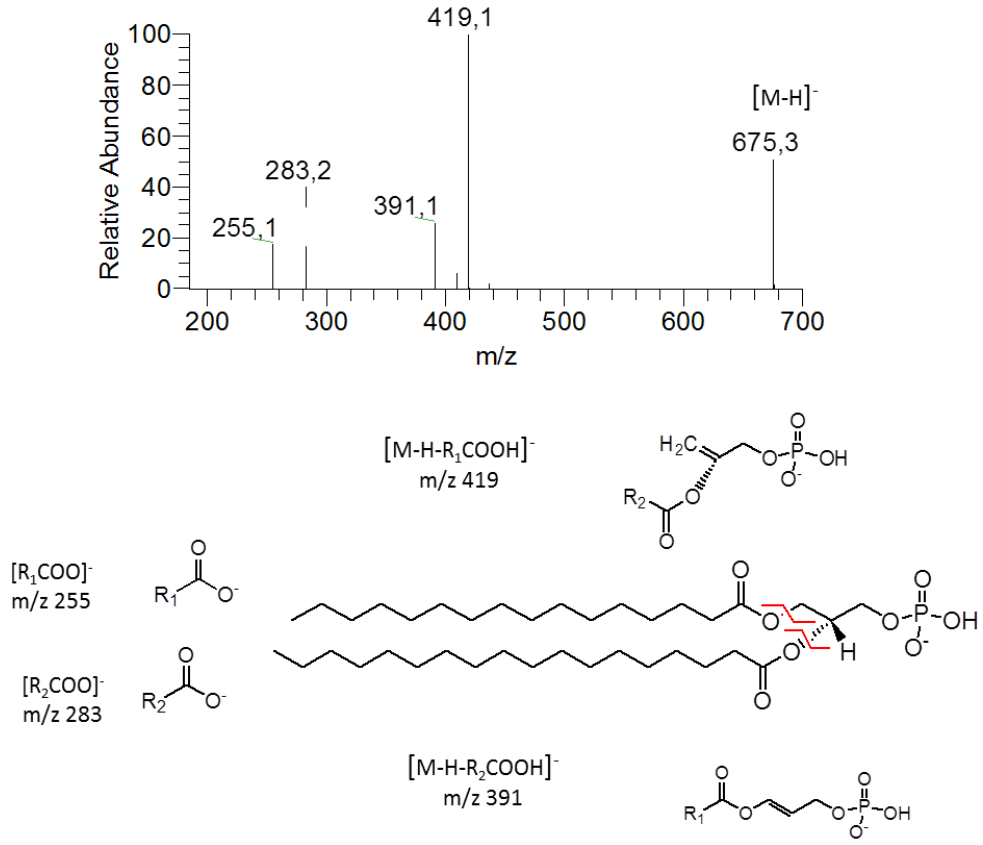

Figure 30: ESI – MS/MS spectrum of the $[M-H]^-$ at *m/z* 675, corresponding to PA (16:00/18:00). Molecular structure of phosphatidic (PA; below) presenting main cleavages correspondent to the fragmentation observed in the MS/MS spectrum of $[M-H]^-$ ion obtained in ESI-ion trap. Fragmentation of $[M-H]^-$ gave the loss of the fatty acids, and ions corresponding to the fatty acyls chains carboxylate anions ($[R_2COO]^-$ and $[R_1COO]^-$).

Interestingly, this class was only separated in the MDA-MB-231 cell line. Therefore, only the profile from this cell line was obtained. The most abundant PA found was PA (16:00/18:00) corresponding to the ion $[M-H]^-$ at *m/z* of 675 followed by PA (16:00/16:00) and PA (18:00/18:00) corresponding to the ion $[M-H]^-$ at *m/z* of 647 and 703 respectively.

PA is a vital cell lipid that acts as a biosynthetic precursor for the formation (directly or indirectly) of triacylglycerols and phospholipids in the cell, and acts as a signaling molecule. PA can be generated by different ways (Figure 10): via the hydrolysis of PC by phospholipase D (PLD), via phosphorylation of DAG by diacyl glycerol kinase (DAGK) and phospholipase C (PLC), and via acylation of LPA by LPA acyltransferase (LPAAT). PA is

degraded by conversion into DAG by lipid phosphate phosphohydrolases (LPPs), keeping PA concentrations at extremely low levels in the cell in normal conditions [103], which could explain the difficulty of separation and / or visualization of the PA band by TLC in MCF10A and T-47D cells lipid extracts.

PLD is an important signaling enzyme implicated in the control of many biological processes, including cell proliferation and survival [104]. PLD expression was shown to be elevated in human breast tumors compared with normal breast tissues [105] indicating a possible role of PLD in human breast tumorigenesis. This is in agreement with our high levels of PA in the high metastatic MDA-MB-231 cells.

ATX, which converts LPC into LPA, is well known to promote metastasis, cell growth, survival, and migration in cancer cells [84], and also described in breast cancer cells [85]. Higher plasma LPA levels are present in patients with ovarian cancer and other gynecologic malignancies, like breast cancer, compared with healthy controls [86]. Since one of the main syntheses of PA is from LPA, differences in LPA levels could also influence our levels of PAs. However, because we have not found LPAs in PL separation, probably due to its low abundance, we can not infer if levels of LPA are related with our high levels of PA in the more metastatic cell lines MDA-MB-231.

Phosphatidylinositol profile

PIs were analyzed by ESI-MS in negative mode, with formation of $[M-H]^-$. This approach permitted to obtain the spectra shown in Figure 31, which revealed the PI $[M-H]^-$ ions present in the TLC spot.

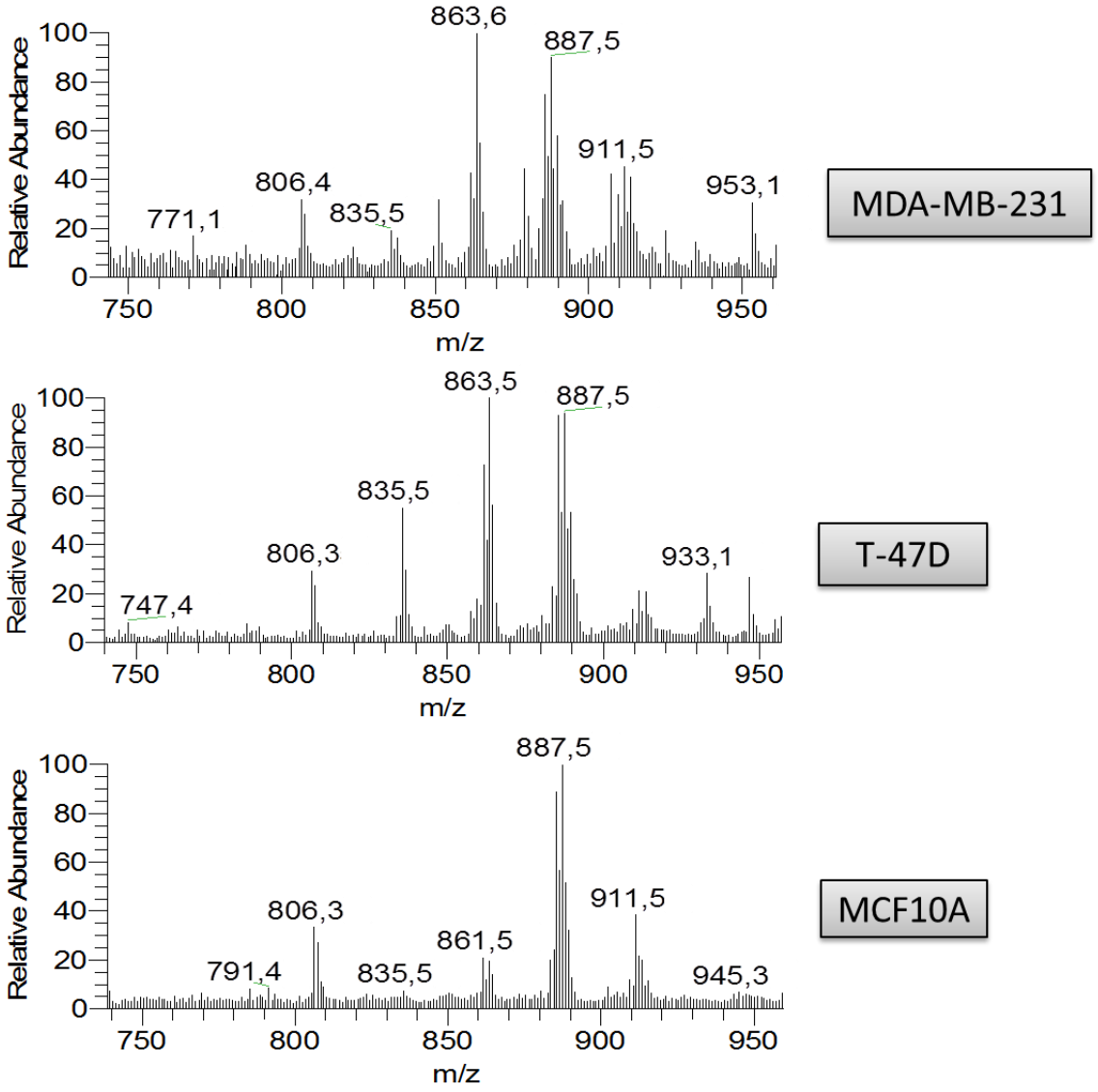

Figure 31: MS spectra obtained by electrospray ionization mass spectrometry analysis of PI extracted from the correspondent spots separated by thin layer chromatography. The PI spot was extracted and MS spectra were acquired in the negative mode obtained using an electrospray ion trap. Y-axis: Relative abundance considering the highest abundant ion as 100 %; x-axis: *m/z* for each ion.

Interpretation of MS/MS spectra of each ion identified in the MS spectra allowed to identify diacyl PIs as explained previously for mouse mammary epithelial cells and resumed in Table 7.

Differences between the spectra corresponding to the three cell types were observed, comparing non tumorigenic cells with cancer cells and between the cancer cells with low and high metastatic potential, underlining once more the idea that PI molecular

species may be target of, or reflect malignant transformation. In the relative PL content of this class, there is a slight decrease with the increase of aggressiveness.

The PIs (observed as $[M-H]^-$) that were most abundant in MCF10A cells were PI (20:03/18:00) at *m/z* of 887 followed by PI (22:05/18:00) at *m/z* 911, and by PI (18:01/18:01 and 18:02/18:00) and PI (16:00/18:01 and 16:01/18:00) at *m/z* of 861 and 835 respectively. In the T-47D and MDA-MB-231 cell lines the most abundant PIs were PI (18:00/18:01) and PI (20:03/18:00) at *m/z* of 863 and 887 respectively, followed by PI (16:00/18:01 and 16:01/18:00) and PI (22:05/18:00) at *m/z* of 835 and 911 respectively.

Observing the differences between non tumorigenic cells and cancer cells, the high relative abundance of PI (18:00/18:01) (*m/z* 863) in both cancer cells is evident. Comparing cancer cell lines, it appears that in the highly metastatic cells the PI (22:05/18:00) increased while PI (16:00/18:01 and 16:01/18:00) decreased. Curiously, regarding these PIs, MCF10A and MDA-MB-231 shared a similar profile compared to the T-47D cells. These again may be related to the similarities in gene expression profiles and therefore in cell type of origin between MDA-MB-231 cells and MCF10A.

PI is responsible for mediating communication between receptors on the cell surface and the extracellular medium, because it is precursor of PIP3, a signalling lipid that modulates cell growth, proliferation and motility [32]. In malignant cells, this messenger process is altered by various mechanisms, as described in the mouse cell lines sections.

In some works with breast cancer tissues the levels of PIs were slightly higher [67], which is not consistent with our results. A more recent study in breast cancer cells showed no substantial differences [75], which could suggest no significant alterations in the total content of this class in the cell, but an alteration in the molecular species which constitute its profile.

Cardiolipin profile

The most complex phospholipid present in eukaryotic cells is CL, because this PL consists of two phosphatidic acids with a glycerol bond. The exact role of cardiolipin in cellular biochemistry is complex; but, it is clear that cardiolipin is necessary for cytochrome C (cyt c) insertion into the mitochondrial membrane, and that it is involved in mitochondrial stability and function. CL obtained from the three different types of cells was analyzed by ESI-MS in negative mode, with formation of both $[M-H]^-$ and $[M-2H]^{2-}$. The Figure 32 represents the spectra of the ions $[M-H]^-$ present in the TLC spot of CL class.

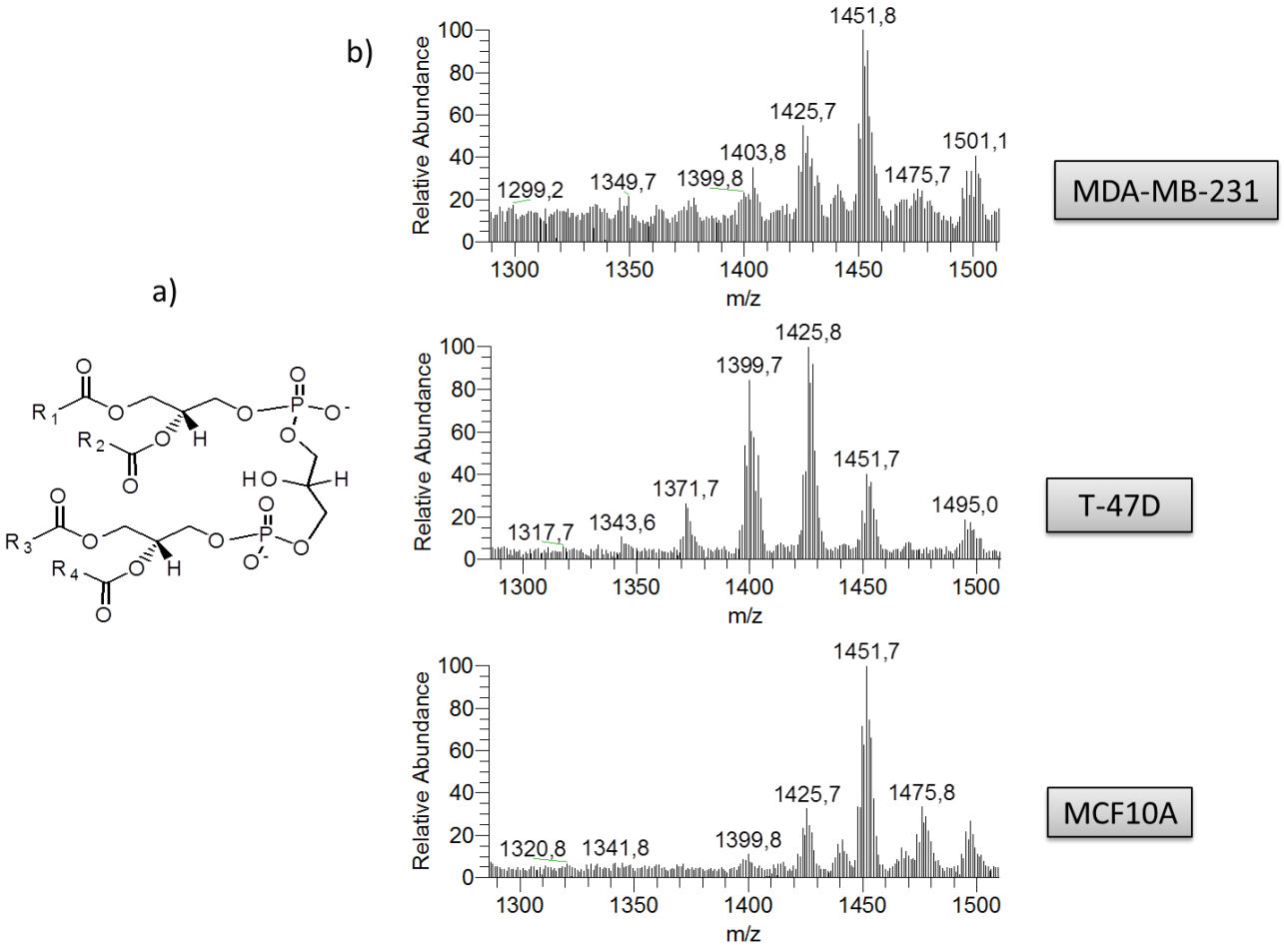

Figure 32: A. cardiolipin (CL) structure; B. MS spectra obtained by electrospray ionization mass spectrometry analysis of CL extracted from the correspondent spots separated by thin layer chromatography. The CL spot was extracted and MS spectra were acquired in the negative mode obtained using an electrospray ion trap. Y-axis: Relative abundance considering the highest abundant ion as 100 %; x-axis: *m/z* for each ion

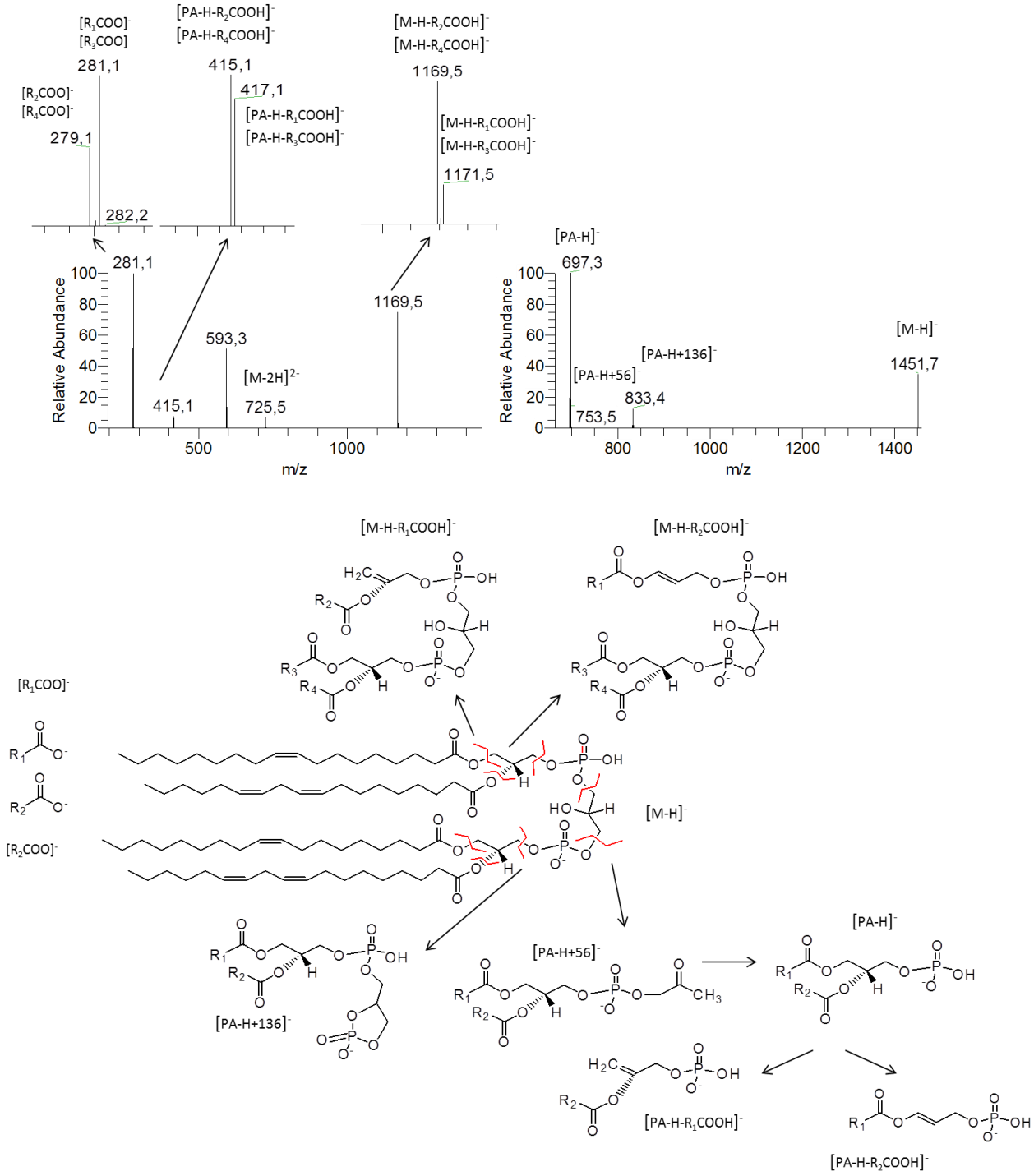

Figure 33: ESI – MS/MS spectrum of the $[M-H]^-$ at *m/z* 1451 and $[M-2H]^{2-}$ at *m/z* 725, corresponding to CL (18:02/18:02/18:01/18:01). Molecular structure cardiolipin (CL; below) presenting main cleavages correspondent to the fragmentation observed in the MS/MS spectrum of $[M-H]^-$ ion obtained in ESI-ion trap. Fragmentation of $[M-2H]^{2-}$ gave more products, as the loss of the fatty acids, the loss of the fatty acids in the PA and ions corresponding to the fatty acyls chains carboxylate anions ($[R_1COO]^-$, $[R_2COO]^-$, $[R_3COO]^-$ and $[R_4COO]^-$).

Analysis of CLs species allowed to identify diacyl CLs as resumed in Table 7. This analysis was achieved by direct interpretation of MS/MS spectra of each ion identified in the MS spectra, both $[M-H]^-$ and $[M-2H]^{2-}$. This is possible because fragmentation of desprotonated ions ($[M-H]^-$ and $[M-2H]^{2-}$) form second product ions, some due to the elimination of each fatty acids [57]. Examples of main product ions of CL are: $[M-H-RCOOH]^-$, the two different PAs ($[PA-H]^-$), PAs with the glycerol ($[PA-H+56]^-$) and with the glycerol plus phosphate group ($[PA-H+136]^-$), the loss of fatty acyls in PAs ($[PA-H-RCOOH]^-$) and the ions corresponding to the fatty acyls chains ($[R_1COO]^-$, $[R_2COO]^-$, $[R_3COO]^-$ and $[R_4COO]^-$) as shown in Figure 33.

The most abundant CLs were CL (18:01/18:01/18:02/18:02) and CL (16:01/18:01/18:01/18:02) corresponding to the ion $[M-H]^-$ at *m/z* 1451 and 1425, respectively, followed by CL (16:00/16:01/18:01/18:02) and CL (18:01/18:02/18:02/20:03 and 18:02/18:02/18:02/20:02) corresponding to the ion $[M-H]^-$ at *m/z* of 1399 and 1475, respectively.

Despite the percentage of CL in the total lipid extract being similar, there were some remarkable differences between the CL profiles of the three different types of cells. Curiously, the profile of the most metastatic MDA-MB-231 cancer cells was more similar to non-tumorigenic MCF10A cells, than to low metastatic T-47D cancer cells, as observed in the PS profiles. The most abundant CL in the MDA-MB-231 and MCF10A was CL (18:01/18:01/18:02/18:02) (*m/z* 1451) while in the T-47D cells the most abundant was CL (16:01/18:01/18:01/18:02) (*m/z* 1425) followed by CL (16:00/16:01/18:01/18:02) (*m/z* 1399), with a higher relative abundance of CL (18:01/18:01/18:02/18:02) (*m/z* 1451). The unique difference between non tumorigenic cells and both cancer cells is the decrease in the relative abundance of CL (18:01/18:02/18:02/20:03 and 18:02/18:02/18:02/20:02) (*m/z* 1475).

In mammalian cells, CL is found almost exclusively in the inner mitochondrial membrane where it is essential for the optimal function of numerous enzymes that are involved in mitochondrial energy metabolism, and when CL is oxidized, is transferred from the inner to the outer membrane, and then helps in the release of cyt c, one of the

fundamental steps of apoptosis. Alterations in the content and/or structure of CL have been reported in several tissues in a variety of pathological settings [106]. The fatty acyl chain composition of CL is highly specific, being predominantly comprised of 18-carbon unsaturated acyl chains, and linoleic acid (18:2) is the most abundant fatty acyl chain in most mammalian tissues [107], which is consistent with our results, as all major four CLs possess at least one 18:02 fatty acid.

Cell viability requires a constant level of energy, and most normal mammalian cells achieve this level of energy through respiration. In 1926, Otto Warburg found that cancer cells produce most of their Adenosine triphosphate (ATP) through glycolysis [108], now known to be a combination of respiration and glycolysis [109]. Indeed, elevated glycolysis is the metabolic hallmark of nearly all tumors, being a correlation between glycolytic ATP production and aggressiveness of the tumor cells [109]. This alteration in the mitochondria of a cancer cell can alter the composition of CL in the membrane, as is shown in the different profiles of the three types of cells in our results. Some studies showed that CL composition and/or content in mouse brain tumor mitochondria differed markedly from those in mitochondria derived from the normal syngeneic host brain tissue [110], indicating, since CL is intimately involved in mitochondrial respiratory functions, the CL abnormalities found will compromise respiratory energy metabolism in brain tumors.

3. Cross comparison between results of mouse and human species

In this study PL content of two cell groups, one from mouse and other from human origin, were analyzed by TLC and MS. The comparison between these two species is important in order to understand if the differences obtained are likely to be conserved among species and therefore, how far it is possible to use another animal model to model the human pathology. TLCs were similar allowing the identification of the major PL classes, although some small differences were observed probably due to experimental details as the elution of TLC, which could be affected by temperature and humidity. One example is human PE class, which eluted more close to the top of the TLC. In mouse cells, the PA spot was not found and analyzed and what we thought that could be the CL spot was not supported by the MS analysis. In spite of these differences, we were able to characterize the profile of most PL classes and to see some differences in some of the major classes of PL that could be important to understand what happens in tumor cells in different stages of malignancy, and between mouse and human cell lines.

Phosphatidilcholine and Lysophosphatidylcholine profile

Observing the percentages of PL content of all cells, it is consistent the increase of PC in the low metastatic cells (MC4-L5 and T-47D) comparing to non-tumorigenic cells (EpH4 and MCF10A). However, in the high metastatic MDA-MB-231 cells, the increase remained, while in the mouse highly metastatic MC4-L2 cells the level of PCs decreased substantially. The LPC class appeared with higher levels in highly metastatic cells and lower levels in both non-tumorigenic cells followed by the low metastatic MC4-L5 and T-47D cells. However, there was a lower increase of LPC in the human MDA-MB-231 cells compared to the increased observed in the mouse MC4-L2 cells. This could be related to the decrease of PC in MC4-L2 cells but not MDA-MD-231 cells, which in the former, could reflect activity of PLA2 to originate LPC.

Looking at the PC profile in all six cell lines, there was no substantial difference between their molecular species compositions. Regarding their relative abundances, akylacyl PCs seemed to be in a higher relative abundance in all mouse cell lines in comparison with human cell lines. The relative abundance of PC (18:01/18:01) and PC (18:00/18:01) appeared to vary but with no specific pattern, because they were higher in all cells except human T-47D and MCF10A cells.

Sphingomyelin profile

This PL class had a similar variance in the relative content comparing the different degrees of aggressiveness in mouse and human cell lines. There was a very slight increase on both cancer cell types compared to non-tumorigenic cells.

In relation to the profile, there was a consistent decrease of SM (18:01/22:00), SM (18:01/24:01) and SM (18:01/24:00) in all ER+ cancer cells (MC4-L5, MC4-L2 and T-47D) relative to SM (18:01/16:00) and SM (18:00/16:00) comparing with non-tumorigenic cells. As we are comparing relative abundances we don't know exactly in absolute levels which SM increase or decrease, but this is an evident difference which could be studied and explored.

In the most metastatic human MDA-MB-321 cells the behavior is different comparing to the other cell lines appearing to be the profile with the highest relative abundance of SM (18:01/24:01) and SM (18:01/24:00). As explained previously, this could be probably because MDA-MB-231 cancer cells is from a different and more aggressiveness type of tumor, called basal like, do not express hormone receptors, consisting of very undifferentiated cells.

Phosphatidylethanolamine profile

Curiously, the relative PL content of PE class was similar among the different degrees of aggressiveness comparing mouse cell lines and human cell lines. The non-tumorigenic cells had an evident higher percentage of PEs compared to both types of cancer cells, which seemed to be characteristic of both mouse and human cell lines. Since we measured relative PL contents, we can not infer that there is a decrease of PEs in cancer cells, but differences in the relative PL content among the different degrees of aggressiveness are identical between mouse and human cells.

However, when we looked to the lipid composition by analysis of MS spectra, we saw a reduced number of alkylacyl PEs species in human cells. Despite this, both highly metastatic MC4-L2 and MDA-MB-231 cells, had a slightly higher relative abundance of some alkylacyl PEs, such as PE (O-18:00/18:01) and PE (O-16:00/18:01) (at *m/z* of 732 and 704 respectively), suggesting that this difference could be related to aggressiveness and / or morphology, since these cells have a more metastatic potential having a more distinguished spindle-shape morphology.

Phosphatidylserine profile

PS content seemed to be similar in all cell types, not having substantial differences in the relative PL content of this class between the different degrees of aggressiveness and between mouse and human cell lines.

Looking to all profiles from mouse and human cells, they all seemed to have a similar PS composition, except for human low metastatic T-47D cells, which had an evident difference in the relative abundance of PS (18:00/18:01) and PS (16:00/18:01 and 16:01/18:00) (at *m/z* of 788 and 760). Curiously there is no known reason for this difference just in the lipid profile of T-47D cell line, therefore, we can not conclude it is characteristic of low metastatic human cancer cells.

Phosphatidylinositol profile

Comparing the relative PL content of PI class in mouse and human cell lines, the behavior was not the same. In the mouse cell lines there was a slightly higher percentage in both cancer cells compared to non-tumorigenic cells. In human cell lines it was exactly the opposite. Still, we can not conclude on whether there was an increase or decrease in absolute PI levels, but its content could be related to PI3K pathway which produces PIPs from PI (more concretely phosphorylates PIP2 resulting in PIP3) and is known to be altered in cancer. The increase or decrease of PIs could be related to the activation of PI3K.

Comparing profiles of mouse and human cell lines, we see some differences in the molecular composition, for example, PI (22:05/18:00) (*m/z* 911) present in human cells but almost unidentifiable in mouse cells lines, suggesting that both species do not have exactly the same PI composition. Another curious difference was in the relative abundance of PI (16:00/18:01 and 16:01/18:00) (*m/z* 835) that appeared to be almost the same in all cell lines, except in T-47D cells were it was higher. There was an evident alteration that was consistent in both mouse and human cell lines: the ratio between the two most abundant PIs, PI (18:00/18:01) (*m/z* 863) and PI (20:03/18:00) (*m/z* 887). In mouse cell lines, the ratio of PI (18:00/18:01) / PI (20:03/18:00) increased in both cancer cells (MC4-L5 and MC4-L2) comparing to non-tumorigenic EpH4 cell line due to a minor relative abundance of PI (20:03/18:00) in both cancer cells. In human cells, the ratio of PI (18:00/18:01) / PI (20:03/18:00) increased in both cancer cells (T-47D and MDA-MB-231) comparing to non-tumorigenic MCF10A cell line due to a higher relative abundance of PI (18:00/18:01) in both cancer cells. Despite their differences in the relative abundance, the variation of the ratio of this two PIs between non-tumorigenic and cancer cells is similar in both mouse and human cell lines indicating an obvious alteration in the fatty acyl composition in cancer cells compared to non-tumorigenic cells.

IV. Conclusion

IV. Conclusion

In this work we described differences and similarities of the phospholipid profile from non-tumorigenic and cancer cells in both mouse and human cell lines. The main goal of the work was to evaluate if non-tumorigenic and cancer cells display differences in PL profile, which could be a consequence of their distinct metabolic state and / or different morphology. Also, this approach was used to search for differences among breast cancer cells with different levels of aggressiveness.

The results obtained allowed us to identify some differences, between non-tumorigenic and cancer cells that were observed both in mouse and human cell lines. Although the same molecular species were seen in all PL classes, the relative abundance of the molecular species changed for SM, PI and CL classes. SM class appeared to have a decrease of the SMs with C16 fatty acids in cancer cells compared to non-tumorigenic cells. Also in all cancer cells dramatic changes in the two most abundant PIs were observed; whereas the ratio PI (18:00/18:01) / PI (20:03/18:00) increased comparing to non-tumorigenic cells.

It was also possible to distinguish the low from the high metastatic cell lines which could be associated to malignant progression in both mouse and human cell lines. The more aggressive cells showed increased relative amounts of LPCs. Alteration in PE profile, more concretely high amount of alkylacyl PEs were also found in the more aggressive cell lines.

Despite having being analyzed only in human cells, CL and PA classes also showed differences. CL class had a minor relative abundance of long chain fatty acids in both cancer cells comparing to non-tumorigenic cells. PA class was only detected in the more metastatic cell line and its high abundance could also be associated to malignant progression.

Comparison of mouse with human cell lines disclosed differences in PLs profile. However, the above mentioned similarities obtained in mouse cell lines, when compared to human cell lines, are likely to be conserved among species and reflect metabolic changes associated to cell morphology, gene expression and cancer progression, directly

related to enzymatic and metabolic activities known to be altered in cancer. Thus, identification of PL classes and their structure open new possibilities for exploration of such alterations in cancer and provide novel biomarkers.

V. Bibliography

V. Bibliography

1. Polyak K: **Breast cancer: origins and evolution**. *J Clin Invest* 2007, **117**(11):3155-3163.
2. Fernandis AZ, Wenk MR: **Lipid-based biomarkers for cancer**. *J Chromatogr B Analyt Technol Biomed Life Sci* 2009, **877**(26):2830-2835.
3. Kamangar F, Dores GM, Anderson WF: **Patterns of cancer incidence, mortality, and prevalence across five continents: defining priorities to reduce cancer disparities in different geographic regions of the world**. *J Clin Oncol* 2006, **24**(14):2137-2150.
4. Weigelt B, Geyer FC, Reis-Filho JS: **Histological types of breast cancer: how special are they?** *Mol Oncol* 2010, **4**(3):192-208.
5. Dumitrescu RG, Cotarla I: **Understanding breast cancer risk -- where do we stand in 2005?** *J Cell Mol Med* 2005, **9**(1):208-221.
6. Ellis IO, Galea M, Broughton N, Locker A, Blamey RW, Elston CW: **Pathological prognostic factors in breast cancer. II. Histological type. Relationship with survival in a large study with long-term follow-up**. *Histopathology* 1992, **20**(6):479-489.
7. Sotiriou C, Pusztai L: **Gene-expression signatures in breast cancer**. *N Engl J Med* 2009, **360**(8):790-800.
8. Masood S: **Estrogen and progesterone receptors in cytology: a comprehensive review**. *Diagn Cytopathol* 1992, **8**(5):475-491.
9. Musgrove EA, Sutherland RL: **Biological determinants of endocrine resistance in breast cancer**. *Nat Rev Cancer* 2009, **9**(9):631-643.
10. Fidler IJ: **The pathogenesis of cancer metastasis: the 'seed and soil' hypothesis revisited**. *Nat Rev Cancer* 2003, **3**(6):453-458.
11. Leitinger B, Hogg N: **The involvement of lipid rafts in the regulation of integrin function**. *J Cell Sci* 2002, **115**(Pt 5):963-972.
12. Brackenbury R, Rutishauser U, Edelman GM: **Distinct calcium-independent and calcium-dependent adhesion systems of chicken embryo cells**. *Proc Natl Acad Sci U S A* 1981, **78**(1):387-391.
13. Hynes RO: **Integrins: bidirectional, allosteric signaling machines**. *Cell* 2002, **110**(6):673-687.
14. Berx G, Van Roy F: **The E-cadherin/catenin complex: an important gatekeeper in breast cancer tumorigenesis and malignant progression**. *Breast Cancer Res* 2001, **3**(5):289-293.
15. Gilcrease MZ, Zhou X, Welch K: **Adhesion-independent alpha6beta4 integrin clustering is mediated by phosphatidylinositol 3-kinase**. *Cancer Res* 2004, **64**(20):7395-7398.
16. Ridley AJ, Schwartz MA, Burridge K, Firtel RA, Ginsberg MH, Borisy G, Parsons JT, Horwitz AR: **Cell migration: integrating signals from front to back**. *Science* 2003, **302**(5651):1704-1709.
17. van Meer G, Voelker DR, Feigenson GW: **Membrane lipids: where they are and how they behave**. *Nat Rev Mol Cell Biol* 2008, **9**(2):112-124.
18. Vereb G, Szollosi J, Matko J, Nagy P, Farkas T, Vigh L, Matyus L, Waldmann TA, Damjanovich S: **Dynamic, yet structured: The cell membrane three decades after the Singer-Nicolson model**. *Proc Natl Acad Sci U S A* 2003, **100**(14):8053-8058.
19. Singer SJ, Nicolson GL: **The fluid mosaic model of the structure of cell membranes**. *Science* 1972, **175**(23):720-731.
20. Eyster KM: **The membrane and lipids as integral participants in signal transduction: lipid signal transduction for the non-lipid biochemist**. *Adv Physiol Educ* 2007, **31**(1):5-16.

21. Escriba PV, Gonzalez-Ros JM, Goni FM, Kinnunen PK, Vigh L, Sanchez-Magraner L, Fernandez AM, Busquets X, Horvath I, Barcelo-Coblijn G: **Membranes: a meeting point for lipids, proteins and therapies**. *J Cell Mol Med* 2008, **12**(3):829-875.
22. Patra SK: **Dissecting lipid raft facilitated cell signaling pathways in cancer**. *Biochim Biophys Acta-Rev Cancer* 2008, **1785**(2):182-206.
23. van Meer G, de Kroon AI: **Lipid map of the mammalian cell**. *J Cell Sci* 2011, **124**(Pt 1):5-8.
24. Hannun YA, Obeid LM: **Principles of bioactive lipid signalling: lessons from sphingolipids**. *Nat Rev Mol Cell Biol* 2008, **9**(2):139-150.
25. Smith ER, Merrill AH, Obeid LM, Hannun YA: **Effects of sphingosine and other sphingolipids on protein kinase C**. In: *Methods in Enzymology.* Edited by Alfred H. Merrill, Jr., Yusuf AH, vol. Volume 312: Academic Press; 2000: 361-373.
26. Hait NC, Oskeritzian CA, Paugh SW, Milstien S, Spiegel S: **Sphingosine kinases, sphingosine 1-phosphate, apoptosis and diseases**. *Biochim Biophys Acta* 2006, **1758**(12):2016-2026.
27. Di Paolo G, De Camilli P: **Phosphoinositides in cell regulation and membrane dynamics**. *Nature* 2006, **443**(7112):651-657.
28. Diamandis EP: **Cancer biomarkers: can we turn recent failures into success?** *J Natl Cancer Inst* 2010, **102**(19):1462-1467.
29. Ackerstaff E, Glunde K, Bhujwalla ZM: **Choline phospholipid metabolism: a target in cancer cells?** *J Cell Biochem* 2003, **90**(3):525-533.
30. Zhao L, Vogt PK: **Class I PI3K in oncogenic cellular transformation**. *Oncogene* 2008, **27**(41):5486-5496.
31. Carnero A, Blanco-Aparicio C, Renner O, Link W, Leal JF: **The PTEN/PI3K/AKT signalling pathway in cancer, therapeutic implications**. *Curr Cancer Drug Targets* 2008, **8**(3):187-198.
32. Wymann MP, Schneiter R: **Lipid signalling in disease**. *Nat Rev Mol Cell Biol* 2008, **9**(2):162-176.
33. Sutphen R, Xu Y, Wilbanks GD, Fiorica J, Grendys EC, Jr., LaPolla JP, Arango H, Hoffman MS, Martino M, Wakeley K *et al*: **Lysophospholipids are potential biomarkers of ovarian cancer**. *Cancer Epidemiol Biomarkers Prev* 2004, **13**(7):1185-1191.
34. Bektas M, Payne SG, Liu H, Goparaju S, Milstien S, Spiegel S: **A novel acylglycerol kinase that produces lysophosphatidic acid modulates cross talk with EGFR in prostate cancer cells**. *J Cell Biol* 2005, **169**(5):801-811.
35. Saddoughi SA, Song P, Ogretmen B: **Roles of bioactive sphingolipids in cancer biology and therapeutics**. *Subcell Biochem* 2008, **49**:413-440.
36. Hla T: **Physiological and pathological actions of sphingosine 1-phosphate**. *Semin Cell Dev Biol* 2004, **15**(5):513-520.
37. Rosen H, Goetzl EJ: **Sphingosine 1-phosphate and its receptors: an autocrine and paracrine network**. *Nat Rev Immunol* 2005, **5**(7):560-570.
38. Carpinteiro A, Dumitru C, Schenck M, Gulbins E: **Ceramide-induced cell death in malignant cells**. *Cancer Lett* 2008, **264**(1):1-10.
39. Ichikawa S, Hirabayashi Y: **Glucosylceramide synthase and glycosphingolipid synthesis**. *Trends Cell Biol* 1998, **8**(5):198-202.
40. Huang Q, Shen H-M, Shui G, Wenk MR, Ong C-N: **Emodin Inhibits Tumor Cell Adhesion through Disruption of the Membrane Lipid Raft-Associated Integrin Signaling Pathway**. *Cancer Res* 2006, **66**.
41. Rossier-Pansier L, Baruthio F, Ruegg C, Mariotti A: **Compartmentalization in Membrane Rafts Defines a Pool of N-Cadherin Associated With Catenins and Not Engaged in Cell–Cell Junctions in Melanoma Cells**. *Journal of Cellular Biochemistry* 2008, **103**:957-971.

42. Causeret M, Taulet N, Comunale F, Favard C, Gauthier-Rouviere C: **N-cadherin association with lipid rafts regulates its dynamic assembly at cell-cell junctions in C2C12 myoblasts**. *Mol Biol Cell* 2005, **16**(5):2168-2180.
43. Zehethofer N, Pinto DM: **Recent developments in tandem mass spectrometry for lipidomic analysis**. *Anal Chim Acta* 2008, **627**(1):62-70.
44. Watson AD: **Thematic review series: systems biology approaches to metabolic and cardiovascular disorders. Lipidomics: a global approach to lipid analysis in biological systems**. *J Lipid Res* 2006, **47**(10):2101-2111.
45. Oresic M, Hanninen VA, Vidal-Puig A: **Lipidomics: a new window to biomedical frontiers**. *Trends Biotechnol* 2008, **26**(12):647-652.
46. Wenk MR: **The emerging field of lipidomics**. *Nat Rev Drug Discov* 2005, **4**(7):594-610.
47. Christie WW: **Rapid separation and quantification of lipid classes by high performance liquid chromatography and mass (light-scattering) detection**. *J Lipid Res* 1985, **26**(4):507-512.
48. Fahy E, Subramaniam S, Brown HA, Glass CK, Merrill AH, Jr., Murphy RC, Raetz CR, Russell DW, Seyama Y, Shaw W *et al*: **A comprehensive classification system for lipids**. *J Lipid Res* 2005, **46**(5):839-861.
49. Hu C, van der Heijden R, Wang M, van der Greef J, Hankemeier T, Xu G: **Analytical strategies in lipidomics and applications in disease biomarker discovery**. *J Chromatogr B Analyt Technol Biomed Life Sci* 2009, **877**(26):2836-2846.
50. Milne S, Ivanova P, Forrester J, Alex Brown H: **Lipidomics: an analysis of cellular lipids by ESI-MS**. *Methods* 2006, **39**(2):92-103.
51. Wolf C, Quinn PJ: **Lipidomics: practical aspects and applications**. *Prog Lipid Res* 2008, **47**(1):15-36.
52. Folch J, Ascoli I, Lees M, Meath JA, Le BN: **Preparation of lipide extracts from brain tissue**. *J Biol Chem* 1951, **191**(2):833-841.
53. Bligh EG, Dyer WJ: **A rapid method of total lipid extraction and purification**. *Can J Biochem Physiol* 1959, **37**(8):911-917.
54. Peterson BL, Cummings BS: **A review of chromatographic methods for the assessment of phospholipids in biological samples**. *Biomed Chromatogr* 2006, **20**(3):227-243.
55. Carrasco-Pancorbo A, Navas-Iglesias N, Cuadros-Rodríguez L: **From lipid analysis towards lipidomics, a new challenge for the analytical chemistry of the 21st century. Part I: Modern lipid analysis**. *TrAC Trends in Analytical Chemistry* 2009, **28**(3):263-278.
56. Want EJ, Cravatt BF, Siuzdak G: **The expanding role of mass spectrometry in metabolite profiling and characterization**. *Chembiochem* 2005, **6**(11):1941-1951.
57. Pulfer M, Murphy RC: **Electrospray mass spectrometry of phospholipids**. *Mass Spectrom Rev* 2003, **22**(5):332-364.
58. Sommerer D, Suss R, Hammerschmidt S, Wirtz H, Arnold K, Schiller J: **Analysis of the phospholipid composition of bronchoalveolar lavage (BAL) fluid from man and minipig by MALDI-TOF mass spectrometry in combination with TLC**. *J Pharm Biomed Anal* 2004, **35**(1):199-206.
59. Fenn JB, Mann M, Meng CK, Wong SF, Whitehouse CM: **Electrospray ionization for mass spectrometry of large biomolecules**. *Science* 1989, **246**(4926):64-71.
60. Watson JT, Sparknman OD: **Introduction to mass spectrometry: instrumentation, applications, and strategies for data interpretation** 4th edn; 2007.
61. Ekman R: **Mass spectrometry: instrumentation, interpretation, and applications** 2009.
62. Taguchi R, Houjou T, Nakanishi H, Yamazaki T, Ishida M, Imagawa M, Shimizu T: **Focused lipidomics by tandem mass spectrometry**. *J Chromatogr B Analyt Technol Biomed Life Sci* 2005, **823**(1):26-36.

63. Cui Z, Thomas MJ: **Phospholipid profiling by tandem mass spectrometry**. *J Chromatogr B Analyt Technol Biomed Life Sci* 2009, **877**(26):2709-2715.
64. Hou W, Zhou H, Elisma F, Bennett SA, Figeys D: **Technological developments in lipidomics**. *Brief Funct Genomic Proteomic* 2008, **7**(5):395-409.
65. Hsu FF, Turk J: **Structural determination of sphingomyelin by tandem mass spectrometry with electrospray ionization**. *J Am Soc Mass Spectrom* 2000, **11**(5):437-449.
66. Merchant TE, Kasimos JN, Vroom T, de Bree E, Iwata JL, de Graaf PW, Glonek T: **Malignant breast tumor phospholipid profiles using P-31 magnetic resonance**. *Cancer Lett* 2002, **176**(2):159-167.
67. Merchant TE, Meneses P, Gierke LW, Den Otter W, Glonek T: **31P magnetic resonance phospholipid profiles of neoplastic human breast tissues**. *Br J Cancer* 1991, **63**(5):693-698.
68. Dill AL, Ifa DR, Manicke NE, Costa AB, Ramos-Vara JA, Knapp DW, Cooks RG: **Lipid profiles of canine invasive transitional cell carcinoma of the urinary bladder and adjacent normal tissue by desorption electrospray ionization imaging mass spectrometry**. *Anal Chem* 2009, **81**(21):8758-8764.
69. Kim Y, Shanta SR, Zhou LH, Kim KP: **Mass spectrometry based cellular phosphoinositides profiling and phospholipid analysis: a brief review**. *Exp Mol Med* 2010, **42**(1):1-11.
70. Kim H, Min HK, Kong G, Moon MH: **Quantitative analysis of phosphatidylcholines and phosphatidylethanolamines in urine of patients with breast cancer by nanoflow liquid chromatography/tandem mass spectrometry**. *Anal Bioanal Chem* 2009, **393**(6-7):1649-1656.
71. Min HK, Kong G, Moon MH: **Quantitative analysis of urinary phospholipids found in patients with breast cancer by nanoflow liquid chromatography-tandem mass spectrometry: II. Negative ion mode analysis of four phospholipid classes**. *Anal Bioanal Chem* 2010, **396**(3):1273-1280.
72. Reichmann E, Schwarz H, Deiner EM, Leitner I, Eilers M, Berger J, Busslinger M, Beug H: **Activation of an inducible c-FosER fusion protein causes loss of epithelial polarity and triggers epithelial-fibroblastoid cell conversion**. *Cell* 1992, **71**(7):1103-1116.
73. Lanari C, Luthy I, Lamb CA, Fabris V, Pagano E, Helguero LA, Sanjuan N, Merani S, Molinolo AA: **Five novel hormone-responsive cell lines derived from murine mammary ductal carcinomas: in vivo and in vitro effects of estrogens and progestins**. *Cancer Res* 2001, **61**(1):293-302.
74. Bartlett GR: **Phosphorus assay in column chromatography**. *J Biol Chem* 1959, **234**(3):466-468.
75. Sterin M, Cohen JS, Ringel I: **Hormone sensitivity is reflected in the phospholipid profiles of breast cancer cell lines**. *Breast Cancer Res Treat* 2004, **87**(1):1-11.
76. Han X, Gross RW: **Shotgun lipidomics: electrospray ionization mass spectrometric analysis and quantitation of cellular lipidomes directly from crude extracts of biological samples**. *Mass Spectrom Rev* 2005, **24**(3):367-412.
77. Hsu FF, Turk J: **Electrospray ionization with low-energy collisionally activated dissociation tandem mass spectrometry of glycerophospholipids: mechanisms of fragmentation and structural characterization**. *J Chromatogr B Analyt Technol Biomed Life Sci* 2009, **877**(26):2673-2695.
78. Katz-Brull R, Seger D, Rivenson-Segal D, Rushkin E, Degani H: **Metabolic markers of breast cancer: enhanced choline metabolism and reduced choline-ether-phospholipid synthesis**. *Cancer Res* 2002, **62**(7):1966-1970.
79. Hoffmann P, Olayioye MA, Moritz RL, Lindeman GJ, Visvader JE, Simpson RJ, Kemp BE: **Breast cancer protein StarD10 identified by three-dimensional separation using free-flow electrophoresis, reversed-phase high-performance liquid chromatography, and**

sodium dodecyl sulfate-polyacrylamide gel electrophoresis. *Electrophoresis* 2005, **26**(6):1029-1037.

80. Murphy NC, Biankin AV, Millar EK, McNeil CM, O'Toole SA, Segara D, Crea P, Olayioye MA, Lee CS, Fox SB *et al*: **Loss of STARD10 expression identifies a group of poor prognosis breast cancers independent of HER2/Neu and triple negative status**. *Int J Cancer* 2010, **126**(6):1445-1453.
81. Olayioye MA, Vehring S, Muller P, Herrmann A, Schiller J, Thiele C, Lindeman GJ, Visvader JE, Pomorski T: **StarD10, a START domain protein overexpressed in breast cancer, functions as a phospholipid transfer protein**. *J Biol Chem* 2005, **280**(29):27436-27442.
82. Murakami M, Kudo I: **Phospholipase A2**. *J Biochem* 2002, **131**(3):285-292.
83. Yamashita S, Yamashita J, Sakamoto K, Inada K, Nakashima Y, Murata K, Saishoji T, Nomura K, Ogawa M: **Increased expression of membrane-associated phospholipase A2 shows malignant potential of human breast cancer cells**. *Cancer* 1993, **71**(10):3058-3064.
84. Tokumura A, Majima E, Kariya Y, Tominaga K, Kogure K, Yasuda K, Fukuzawa K: **Identification of human plasma lysophospholipase D, a lysophosphatidic acid-producing enzyme, as autotaxin, a multifunctional phosphodiesterase**. *J Biol Chem* 2002, **277**(42):39436-39442.
85. Yang SY, Lee J, Park CG, Kim S, Hong S, Chung HC, Min SK, Han JW, Lee HW, Lee HY: **Expression of autotaxin (NPP-2) is closely linked to invasiveness of breast cancer cells**. *Clin Exp Metastasis* 2002, **19**(7):603-608.
86. Xu Y, Shen Z, Wiper DW, Wu M, Morton RE, Elson P, Kennedy AW, Belinson J, Markman M, Casey G: **Lysophosphatidic acid as a potential biomarker for ovarian and other gynecologic cancers**. *JAMA* 1998, **280**(8):719-723.
87. Okita M, Gaudette DC, Mills GB, Holub BJ: **Elevated levels and altered fatty acid composition of plasma lysophosphatidylcholine(lysoPC) in ovarian cancer patients**. *Int J Cancer* 1997, **71**(1):31-34.
88. Ogretmen B: **Sphingolipids in cancer: Regulation of pathogenesis and therapy**. *FEBS Letters* 2006, **580**(23):5467-5476.
89. Koyanagi S, Kuga M, Soeda S, Hosoda Y, Yokomatsu T, Takechi H, Akiyama T, Shibuya S, Shimeno H: **Elevation of de novo ceramide synthesis in tumor masses and the role of microsomal dihydroceramide synthase**. *Int J Cancer* 2003, **105**(1):1-6.
90. Kim CW, Lee HM, Lee TH, Kang C, Kleinman HK, Gho YS: **Extracellular membrane vesicles from tumor cells promote angiogenesis via sphingomyelin**. *Cancer Res* 2002, **62**(21):6312-6317.
91. Patra SK: **Dissecting lipid raft facilitated cell signaling pathways in cancer**. *Biochim Biophys Acta* 2008, **1785**(2):182-206.
92. Seijo L, Merchant TE, van der Ven LT, Minsky BD, Glonek T: **Meningioma phospholipid profiles measured by 31P nuclear magnetic resonance spectroscopy**. *Lipids* 1994, **29**(5):359-364.
93. Vance JE, Steenbergen R: **Metabolism and functions of phosphatidylserine**. *Prog Lipid Res* 2005, **44**(4):207-234.
94. Shi J, Pipe SW, Rasmussen JT, Heegaard CW, Gilbert GE: **Lactadherin blocks thrombosis and hemostasis in vivo: correlation with platelet phosphatidylserine exposure**. *J Thromb Haemost* 2008, **6**(7):1167-1174.
95. Wolfs JL, Comfurius P, Rasmussen JT, Keuren JF, Lindhout T, Zwaal RF, Bevers EM: **Activated scramblase and inhibited aminophospholipid translocase cause phosphatidylserine exposure in a distinct platelet fraction**. *Cell Mol Life Sci* 2005, **62**(13):1514-1525.
96. Stace CL, Ktistakis NT: **Phosphatidic acid- and phosphatidylserine-binding proteins**. *Biochim Biophys Acta* 2006, **1761**(8):913-926.

97. Yeung T, Gilbert GE, Shi J, Silvius J, Kapus A, Grinstein S: **Membrane phosphatidylserine regulates surface charge and protein localization**. *Science* 2008, **319**(5860):210-213.
98. Dobrzynska I, Szachowicz-Petelska B, Sulkowski S, Figaszewski Z: **Changes in electric charge and phospholipids composition in human colorectal cancer cells**. *Mol Cell Biochem* 2005, **276**(1-2):113-119.
99. Jiang BH, Liu LZ: **PI3K/PTEN signaling in tumorigenesis and angiogenesis**. *Biochim Biophys Acta* 2008, **1784**(1):150-158.
100. Hughes-Fulford M, Li CF, Boonyaratanakornkit J, Sayyah S: **Arachidonic acid activates phosphatidylinositol 3-kinase signaling and induces gene expression in prostate cancer**. *Cancer Res* 2006, **66**(3):1427-1433.
101. Larijani B, Dufourc EJ: **Polyunsaturated phosphatidylinositol and diacylglycerol substantially modify the fluidity and polymorphism of biomembranes: a solid-state deuterium NMR study**. *Lipids* 2006, **41**(10):925-932.
102. Murph M, Tanaka T, Pang J, Felix E, Liu S, Trost R, Godwin AK, Newman R, Mills G: **Liquid chromatography mass spectrometry for quantifying plasma lysophospholipids: potential biomarkers for cancer diagnosis**. *Methods Enzymol* 2007, **433**:1-25.
103. Brindley DN, Waggoner DW: **Mammalian lipid phosphate phosphohydrolases**. *J Biol Chem* 1998, **273**(38):24281-24284.
104. Gomez-Cambronero J: **New concepts in phospholipase D signaling in inflammation and cancer**. *ScientificWorldJournal* 2010, **10**:1356-1369.
105. Noh DY, Ahn SJ, Lee RA, Park IA, Kim JH, Suh PG, Ryu SH, Lee KH, Han JS: **Overexpression of phospholipase D1 in human breast cancer tissues**. *Cancer Lett* 2000, **161**(2):207-214.
106. Chicco AJ, Sparagna GC: **Role of cardiolipin alterations in mitochondrial dysfunction and disease**. *Am J Physiol Cell Physiol* 2007, **292**(1):C33-44.
107. Hostetler KY, Galesloot JM, Boer P, Van Den Bosch H: **Further studies on the formation of cardiolipin and phosphatidylglycerol in rat liver mitochondria. Effect of divalent cations and the fatty acid composition of CDP-diglyceride**. *Biochim Biophys Acta* 1975, **380**(3):382-389.
108. Warburg O: **On the origin of cancer cells**. *Science* 1956, **123**(3191):309-314.
109. Gogvadze V, Orrenius S, Zhivotovsky B: **Mitochondria in cancer cells: what is so special about them?** *Trends Cell Biol* 2008, **18**(4):165-173.
110. Kiebish MA, Han X, Cheng H, Chuang JH, Seyfried TN: **Cardiolipin and electron transport chain abnormalities in mouse brain tumor mitochondria: lipidomic evidence supporting the Warburg theory of cancer**. *J Lipid Res* 2008, **49**(12):2545-2556.